

**IMPLEMENTING THE HOT WATER-WAG FOR  
ENHANCING HEAVY OIL RECOVERY IN A  
FRACTURED CARBONATE RESERVOIR**

**A THESIS SUBMITTED TO THE GRADUATE  
SCHOOL OF APPLIED SCIENCES  
OF  
NEAR EAST UNIVERSITY**

**By  
MUSTAFA HASAN HAMAD**

**In Partial Fulfillment of the Requirements for  
The Degree of Master of Science  
In  
Petroleum and Natural Gas Engineering**

**NICOSIA, 2021**

**MUSTAFA HASAN  
HAMAD**

**IMPLEMENTING THE HOT WATER-WAG FOR ENHANCING HEAVY OIL  
RECOVERY IN A FRACTURED CARBONATE RESERVOIR**

**NEU  
2021**

**IMPLEMENTING THE HOT WATER-WAG FOR  
ENHANCING HEAVY OIL RECOVERY IN A  
FRACTURED CARBONATE RESERVOIR**

**A THESIS SUBMITTED TO THE GRADUATE  
SCHOOL OF APPLIED SCIENCES  
OF  
NEAR EAST UNIVERSITY**

**By  
MUSTAFA HASAN HAMAD**

**In Partial Fulfillment of the Requirements for  
The Degree of Master of Science  
In  
Petroleum and Natural Gas Engineering**

**NICOSIA, 2021**

**Mustafa Hasan HAMAD: IMPLEMENTING THE HOT WATER-WAG FOR  
ENHANCING HEAVY OIL RECOVERY IN A FRACTURED CARBONATE  
RESERVOIR**

**Approval of Director of Institute of Graduate  
Studies**

**Prof. Dr. K. Hüsni Can BAŞER**

**We certify that this thesis is satisfactory for the award of the degree of Masters of Science in  
Petroleum and Natural Gas Engineering**

**Examining Committee in Charge:**



**Prof. Dr. Cavit ATALAR**

Committee Chairman, Petroleum and Natural Gas  
Engineering Department, NEU



**Prof. Dr. Salih SANER**

Supervisor, Petroleum and Natural Gas Engineering  
Department, NEU



**Assist. Prof. Dr. Süleyman AŞIR**

Materials Sciences and Nanotechnology  
Engineering Department, NEU

I hereby declare that all information in this document has been obtained and presented in accordance with academic rules and ethical conduct. I also declare that, as required by these rules and conduct, I have fully cited and referenced all material and results that are not original to this work.

Name, Last Name: MUSTAFA HASAN HAMAD

Signature:

A handwritten signature in blue ink, consisting of a large, stylized loop followed by a horizontal line and a small mark.

Date: 28/06/2021

## **ACKNOWLEDGEMENT**

Firstly, I would like to express my honest gratitude to my research supervisor Prof. Dr. SALIH SANER, for his bright guidance and provision in this work. His time and effort made it possible for me to complete this work.

It is a great pleasure to thank everyone who supported me during my project. I am highly appreciated and thankful to the chairman Prof. Dr. CAVIT ATALAR for his continuous support, advising and encouragement, and thankful for all professors, doctors and lecturers which they had been teaching me during this journey and study.

I want to thank to my classmates for their help which continued especially during quarantine time while COVID-19 world issue, without them I could not complete this study, it is great pleasure to thank to my coworkers, they covered me at the beginning of first and second coursework semesters, without their help may I could not travel to Northern Cyprus, they helped me to keep staying in the oilfield work.

Finally, I would like to offer my deepest appreciation to my family, Father, Mother, Brothers and Sisters for their continues support and for their motivation and for the fact that without their motivation, I wouldn't accomplish this study.

**To my family...**

## ABSTRACT

In recent years, with the technological developments, heavy oil is produced with enhanced oil recovery (EOR) methods mainly using thermal methods. The recovery factor for producing heavy oil with natural drive mechanisms doesn't exceed 20%, and in many cases doesn't produce at all. However, high temperature injection methods aim to maximize the recovery factor in heavy oil reservoirs.

Heavy oil reservoirs are challenging cases due to the extreme difficulties in terms of oil viscosity which makes flow through pores difficult. The conventional injection methods in heavy oil reservoirs is indeed unwanted as it doesn't help to produce heavy oil effectively and at the same time it causes production problems. Thermal water injection with the use of CO<sub>2</sub> as gas injection can help to maximize the oil recovery factor through reducing heavy oil viscosity. A definite effective hot water-water-alternating gas (WAG) method will be used with practical steps that aims to improve oil recovery and achieves the objective of this study successfully.

CMG-STARs simulation software has been used to run a field model with the use of EOR to optimize the overall production. Hot-water flooding, CO<sub>2</sub> flooding and Hot-WAG injection have been investigated based on water-cut, cumulative oil production and GOR results. The result of this study concluded that hot WAG injection is very desirable and provides best oil recovery compared to hot water flooding and gas flooding injection. Additionally, higher injection temperature and 12-month cycle has provided greater oil recovery, which therefore been selected as best scenarios.

**Keywords:** Heavy oil carbonate reservoir, fractured reservoir, hot water flooding, hot WAG injection, CO<sub>2</sub> flooding.

## ÖZET

Son yıllarda teknolojik gelişmelerle birlikte ağır petrol, ağırlıklı olarak termal yöntemler kullanılarak geliştirilmiş petrol üretimi (EOR) yöntemleriyle çıkarılmaktadır. Doğal tahrik mekanizmaları ile ağır petrol üretmek için geri kazanım faktörü %20' yi geçmez ve çoğu durumda hiç üretim yapılamaz. Bununla birlikte, yüksek sıcaklıkta enjeksiyon yöntemleri, ağır petrol rezervuarlarında üretim faktörünü maksimize etmeyi amaçlamaktadır.

Ağır petrol rezervuarları, gözeneklerden akışı zorlaştıran petrol viskozitesi nedeniyle aşırı zorluklar oluşturur. Ağır petrol rezervuarındaki geleneksel enjeksiyon yöntemleri, ağır petrolün etkin bir şekilde üretilmesine yardımcı olmadığından ve aynı zamanda üretim sorunlarına neden olduğundan gerçekten tercih edilmeyen bir durumdur. Gaz enjeksiyonu olarak CO<sub>2</sub> kullanımıyla termal su enjeksiyonu, ağır petrol viskozitesini azaltarak petrol üretim faktörünü en üst düzeye çıkarmaya yardımcı olabilir. Petrol üretimini artırmayı amaçlayan ve bu çalışmanın amacına başarılı bir şekilde ulaşan kesin etkili bir sıcak su-gaz nöbetleşe enjeksiyon (WAG) yöntemi pratik adımlarla kullanılmaktadır.

CMG-STARs simülasyon yazılımı, genel EOR üretimini optimize etmek için bir saha modeli çalıştırmak için kullanılacaktır. Bu çalışma, kırık karbonat rezervuarlarında ağır petrolün üretim faktörünü geliştirmek için miscible CO<sub>2</sub> kullanımıyla birlikte sıcak WAG enjeksiyonuna ek olarak sıcak su enjeksiyonunun kullanımını araştırmayı amaçlamaktadır.

**Anahtar Kelimeler:** Ağır petrol karbonat rezervuarı, kırıklı rezervuarı, sıcak su ötelemesi, sıcak WAG enjeksiyonu, miscible CO<sub>2</sub> ötelemesi.

# TABLE OF CONTENT

<b>ACKNOWLEDGEMENT</b> .....	ii
<b>ABSTRACT</b> .....	iv
<b>ÖZET</b> .....	v
<b>LIST OF TABLES</b> .....	ix
<b>LIST OF FIGURES</b> .....	x
<b>LIST OF SYMBOLS AND ABBREVIATIONS</b> .....	xiv
<b>CHAPTER 1 INTRODUCTION</b>	
1.1 Background.....	1
1.2 Objectives of the Study.....	3
1.3 Problem Statement of the Research Study .....	3
1.4 Organization of the Study.....	4
<b>CHAPTER 2 LITERATURE REVIEW</b>	
2.1 Heavy Oil Reservoir .....	5
2.1.1 Heavy oil characteristics.....	6
2.1.2 Heavy oil extraction methods .....	7
2.2 Naturally Fractured Reservoirs.....	8
2.3 EOR for Heavy Oil Extraction .....	10
2.3.1 Thermal flooding .....	11
2.3.2 Hot water flooding.....	11
2.3.3 Gas flooding .....	12
2.3.4 WAG.....	12

2.3.5 WAG application in Gyda oil field.....	14
2.3.6 Hot WAG.....	15
2.4 Miscible EOR .....	15
2.4.1 Fundamentals and mechanism of miscible CO <sub>2</sub> flooding .....	15
2.4.3 CO <sub>2</sub> Solubility in Oil.....	17
2.5 Immiscible CO <sub>2</sub> Flooding EOR.....	17
2.6 Screening Rules for CO <sub>2</sub> Flooding .....	18

### **CHAPTER 3 METHODOLOGY**

3.1 Reservoir Description .....	19
3.2 Reservoir Simulation Model.....	19
3.3 Simulation process.....	23
3.4 Reservoir Fluid Characteristics .....	23
3.5. Well Properties .....	27
3.6 Case Studies.....	28
3.5.1 Hot WAG injection.....	28
3.5.2 CO <sub>2</sub> Flooding .....	29
3.5.3 Hot Water Flooding.....	30

### **CHAPTER 4 RESULTS AND DISCUSSIONS**

4.1 Hot-Water Flooding Scenarios .....	31
4.1.1 Hot 190 °F-water flooding at 2400 psi .....	31
4.1.2 Hot 190 °F-water flooding at 2700 psi .....	33
4.1.3 Hot 190 °F-water flooding at 3000 psi .....	34

4.2 CO <sub>2</sub> Flooding Scenarios .....	36
4.2.1 CO <sub>2</sub> flooding at 2400 psi .....	36
4.2.3 CO <sub>2</sub> flooding at 3000 psi .....	40
4.3 Hot WAG Injection Scenarios .....	42
4.3.1 Hot 190 °F WAG injection 1-month.....	42
4.3.2 Hot 200 °F WAG injection 1-month.....	44
4.3.3 Hot 211°F WAG injection 1-month.....	45
4.3.4 Hot 190 °F WAG injection at 2700 psi 1-month.....	47
4.3.5 Hot 190 °F WAG injection 12-month.....	48
4.3.6 Hot 200 °F WAG injection 12-month.....	50
4.3.7 Hot 211 °F WAG injection 12-month.....	51
4.3.8 Hot 190 °F WAG injection at 2700 psi 12-month .....	53
4.3.9 Hot 190 °F WAG injection at 2400 psi 6-month .....	54
4.4 Discussions .....	56

## **CHAPTER 5 CONCLUSIONS AND RECOMMENDATIONS**

5.1 Conclusions .....	61
5.2 Recommendations .....	62
<b>REFERENCES</b> .....	63

## **APPENDICES**

Appendix 1: Hot-Water-Flooding CMG-STARS Data .....	68
Appendix 2: Similarity Report .....	93
Appendix 3: Ethical Approval Letter .....	94

## LIST OF TABLES

<b>Table 2.1:</b> Crude oil classification by the National Petroleum Agency of Brazil.....	5
<b>Table 2.2:</b> Types of thermal and non-thermal recovery methods.....	8
<b>Table 3.1:</b> Input parameters used in this study.....	20
<b>Table 3.2:</b> Well Properties.....	27
<b>Table 3.3:</b> Hot WAG injection scenario.....	29

## LIST OF FIGURES

<b>Figure 1.1:</b> Schematic drawing of the hot water-WAG injection method to enhance heavy oil recovery.....	2
<b>Figure 2.1:</b> Heavy oil classification.....	6
<b>Figure 2.2:</b> Viscosity-temperature relationship of an Athabasca Bitumen.....	7
<b>Figure 2.3:</b> Idealization of a dual-porosity medium.....	10
<b>Figure 2.4:</b> Recovery factor of different recovery mechanisms.....	13
<b>Figure 2.5:</b> Gyda field historical daily oil and cumulative oil productions, and water cut .....	14
<b>Figure 3.1:</b> 3D Reservoir Model.....	21
<b>Figure 3.2a:</b> 2D Original reservoir temperature distribution 139 °F in the Model.....	22
<b>Figure 3.2b:</b> 2D Reservoir temperature distribution after injection implementation.....	22
<b>Figure 3.3:</b> Relative permeability curve for studied simulation model.....	24
<b>Figure 3.4:</b> Gas relative permeability curve for studied simulation model.....	24
<b>Figure 3.5:</b> Three-phase fluid for studied simulation model .....	25
<b>Figure 3.6:</b> Oil density versus Pressure .....	25
<b>Figure 3.7:</b> Oil viscosity versus temperature .....	26
<b>Figure 3.8:</b> Gas oil ratio versus Pressure .....	27
<b>Figure 3.9:</b> Hot WAG injection rate versus time for one-year hot WAG scenario .....	28
<b>Figure 3.10:</b> CO <sub>2</sub> gas injection rate versus time.....	29
<b>Figure 3.11:</b> Hot water injection rate versus time.....	30

<b>Figure 4.1a:</b> OPR, WCT, and WOR versus time for hot 190 oF-water flooding at 2400 psi .....	32
<b>Figure 4.1b:</b> Cumulative oil production versus time for hot 190 oF-water flooding at 2400 psi .....	32
<b>Figure 4.2a:</b> OPR, WCT, and WOR versus time for hot 190 oF-water flooding at 2700 psi .....	33
<b>Figure 4.2b:</b> Cumulative oil production versus time for hot 190 oF-water flooding at 2700 psi .....	34
<b>Figure 4.3a:</b> OPR, WCT, and WOR versus time for hot 190 oF-water flooding at 3000 psi .....	35
<b>Figure 4.3b:</b> Cumulative oil production versus time for hot 190 oF-water flooding at 3000 psi .....	35
<b>Figure 4.3C:</b> WPR and GPR versus time for hot 190 °F-water flooding at 3000 psi.....	36
<b>Figure 4.4a:</b> OPR, WCT, and WOR versus time for CO <sub>2</sub> flooding at 2400 psi.....	37
<b>Figure 4.4b:</b> Cumulative oil production versus time for CO <sub>2</sub> flooding at 2400 psi .....	38
<b>Figure 4.5a:</b> OPR, WCT, and WOR versus time for CO <sub>2</sub> flooding at 2700 psi .....	39
<b>Figure 4.5b:</b> Cumulative oil production versus time for CO <sub>2</sub> flooding at 2700 psi .....	39
<b>Figure 4.6a:</b> OPR, WCT, and WOR versus time for CO <sub>2</sub> flooding at 3000 psi .....	40
<b>Figure 4.6b:</b> Cumulative oil production versus time for CO <sub>2</sub> flooding at 3000 psi .....	41
<b>Figure 4.6C:</b> Gas and water production rate versus time for CO <sub>2</sub> flooding at 3000 psi .....	42
<b>Figure 4.7a:</b> OPR, WCT, and WOR versus time for hot 190 oF WAG injection 1- month.....	43
<b>Figure 4.7b:</b> Cumulative oil production versus time for hot 190 oF WAG injection 1-month.....	43
<b>Figure 4.8a:</b> OPR, WCT, and WOR versus time for hot 200 oF WAG injection 1- month.....	44

<b>Figure 4.8b:</b> Cumulative oil production versus time for hot 200 oF WAG injection 1-month.....	45
<b>Figure 4.9a:</b> OPR, WCT, and WOR versus time for hot 211 oF WAG injection 1-month.....	46
<b>Figure 4.9b:</b> Cumulative oil production versus time for hot 211 oF WAG injection 1-month.....	46
<b>Figure 4.10a:</b> OPR, WCT, and WOR versus time for hot 190 oF WAG injection at 2700 psi-1-month.....	47
<b>Figure 4.10b:</b> Cumulative oil production versus time for hot 190 oF WAG injection at 2700 psi-1-month.....	48
<b>Figure 4.11a:</b> OPR, WCT, and WOR versus time for hot 190 oF WAG injection 12-month.....	49
<b>Figure 4.11b:</b> Cumulative oil production versus time for hot 190 oF WAG injection 12-month.....	49
<b>Figure 4.12a:</b> OPR, WCT, and WOR versus time for hot 200 oF WAG injection 12-month.....	50
<b>Figure 4.12b:</b> Cumulative oil production versus time for hot 200 oF WAG injection 12-month.....	51
<b>Figure 4.13a:</b> OPR, WCT, and WOR versus time for hot 211 oF WAG injection 12-month.....	52
<b>Figure 4.13b:</b> Cumulative oil production versus time for hot 211 oF WAG injection 12-month.....	52
<b>Figure 4.14a:</b> OPR, WCT, and WOR versus time for hot 190 oF WAG injection at 2700 psi 12-month.....	53
<b>Figure 4.14b:</b> Cumulative oil production versus time for hot 190 oF WAG injection at 2700 psi 12-month .....	54
<b>Figure 4.15a:</b> OPR, WCT, and WOR versus time for hot 190 oF WAG injection at 2400 psi 6-month .....	55
<b>Figure 4.15b:</b> Cumulative oil production versus time for hot 190 oF WAG injection at 2400 psi 6-month.....	55

<b>Figure 4.16:</b> Well pressure Versus Time for hot WAG injection.....	56
<b>Figure 4.17a:</b> 3D model for hot WAG injection scenario (Base-Case) .....	57
<b>Figure 4.17b:</b> 3D model for hot WAG injection scenario (after implementing hot WAG injection) .....	58
<b>Figure 4.18:</b> Cumulative oil production for different CO2 and hot water-Flooding Scenarios .....	59
<b>Figure 4.19:</b> Cumulative oil production for one month and six-month hot WAG scenarios .....	60
<b>Figure 4.20:</b> Cumulative oil production for twelve-month hot WAG scenarios .....	60

## LIST OF SYMBOLS AND ABBREVIATIONS

<b>Ø</b>	Porosity
<b>Ø fracture</b>	Porosity of Fracture
<b>K<sub>x</sub></b>	Permeability in X Direction
<b>K<sub>y</sub></b>	Permeability in Y Direction
<b>K<sub>z</sub></b>	Permeability in Z Direction
<b>OPr</b>	Oil Production Rate
<b>WOR</b>	Water Oil Ratio
<b>GOC</b>	Gas Oil Contact
<b>WAG</b>	Water Alternating Gas
<b>IWAG</b>	Immiscible Water Alternating Gas
<b>EOR</b>	Enhanced Oil Recovery
<b>CO<sub>2</sub></b>	Carbon Dioxide
<b>API</b>	American Petroleum Institute
<b>GOR</b>	Gas Oil Ratio
<b>CSS</b>	Cyclic Steam Stimulation
<b>SAGD</b>	Steam Assisted Gravity Drainage
<b>VAPEX</b>	Vapor-Assisted Petroleum Extraction

<b>CHOPS</b>	Cold Heavy Oil Production with Sand
<b>NFR</b>	Naturally Fractured Reservoir
<b>IOR</b>	Improved Oil Recovery
<b>DP</b>	Dual Porosity
<b>IFT</b>	Interfacial Tension
<b>MSCF</b>	Thousand Standard Cubic Feet Per Day
<b>MMP</b>	Minimum Miscibility Pressure
<b>OOIP</b>	Original Oil in Place
<b>MPA</b>	Megapascal
<b>CP</b>	Centipoise
<b>PV</b>	Pore Volume
<b>°C</b>	Celsius Degree
<b>°F</b>	Fahrenheit Degree
<b>FT</b>	Feet
<b>WOC</b>	Water Oil Contact
<b>PVT</b>	Pressure-Volume-Temperature
<b>PSI</b>	Pound Per Square Inch
<b>PPM</b>	Parts Per Million

<b>FT<sup>3</sup></b>	Cubic foot
<b>BBL</b>	Barrel
<b>SW</b>	Water Saturation
<b>Kr</b>	Relative Permeability
<b>Krw</b>	Relative Permeability to Water
<b>Krow</b>	Relative Permeability to Oil in Presence of Water
<b>Bpd</b>	Barrel Per Day
<b>BHP</b>	Bottom Hole Pressure
<b>WCT</b>	Water Cut Rate
<b>2D</b>	Two Dimensional
<b>3D</b>	Three Dimensional
<b>ft<sup>3</sup>/d</b>	Cubic Foot Per Day

# CHAPTER 1

## INTRODUCTION

### 1.1 Background

Throughout the years, the energy demands of countries have increased rapidly and the need for extra resources became the most important global issue. One of these resources is the oil from heavy oil reservoirs, which is considered as an unconventional resource and very difficult to produce compared to conventional oil reservoirs. There are around 6 trillion barrels of heavy oil in place in the world (Curtis et al., 2002). Heavy oil has a density of less than 20° API gravity with extreme high viscosity at reservoir conditions (Batzle et al., 2006). On the other hand, if the fractured carbonate reservoir is of concern, another complication which regular secondary recovery methods like water-flooding or gas injection do not help to increase the recovery effectively, because using secondary recovery methods will result in production problems mainly excessive water production problem or gas coning. Therefore, other enhanced oil recovery (EOR) methods need to be considered, including polymer-flooding or thermal methods.

In fact, heavy oil is not produced normally due to its viscosity, thermal or chemical methods are used to reduce its viscosity or breakdown its heavy components. Heating methods are common in Canada to produce heavy oil through heating which results in viscosity reduction (Butler, 1991). Hot water flooding and hot water alternating gas (WAG) injection is studied in this project using simulation technique to enhance oil recovery in fractured carbonate heavy oil reservoirs. Figure 1.1 shows hot-WAG injection technique which hot water and CO<sub>2</sub> is used in the process. As seen in Figure 1.1 CO<sub>2</sub> has been injected then hot water is injected in which both fluids contribute to lower oil viscosity and push the oil toward the production well. Therefore, both water and gas injection will contribute to recover the residual oil through viscosity reduction and pushing the oil toward the production well.

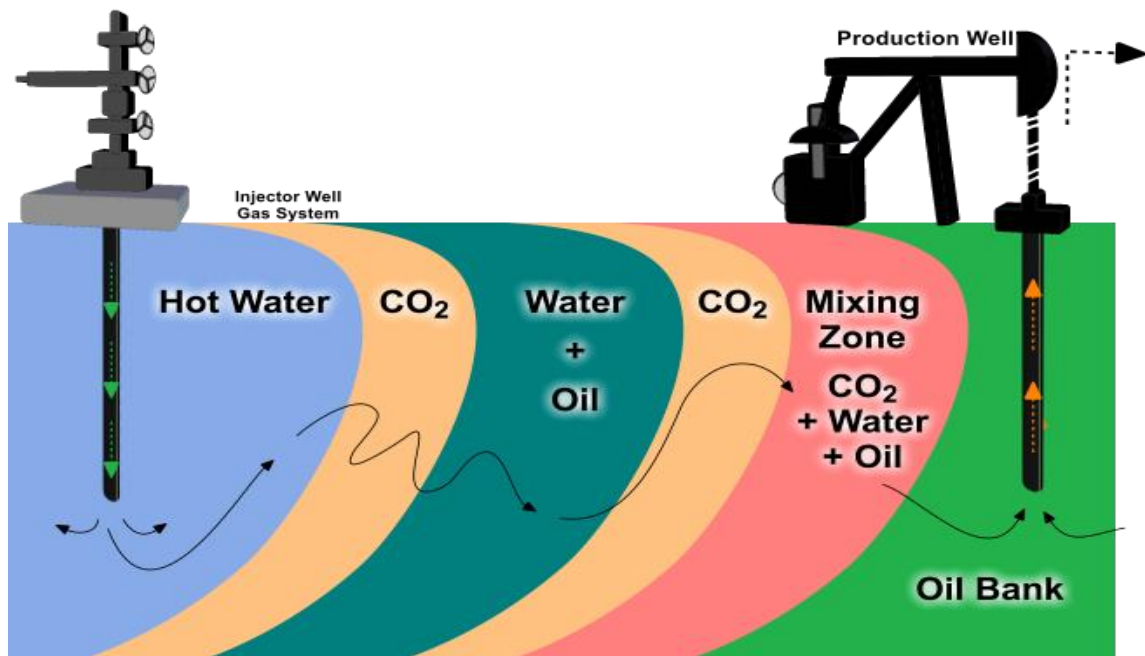


Figure 1.1: Schematic drawing of the hot water-WAG injection method to enhance heavy oil recovery (Adjtoutah, 2019)

In case of extremely large fractures, thermal methods have proven their effectiveness in heavy oil reservoirs around the globe, which it helped to maximize oil recovery without water production issues. As seen in Figure 1.1, the hot water and CO<sub>2</sub> injection alternately aims to push the oil toward the production tube, miscible CO<sub>2</sub> is reducing heavy oil viscosity and resulting in greater oil recovery. In this study, hot water flooding and hot water-alternating gas has been used to investigate their effectiveness in a fractured carbonate heavy oil reservoir. Intensive simulation procedure has been used with respect to the studied subject and a sensitivity analysis has been done to show the impact of different parameters, including; injection cycle, injection amount, injection temperature, injection pattern and injection well location on the recovery factor. Results are analyzed considering water-cut, GOR, collective oil production, and reservoir pressure parameters.

## **1.2 Objectives of the Study**

The following are the main goals of this study:

1. Investigate the recovery factor in a fractured carbonate heavy oil reservoir.
  - a. Conduction intensive simulation work using CMG-STAR3 through using hot water flooding and Hot-WAG EOR techniques to enhance oil recovery method.
  - b. Comparing various methods in terms of oil recovery, water-cut and GOR in order to select the best scenario among them.

## **1.3 Problem Statement of the Research Study**

Heavy oil reservoirs have been produced with enhanced oil recovery methods due to difficulties caused by high viscosity where recovery factor with natural drive mechanisms doesn't exceed 20%. Using high temperature fluid injection methods can significantly contribute in reducing the viscosity and upgrading the heavy oil, which in turn results in increasing oil recovery. Hot-WAG injection method with using hot miscible CO<sub>2</sub> has been studied and analyzed in this paper, which the hot water and hot CO<sub>2</sub> together may help to reduce viscosity and upgrade the heavy oil effectively. Hot-water injection and WAG injection both contribute to reduce the viscosity of oil in different ways, when WAG is used, the water helps to push the residual oil, while the gas in WAG injection helps to reduce the viscosity of oil and lightening it which can result in better recovery of heavy oil.

After achieving the objectives, this study helps the petroleum industry and researchers to obtain information about the following:

1. Understanding unconventional heavy oil reservoirs and the recovery methods required to achieve a suitable recovery factor.
2. How to deal with heavy oil reservoirs with the existence of extremely large fractures and which methods will be used to ensure an effective recovery process.

3. A clear methodology will be used which helps to understand the mechanism of using heating method in heavy oil reservoirs, and to understand certain factors affecting oil recovery in fractured heavy oil reservoirs.

Additionally, this study also involves open fractures that affect the production performance as fractures have a massive impact on overall oil production.

These points will contribute to provide a greater knowledge regarding using heating method to recover heavy oil effectively and minimizing production problems resulted from the fractures within the reservoir, or the high viscous oil.

#### **1.4 Organization of the Study**

Chapter 1 is an introduction which is an overview about the topic, and the main problem of producing heavy oil from fractured reservoir. The list of the objectives of this study is also discussed in this chapter.

Chapter 2 includes literature review. A detailed literature study has been discussed in this chapter, which involves, subjects related to this topic, including EOR methods, heavy oil reservoir, and fractured reservoirs.

Chapter 3 describes the methodology applied. In this chapter, all the procedures involved to complete this project are discussed and mentioned in detail, and all the reservoir rock and fluid data are listed in addition to injection scenarios.

Chapter 4 includes results and discussion obtained in this study. The simulation results are analyzed and discussed in this chapter.

Chapter 5 is conclusions and recommendations. In this chapter, the conclusive remarks are listed in addition to some recommendations for further study.

## CHAPTER 2

### LITERATURE REVIEW

#### 2.1 Heavy Oil Reservoir

Ancheyta et al (2007) and IEA (2005), indicated that two distinct sorts of crude oil exist in the oil reservoirs, one is light oil and the other one is heavy oil. There is a major contrast between these two raw petroleum types regarding composition, recovery and process strategy. The production techniques as well as refining techniques for heavy oil in terms of cost and handling is higher because of sulfur substance and viscosity of the heavy oil. Heavy oil essentially contains a lower amount of light components and more prominent amount of heavy parts contrasted with light oil. Heavy oil contains wax components in which these components own higher atomic structure. These heavy components can make a negative impact on the heavy oil production by contrarily influencing heavy oil mobility (Speight, 2016). Table 2.1 classifies crude oil based on API and specific gravity of crude oil. Here four groups have been designed.

**Table 2.1** Sorting of crude oil based on density by the National Petroleum Agency of Brazil  
(National Petroleum Agency of Brazil, 2000)

<b>Classification</b>	<b>API°</b>	<b>Specific Gravity</b>
Light Crude Oil	>31.1°	<870 Kg/m <sup>3</sup>
Medium Crude Oil	22.3° - 31.1°	870-920 Kg/m <sup>3</sup>
Heavy Crude Oil	10° - 22.3°	920-1000 Kg/ m <sup>3</sup>
Extra Heavy Crude Oil	<10°	>1000 Kg/ m <sup>3</sup>

Heavy oil accounts for a sizable portion of the globe's undiscovered hydrocarbon reserves. High viscosity and density at air circumstances make recovery harder in comparison to lighter crudes, resulting in low recovery factors. Hence, heavy crude oil has an important potential but has not been totally developed yet, which still exploration is implementing in various areas as heavy oil

could be relied to be an enormous supporter of the energy of the globe's requests in the future. Nevertheless, the innovative expenses per barrel are presently a lot higher than for regular lighter crude oil.

### 2.1.1 Heavy oil characteristics

Heavy oil is characterized with very high viscosity compared to lighter crude oil; therefore, it is considered as an unconventional oil reservoir. The API gravity is very low between  $10^{\circ}$  to  $20^{\circ}$  with a consideration of oil with  $10^{\circ}$  API as extra heavy oil as shown in Figure 2.1 At reservoir conditions, very heavy oil or natural bitumen is largely immobile.

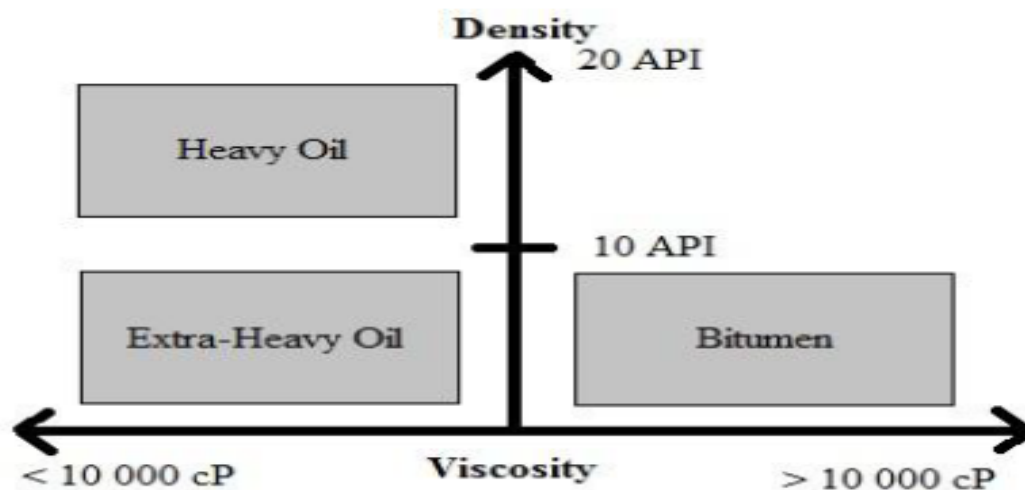


**Figure 2.1:** Heavy oil classification (Saniere et al, 2004)

Thermal method is the main known method for extracting heavy oil due to the effect of temperature on viscosity which with increasing the temperature, the viscosity is reduced as shown in Figure 2.2. from the figure, it's clear that the Bitumen is under oil density of 10 API, and extreme high viscosity. The extra heavy oil is also under 10 API oil density while the heavy oil is between 20 API to 10 API.

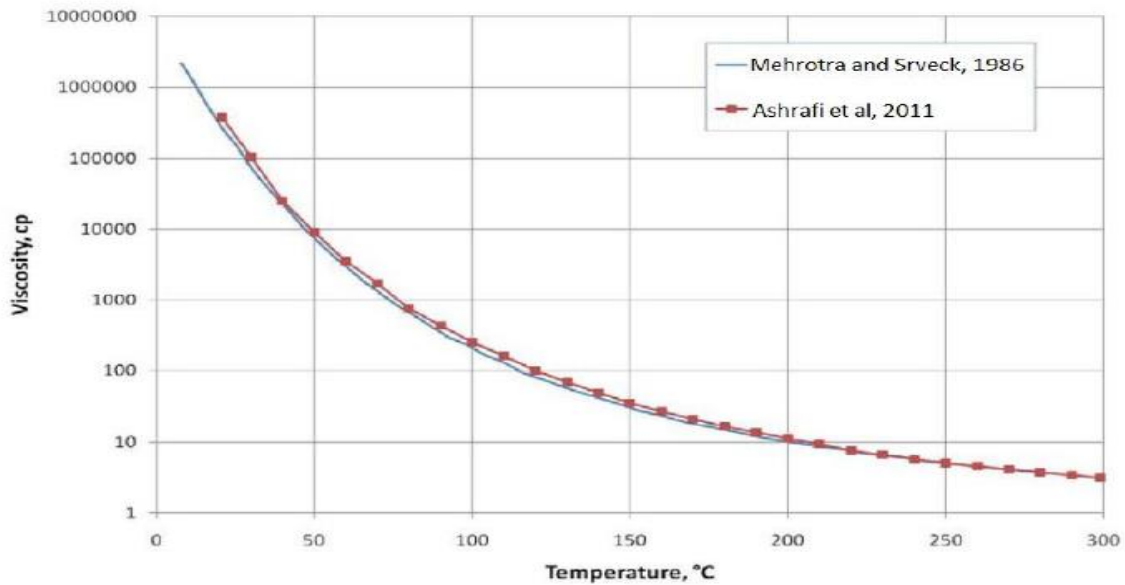


**Figure 2.2:** Athabasca Bitumen's viscosity-temperature relationship (Ashrafi et. al 2011)

### 2.1.2 Heavy oil extraction methods

Recovery from heavy oil is a basic procedure which involves difficulties and multifaceted nature because of the qualities of the crude oil. According to Speight (2013), the problems arise mostly as a result of the heavier viscosity and explicit gravity, as well as the presence of various components within the heavy oil, such as higher nitrogen, sulfur, and asphaltene. In any case, with all the troubles and difficulties, it is important to note that heavy oil is important in satisfying future vitality needs (Speight, 2013; Meyer, 1997). There are two main methods to recover heavy oil reservoirs, thermal and nonthermal methods. Table 2.2 illustrates the methods used to extract heavy oil.

**Table 2.2:** Types of thermal and non-thermal heavy oil recovery methods

<b>Thermal Recovery Methods</b>	<b>Nonthermal Recovery Methods</b>
Cyclic Steam Stimulation/injection (CSS)	Waterflooding
Steam injection	Polymer injection
In-Situ Combustion	Vapor-Assisted Petroleum Extraction (VAPEX)
Steam Assisted Gravity Drainage (SAGD)	Alkali-Surfactant Injection
Electromagnetic Heating	CO <sub>2</sub> Injection
Steam Over Solvent Injection	Cold Heavy Oil Production With Sand (CHOPS)
Nanocatalyst	Foamy Heavy Oil Production

## 2.2 Naturally Fractured Reservoirs

Fractures are the result of landforms such as bending, faulting, and the release of overburden pressure. Naturally fractured reservoirs (NFR) contain a large amount of residual conventional hydrocarbons and are the most profitable oilfield on the planet (Aguilera, 1998; Bratton et al., 2006; Lemonnier and Bourbiaux, 2010). Fractured carbonate reservoirs include a substantial portion of these reservoirs, accounting for sixty percent of the globe's oil and forty percent of the globe's gas. Fractures frequently impact production behavior in naturally fractured reservoirs. Fractures have a significant impact on the performance of the reservoir and the total oil recovery from primary recovery to tertiary oil recovery (enhanced oil) recovery stages. The existence of cracks in a reservoir has a significant impact on fluid flow, resulting in a decrease in oil and gas recovery in conventional reservoirs.

Aside from maximizing the oil recovery, fractures can likewise hinder hydrocarbon production and extraction by serving as baffles and flow barriers (Bourbiaux, 2010; Spence et al., 2014). Fractures provide a path that ease the fluid flow within the formation, which in case water is injected, the water flows through the high permeable fractured layers and results in excessive water production. This will have a very negative impact on oil recovery and it also results in

additional massive treatment costs. Therefore, it's very important to consider the fracture effect on overall oil recovery.

While the DP model is useful for showing and analyzing stream forms in NFR, it has certain limitations (Warren and Root, 1963; Gringarten, 1984, 1987; Moench, 1984; Chen, 1989). To recreate flow conduct in fractured reservoirs, Barenblatt et al. (1960) proposed this model, while Warren & Root (1963) developed it to show pressure transient behavior in well-tests from NFR. To simulate outcrop cracks, a reservoir model consists of cells with gaps to represent the fractures (Figure 2.3).

The following are the inclusive suppositions of the dual-porosity (DP) pattern:

1. The DP model comprises two areas with different porosities, where grids are showing fractures inside the formation.
2. The matrix forms the formation material with insignificant permeability however critical pore volume fraction that is giving the vital porosity of the reservoir framework.
3. Fractures deliver extra permeability if fractures are interconnected to each other with respect to fluid flow from the formation which has a low porosity.
4. Matrix and fracture flow is possible, but not between matrix squares or from the matrix straight into the well.
5. Matrix and fracture systems are considered to be continuous in the DP model.

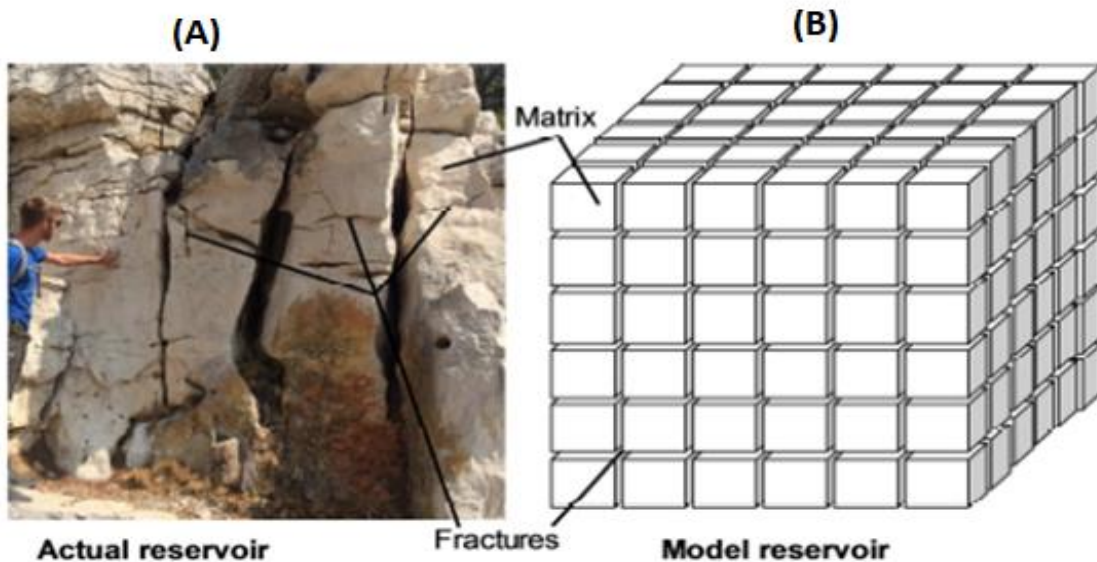


**Figure 2.3:** Two-porosity medium in its idealized form. (a) Well-test image of a fractured and jointed carbonate reservoir (Barremian, Lower Cretaceous, Cassis, France), and (b) reservoir simulation model (Warren and Root, 1963)

### 2.3 EOR for Heavy Oil Extraction

Two main categories of EOR methods for heavy oil exist: increasing sweep efficiency and increasing displacement efficacy (Hite and Bondor, 2004). This is the difference between microscopic and macroscale. Macrorecovery is a measure of how well dislodged liquid interacts with reservoir oil-bearing areas. When the dislodging liquid interacts with the oil, microscopic recovery refers to the degree to which the leftover oil is reassembled by the liquid.

Oil viscosity can be controlled via thermal oil recovery techniques, such as cyclic and flooding steam, as well as high temperature water injection (Zerafat et al., 2011), or through chemical treatments, such as polymer flooding (Taber et al., 1997b). As the dislodging liquid interacts with the oil-bearing reservoir portions, macroscopic sweep efficiency is determined.

Productivity is impacted by heterogeneity in a reservoir's fluid stream limit (Petrowiki.org, 2014). It has a high capability of movement. Viscous-fingering occurs when the displaced fluid has a considerably greater mobility than the displaced fluid. On the field, the physical arrangement of injectors and producers has a significant impact on production performance. The rock lattice is also an important component in the design (Terry, 2001). Other important elements are reservoir thickness, porousness, production rate, and liquid contact.

### **2.3.1 Thermal flooding**

Heavy oil production has been dominated by thermal flooding for over 40 years (Taber et al., 1997b). To remove excess oil, thermal methods use a variety of components, but the basic concept is that crude oil viscosity decreases with increasing temperature. In the case of very heavy crude oil (10-20 API), a temperature increase of 300-400 K (27-127 oC) will result in a viscosity that is among the streaming extent (Lake, 2010). The viscosity decrease is smaller for lighter crudes.

### **2.3.2 Hot water flooding**

Heavy oil reservoirs can be improved by lowering heavy oil viscosity and increasing mobility ratio through the use of hot water flooding. This approach involves injecting hot water into the reservoir, which warms it and reduces the amount of residual oil (Alajmi et al., 2009; Alvarez and Han, 2013). To maintain or raise pressure, hot water injection increases the reservoir's thermal expansion rate (Zhao, et al., 2013). When compared to steam flooding, hot-water flooding is more efficient and economical.

During the procedure of hot water flooding, a critical key is the manner by which to productively lessen viscosity of heavy oil by warming heavy oil reservoir to arrive at high temperature with the goal that heavy oil can flow into production wellbore without much of a stretch (Venkatesan, et al., 1986).

Temperature field dispersion of reservoir utilizing high temperature water flooding can reflect the warm impact of heated water on the reservoir which likewise determines the temperature of oil zones. Additionally, it tends to be utilized to comprehend flow condition of the reservoir fluids and examine the temperature change of the reservoir, which is additionally the significant parameter to foresee properties of the reservoir.

### **2.3.3 Gas flooding**

Gas flooding is one of the ways that may be used to enhance the miscibility between gas and reservoir oil. Both macroscopic and microscopic recovery are improved by gas flooding. Miscibility can take two forms. As soon as the injected liquid is mixed with the oil, it becomes miscible on first touch. As the injected liquid travels through the reservoir, it comes into contact with miscible materials on many occasions, and miscible situations are generated in position by changing the composition of the injected liquid or hydrocarbon (Arshad et al., 2009).

Full miscibility results in the elimination of the interfacial tension between the rock and fluid, resulting in the capillary number being infinite. This causes a tiny displacement to increase (Terry, 2001). Swelling and oil viscosity reduction are further aided by secondary recovery system gas flooding. The relative permeability to oil is improved by swelling (Arshad et al., 2009). Macroscopic healing is maximized by using secondary recovery methods. It is a known fact that viscous fingering can occur due to the difference in density between injected fluid and reservoir fluid.

The followings are the main functions of gas flooding:

1. Disintegrating the crude oil's lighter components.
2. The creation of miscibility when pressure is high enough.
3. It is also possible to improve gravity drainage in dip reservoirs.
4. Swelling increases, the amount of oil.
5. The oil viscosity is decreasing.
6. Displacement of incompressible gas
7. Gas lift has an impact on high water-cut wells if gas gets through (Taber et al, 1997a).

### 2.3.4 WAG

Water-alternating-gas (WAG) injection is the standard method for improving the recovery factor because to its high capability for mobilizing residual oil and regulating gas mobility. Gas flooding and water flooding are utilized to replace water in the recovery process. Reservoir heterogeneity, rock type, and liquid characteristics are the most important factors to consider while injecting WAG (Ebadati et al., 2018). Based on a study made by Amir Hossein (Ebadati et al., 2018) the study conducted in their paper aims to investigate five recovery mechanisms including water-flooding, WAG injection and hot WAG injection and their impact on recovery factor of an Iranian oil field. One of Iran's reservoirs has been subjected to water floods for a long time, and the recovery factor is 42 percent. A substantial influence on recovery factor was found with both water alternating gas injection and high temperature water alternating gas injection. They found that both WAG injection and hot WAG injection provided the best oil recovery, as shown in Figure 2.4. This demonstrates the effectiveness of the WAG approach in recovering more oil than any other method.

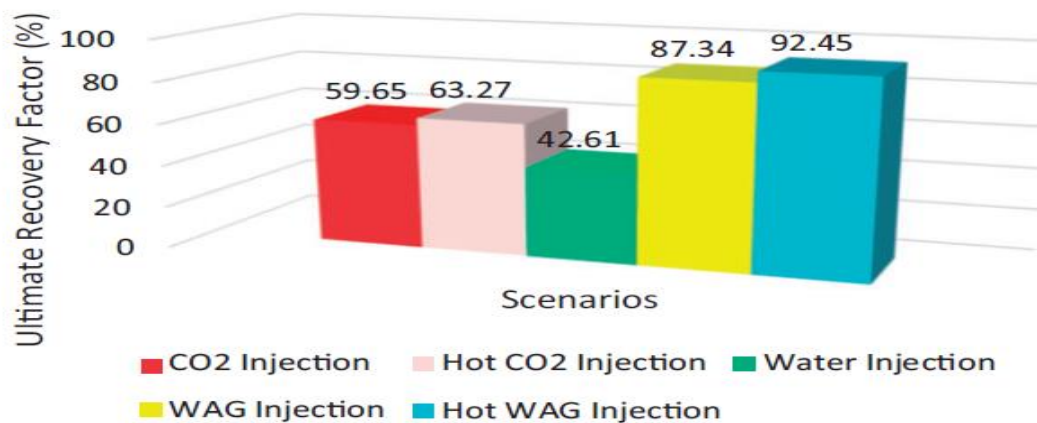


**Figure 2.4:** Recovery factor of different recovery mechanisms

Additionally, choice of this injection liquid is completely subject to the accessibility of these liquids, value (economy), and reservoir attributes and that is the reason that ongoing innovations and examinations are progressively focused on progress of past procedures and direct ideal approaches to accomplish the harmony between effective parameters, for example, Costs and time (Davaranah and Mirshekari, 2018; Davaranah et al., 2018; Kamali and Cinar, 2014;

Pinerez et al., 2016). As a result of reservoir condition and liquid type, recovery techniques may be classified into the following categories: Steam cycle injection, steam cycle flooding and enriched gas injection are all terms used to describe the process of injecting a gas (Davarpناه, 2018; Lee et al., 2018; Lei et al., 2016; Person et al., 2017; Sorbie, 2013; Xuezhong et al., 2016).

### 2.3.5 WAG application in Gyda oil field

Gyda is a well-established oil field in the North Sea. In Gyda, falling oil recovery and growing water-cuts are causing problems for the company. Researchers looked at the Gyda field's potential for further oil and gas production. According to the simulation result of WAG cycle times over a half-year period, there is an increase in efficiency when injector and producer are far apart. When the producer and injector are close and have great communication, shorter WAG cycles are preferable. A good oil recovery does not require a long WAG cycle. An improvement in recovery of 1.4 percent may be achieved with WAG injection on Gyda using dry injection gas.

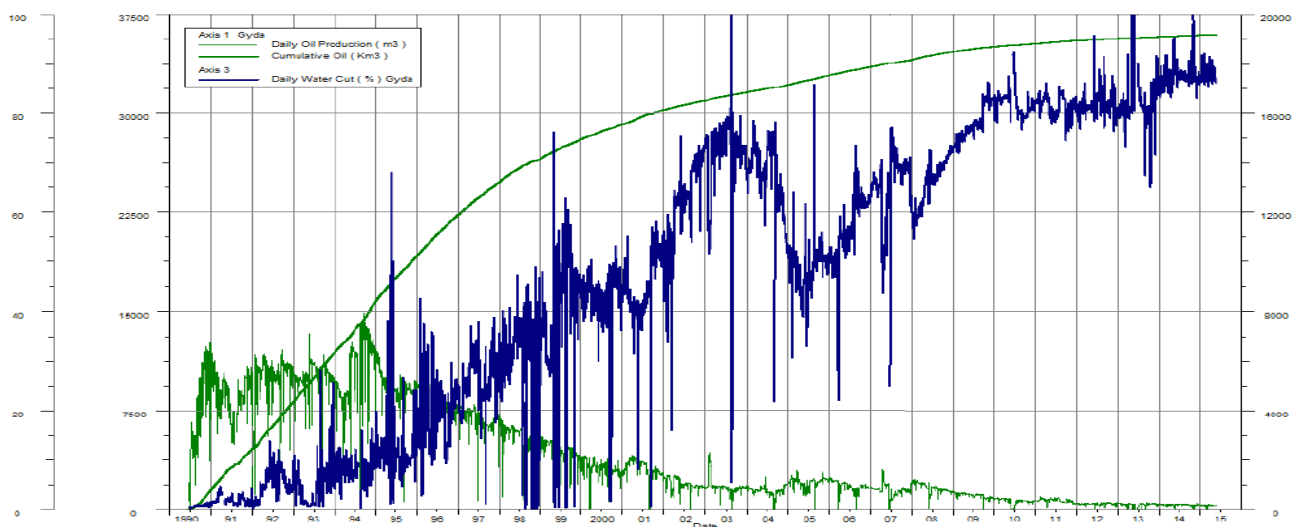


**Figure 2.5:** Gyda field historical daily oil and cumulative oil productions, and water cut (Mari. A, 2005)

### **2.3.6 Hot WAG**

Gas injection is the second most improved oil recovery method that has been used after thermal recovery techniques. In order to ensure better contact between the injected gas with reservoir fluids, water is injected with gas in a cyclic case known as a water-alternating gas (WAG) injection. A study made by Dorostkar (2009) to use hot immiscible water-alternating gas injection on a fractured sand pack.

A mix of heat, solvent, and flooding techniques is used in the hot IWAG approach. To heat CO<sub>2</sub>, hot water and superheated CO<sub>2</sub> is recommended. CO<sub>2</sub> and warm water injections into the sand packs. Testing was done in the lab on fractured and regular sand packs to see which one performed better. Injection of water and CO<sub>2</sub> was carried out at a slow and steady speed, using slugs of 0.05 PV in diameter.

Using similar circumstances, boiling water and hot CO<sub>2</sub> were injected again, and enhanced oil recovery from each sand pack was determined. Researchers found that injecting hot WAG into conventional and fractured sand packs might significantly increase the amount of oil recovered.

## **2.4 Miscible EOR**

Supercritical CO<sub>2</sub> is used in miscible EOR to displace oil from a depleted oil reserve. Adding CO<sub>2</sub> to the mix increases the recovery of crude oil by dissolving, expanding, and decreasing its viscosity. 1–2\$/Mscf is the cost of injecting CO<sub>2</sub> (Manrique et al., 2007). In the United States, the majority of CO<sub>2</sub> flooding occurs. Miscible oil replacement in high-depth reservoirs is accomplished using hydrocarbon gases (natural gas and flue gas) and compressed nitrogen. There is a possibility that these displacements are merely "pressure maintenance" in the reservoir (Plasynski et al., 2009; Farajzadeh et al., 2009).

### **2.4.1 Fundamentals and mechanism of miscible CO<sub>2</sub> flooding**

This may be achieved by CO<sub>2</sub> flooding in low permeability and light oil reservoirs (Kulkarni, 2003). CO<sub>2</sub> storage also decreases ambient gas emissions. At first contact or after many contacts, gas miscible flooding improves volumetric sweeping and displacement efficiency,

respectively (Claridge, 1972; Mathiassen, 2003). CO<sub>2</sub> flooding of poor permeability and light oil reservoirs can achieve this (Kulkarni, 2003). As a bonus, CO<sub>2</sub> storage reduces ambient gas emissions as well. Gas miscible flooding enhances volumetric sweeping and displacement efficiency, respectively, at initial contact and after numerous contacts (Claridge, 1972; Mathiassen, 2003).

Activating the oil's light component, decreasing its density, vaporizing it and merging it with other oil, and reducing interfacial tension are all necessary for miscible CO<sub>2</sub> flooding to occur (Thomas, 2001). CO<sub>2</sub> injected into crude oil disintegrates completely at the basic miscibility pressure (MMP). As determined by thin cylinder tests or numerical relationships, the CO<sub>2</sub> advancement pressure is indicated as the pressure at which over eighty percent of the oil in place set up (OOIP) is produced (Holm and Josendal, 1974). Oil recovery of at least 90 percent is employed as a rule-of-thumb for determining the minimum miscibility pressure on an industrial scale, however (MMP).

By vaporizing intermediate and high molecular weight hydrocarbons from reservoir oil into CO<sub>2</sub> (vaporized gas-drive method), and then dissolving a part of the injected CO<sub>2</sub> into oil (condensed gas-drive process), miscibility between CO<sub>2</sub> and reservoir oil may be obtained (Merchant, 2015). There is no interface formed between the oil and CO<sub>2</sub> as a result of this mass exchange, and a change zone is formed that is miscible with both oil and CO<sub>2</sub> (Jarrell, et al., 2002). In addition to initial contact, CO<sub>2</sub> miscible flooding also comprises disintegrating gas drive and collecting gas drive

When miscible solvents are mixed with stored oil to the fullest degree and the mixture remains in a single stage, this is called first contact the oil can be recovered more effectively through single or multiple interactions (Bonder, 1992).

By infusing lean gases or CO<sub>2</sub> into the oil, the disintegrating gas-drive measure (high-pressure gas drive) achieves dynamic miscibility (Stalkup, 1983). It achieves dynamic miscibility by in situ moving middle of the road subatomic pressure hydrocarbons from rich dissolvable reservoir oil to lean reservoir oil using a buildup measure (consolidating gas drive) (Holm and Josendal, 1987).

### **2.4.3 Solubility of CO<sub>2</sub> in Oil**

CO<sub>2</sub> miscibility in oil is mostly determined by certain parameters, including injection pressure, temperature, and oil gravity. As pressure and API gravity increase, CO<sub>2</sub> miscibility in raw petroleum decreases. Oil production and bubble pressure, on the other hand, become more stronger at temperatures that are below the CO<sub>2</sub> basic temperature. Super-basic CO<sub>2</sub> is more successful than sub-basic CO<sub>2</sub> for removing hydrocarbons from oil (Farajzadeh, et al., 2009). In a typical mathematical approach, Emera and Sarma have developed extremely precise relationships between CO<sub>2</sub> solubility in oil and oil expansion and thickness, and their results have been validated using experimental data that has been widely disseminated.

Oil viscosities up to 12,000 cp and pressures up to 34.5 MPa may be calculated using these calculations. Oil temperatures up to 140°C can also be calculated using the same principles. Al Jarba and Al Anazi have also checked this for free. When the temperature of CO<sub>2</sub> is higher than the basic temperature (under any pressure condition), two links have been made for its solubility in oil (under pressures under CO<sub>2</sub> liquefaction pressure).

### **2.5 Immiscible CO<sub>2</sub> Flooding EOR**

Immiscible flooding requires a fluid drive and a reduction in oil viscosity. When the reservoir pressure is below the minimum miscible pressure (MMP) or the reservoir oil composition is unfavorable, CO<sub>2</sub> and oil will not form a single phase (i.e., immiscible). This causes oil swelling and viscosity decrease as well as solution gas formation. This in turn improves the sweeping efficiency and facilitates further oil recovery. Pressure and temperature affect CO<sub>2</sub> miscibility via crude oil.

The cycle of oil growth and decline overwhelms the CO<sub>2</sub>-EOR approach. The oil swells and its viscosity decrease as CO<sub>2</sub> is dissolved in it, thus injecting CO<sub>2</sub> into the reservoir should result in oil production. For low pressure applications, however, CO<sub>2</sub> dissolvability in oil is the most important factor for CO<sub>2</sub>-EOR feasibility. Below are detailed illustrations of CO<sub>2</sub> dissolvability in oil and the corresponding oil expansion and consistency.

## **2.6 Screening Rules for CO<sub>2</sub> Flooding**

Among the criteria used to screen for miscible CO<sub>2</sub> flooding are the minimum miscibility pressure (MMP), residual oil saturation, pay-zone thickness, crude petroleum gravity, and density (Mathiassen, 2003). The National Petroleum Council summarizes the best reservoir requirements for CO<sub>2</sub> miscible flooding in beginning screening. This would depend on the size of the reservoir and the hydrocarbon recovery potential.

When the temperature of the reservoir is higher than 120°F, extra pressure of 200 to 500 psi is needed to reach miscibility condition, for example. 0.6–0.8 g/cc is the thickness of CO<sub>2</sub> depending on the infusion depth, which influences the surrounding temperature and pressure (Sheppard, 2007). A profundity of more than 800 meters is required for the CO<sub>2</sub> injection (either fluid or supercritical). When it comes to CO<sub>2</sub> storage, reservoirs with a high salinity level are more vulnerable.

## CHAPTER 3

### METHODOLOGY

This study is numerical simulation modelling using CMG-STAR5 software, which is a thermal compositional reservoir simulator to create the hypothetical reservoir simulation model by inputting the required parameters. This chapter starts with the introduction of the reservoir studied in this project. Later on, completion of the project is discussed.

#### 3.1 Reservoir Description

A Cartesian model of 40 x 40 x 10 was created in this project using the CMG-STAR5., which is a thermal compositional reservoir simulator, the 40 x 40 x 10 grid dimensions and properties for matrix and fracture grids are given in Table 3.1. Initial reservoir pressure is 2100 psi. Initial reservoir temperature is 139 °F. The reservoir is located at 4500 ft depth. Additionally, an infinite water aquifer is assumed to exist in this study, and was located at the bottom layer of the formation connected to the fractures within the reservoir model. Water oil contact WOC is located at 4600 ft depth. Generated compositional PVT data required for CMG-STAR5 software. Table 3.1 shows oil viscosity, oil density °API, gas oil ratio GOR, gas gravity, reservoir temperature, water density, reservoir pressure and water salinity. The reservoir model consists of 16,000 cells, each cell has a thickness of 10 ft.

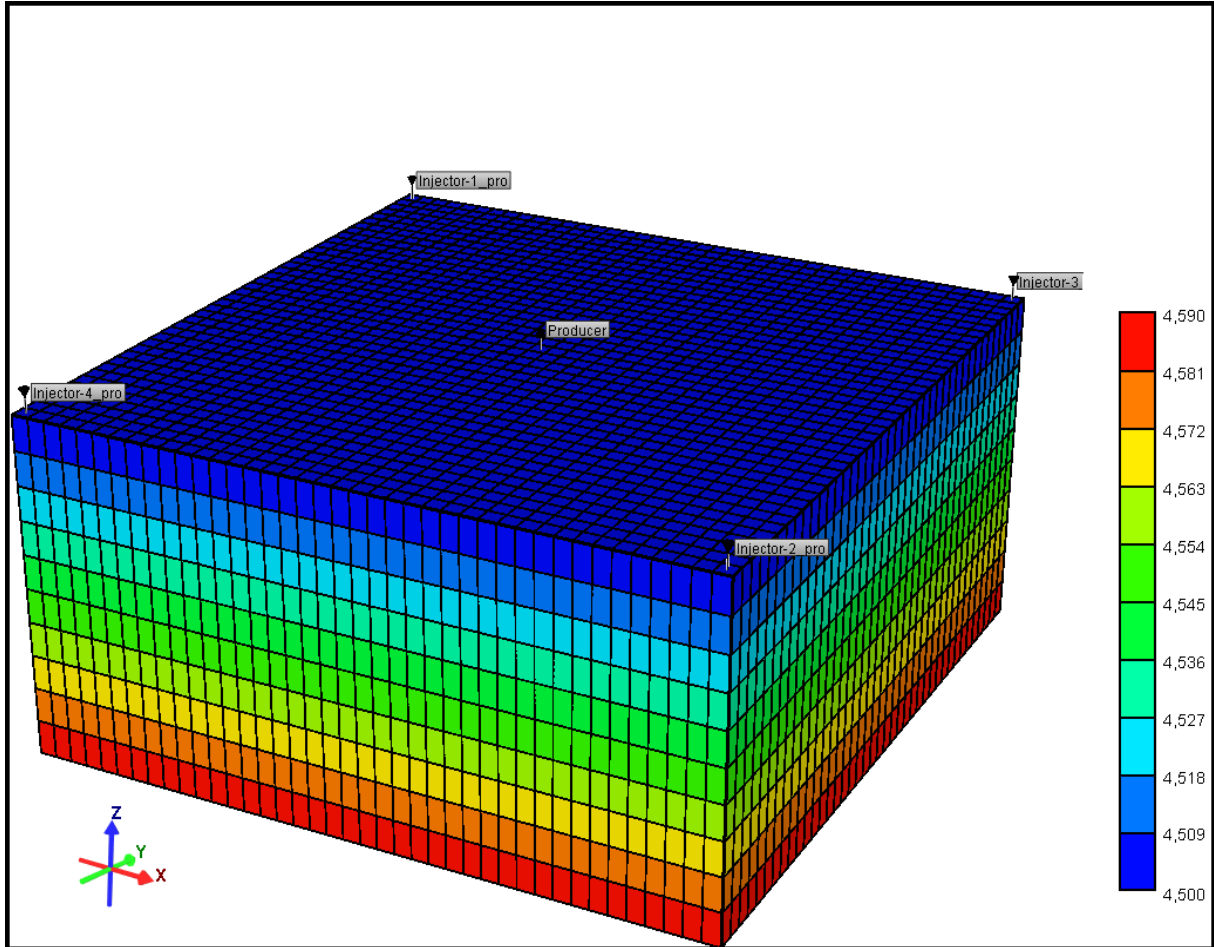
#### 3.2 Reservoir Simulation Model

CMG-STAR5 2015 used to investigate the impact of hot-WAG, hot water flooding, and CO<sub>2</sub> flooding methods on reservoir performance. The created reservoir is an imaginary model. The reservoir contains heavy oil, water, gas, and CO<sub>2</sub>. Additionally, the reservoir contains an infinite aquifer at the bottom of the reservoir and the heavy oil density is 17 °API. Five wells were used, four wells as injectors and one well as producer. Figure 3.1 shows the 3D reservoir model in terms of reservoir depth and well locations in the model.

**Table 3.1:** Input parameters used in this study

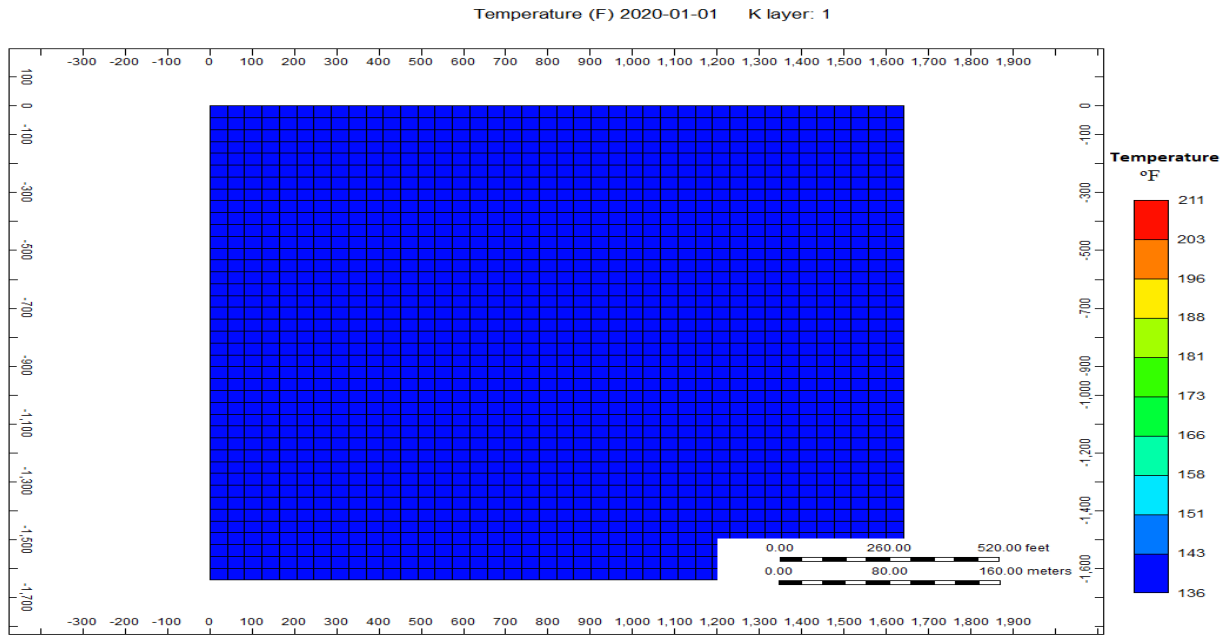
Parameters	Value
Matrix Permeability (Kx,Ky) (mD)	30-35
Matrix Permeability (Kz) (mD)	0.3-0.35
Fracture Permeability (Kx,Ky) (mD)	1120-2100
Fracture Permeability (Kz) (mD)	150
Matrix Porosity $\emptyset$ (Fraction)	0.12-0.14
Fracture Porosity $\emptyset$ (Fraction)	0.002-0.004
Fracture Spacing (Ft)	0.001
Number of layers	10
Reservoir Pressure (Psi)	2100
Reservoir Temperature ( $^{\circ}$ F)	139
Oil Density ( $^{\circ}$ API)	17
Water Density (lb/ft <sup>3</sup> )	64.9423
WOC Depth (Ft)	4600
Pay zone thickness (ft)	100
GOR (ft <sup>3</sup> /bbl)	350
Oil viscosity (Cp) @104 $^{\circ}$ F	412
Water salinity in ppm	35000
Gas gravity (Air = 1)	0.842
Oil Saturation	0.8
Water Saturation	0.2

Figure 3.1 shows the oil field-reservoir simulation model which illustrates the top of the formation layers. Each colour represents a different layer and depth within four injector wells were spotted in corners and one producer well in the centre, the wells were perforated from layer three to layer eight in the model.



**Figure 3.1:** 3D Reservoir Model

Hot fluid injection (hot WAG injection, hot water flooding, and CO<sub>2</sub> flooding) has been used to reduce heavy oil viscosity and upgrade it to maximize oil production. Figure 3.2 shows the 2D reservoir model before and after EOR was implemented. Figure 3.2a shows original reservoir temperature distribution 139 °F in the model before injecting hot water-alternating gas. Figure 3.2b shows the reservoir model after 1 year and 6 years of injection respectively. Based on Figure 3.2, the reservoir temperature is distributed effectively after EOR implementation which results in upgrading heavy oil and maximize oil recovery.



**Figure 3.2a:** 2D Original reservoir temperature distribution 139 °F in the Model

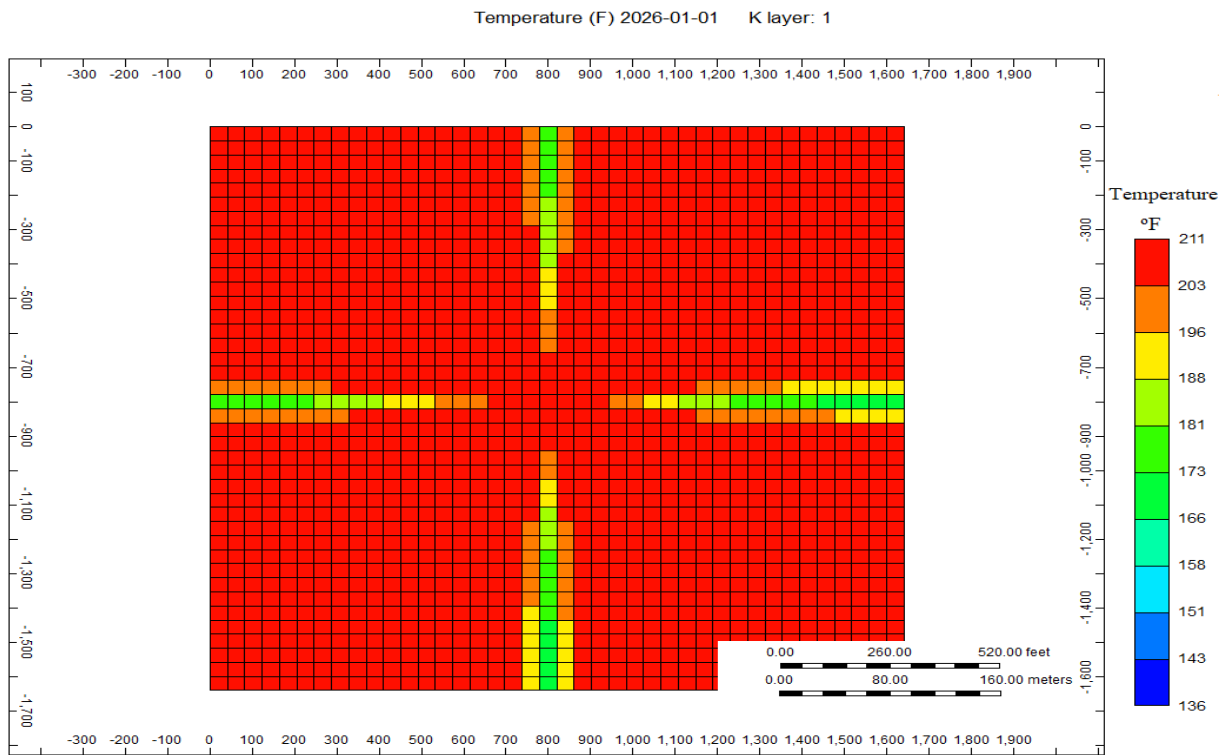


**Figure 3.2b:** 2D Reservoir temperature distribution after injection implementation

### 3.3 Simulation Process

The following points refers to all the steps used to complete simulation work:

1. Build a dual-porosity reservoir model in CMG-STARS 2015 and assume an infinite water aquifer exists and connected to fractures within the bottom layer.
2. Input all the required parameters and sections within CMG-STARS and run the model.
3. Four injector and one producer wells are used in the model.
4. Forecasting simulation start date 01 January 2020 and ended 01 January 2026.
5. Apply hot-water flooding and analyse the result.
6. Repeat Step 5 using CO<sub>2</sub> flooding.
7. Repeat Steps 5 and 6 using hot WAG injection instead.
8. Compare the results and evaluate them.
9. Analyse the results and select the optimum scenario for each case.

### 3.4 Reservoir Fluid Characteristics

Generated relative permeability in CMG-Builder by correlation is used in simulation. Relative permeability is a measure of the permeability effectiveness of a phase to another phase (Figure 3.3). Figure 3.3 shows that the water relative permeability starts to increase when water saturation reaches  $S_{wi}$  at 0.31 water saturation as denoted in red colour and the oil relative permeability reduces over time with increasing water saturation as represented in blue colour. Other reservoir properties are mentioned in the appendix section. Moreover, Figure 3.4 shows the gas relative permeability curve versus liquid saturation as denoted in red colour. Based on the plot, the gas relative permeability reduces over time until it reaches zero at liquid saturation of 83%. In contrast, the oil-gas relative permeability increases as gas relative permeability reduces over time as denoted in blue colour. The oil to gas relative permeability increases from 0 when liquid saturation is 0%. To 0.3 oil to gas relative permeability when liquid saturation is at maximum rate of 100%.

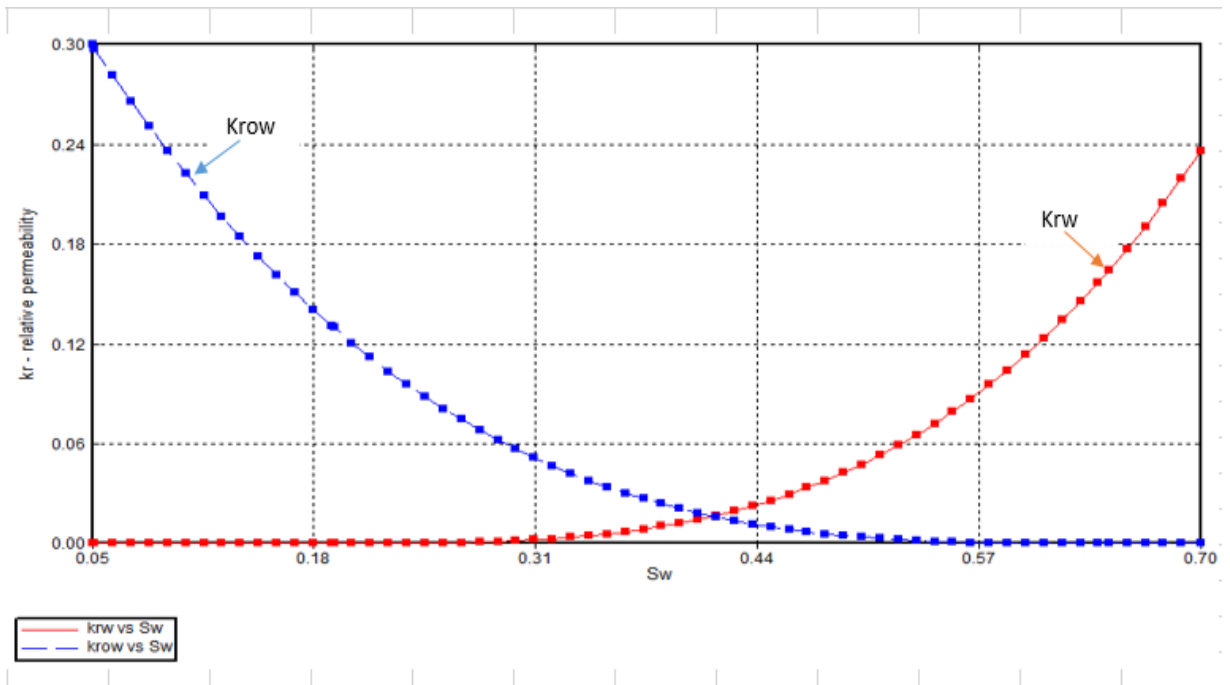


**Figure 3.3:** Relative permeability curve for studied simulation model

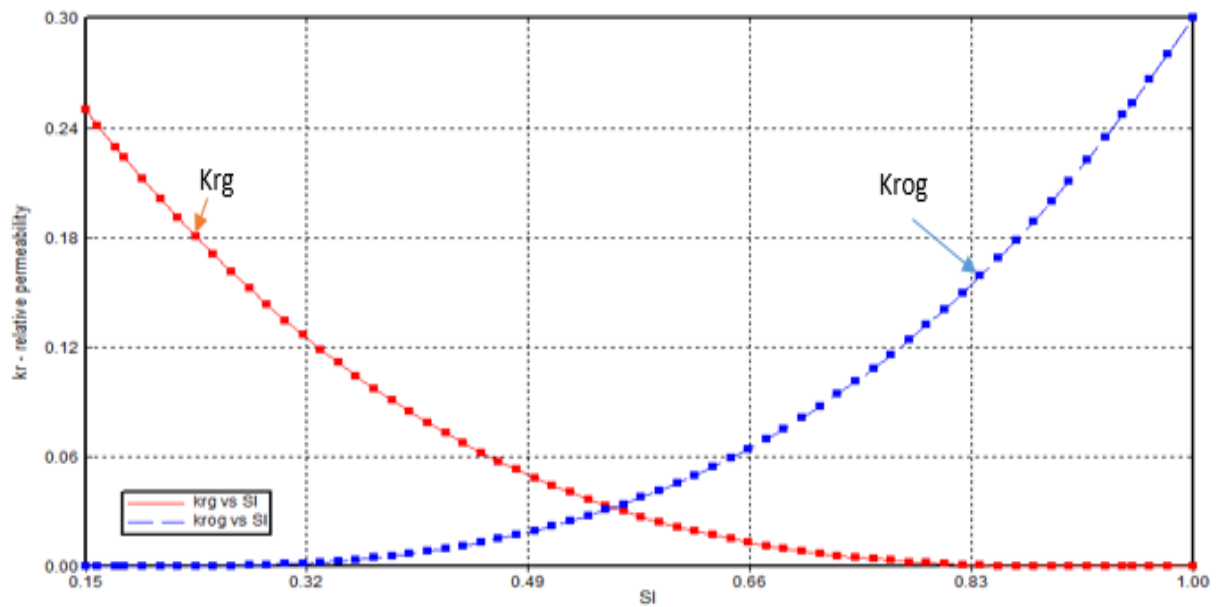


**Figure 3.4:** Gas relative permeability curve for studied simulation model

Three-phase fluid for the studied reservoir is shown in Figure 3.5. Based on the graph, the oil phase saturation has reached about 0.8 as shown in the plot and the water saturation is over 0.2. Figure 3.6 shows the oil density versus pressure for the studied field. Based on figure 3.6, the oil density is 57.6 lb/ft<sup>3</sup>, while it reduces to 53.2 lb/ft<sup>3</sup> at pressure of 2300 psi.

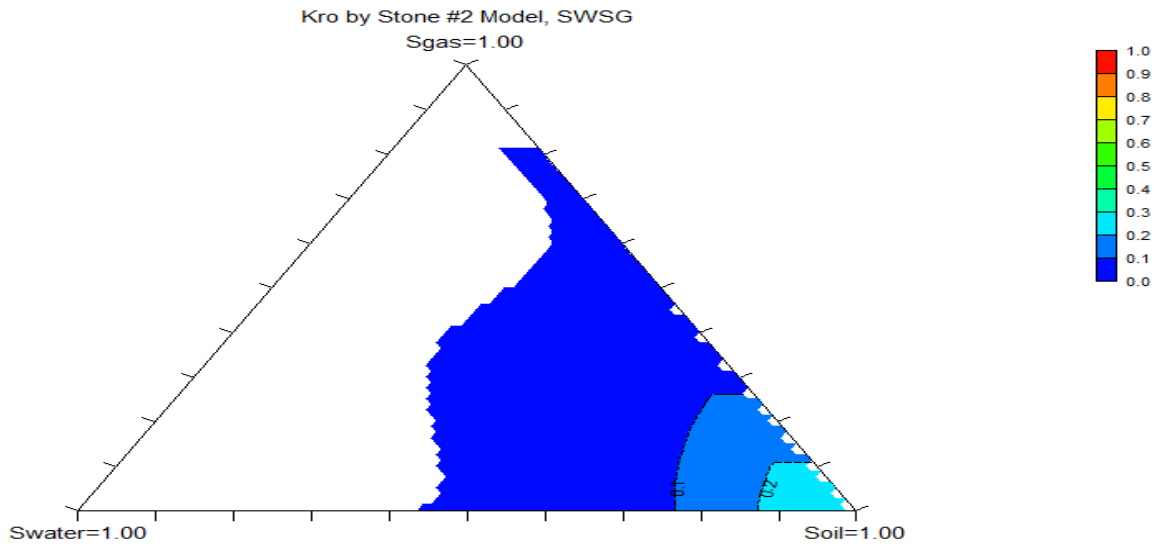


**Figure 3.5:** Three-phase fluid for studied simulation model

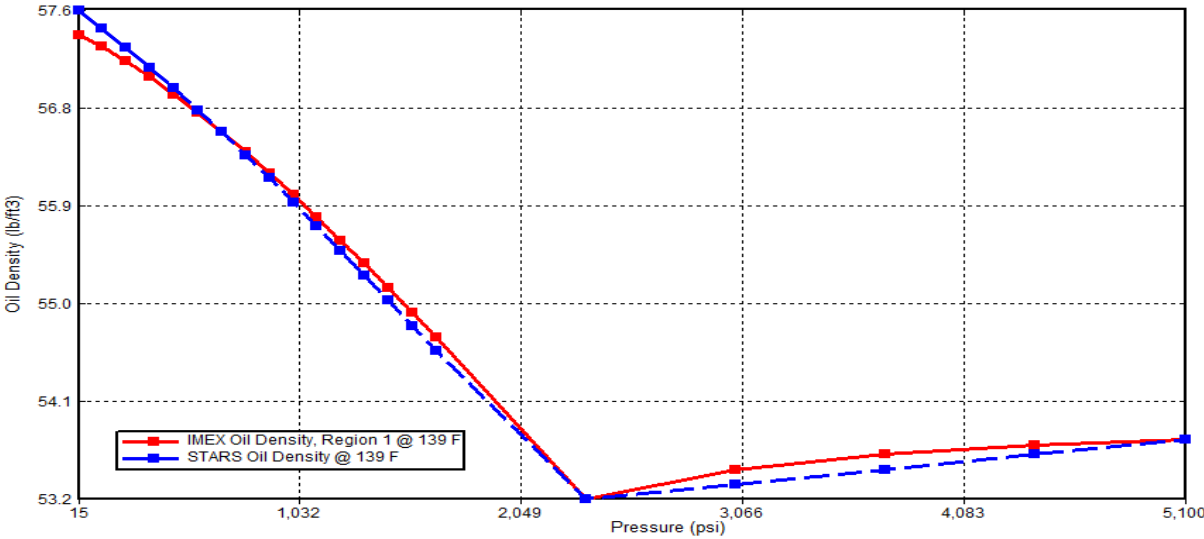


**Figure 3.6:** Oil density versus Pressure

Oil viscosity versus temperature is shown in Figure 3.7. Based on the plot, at temperature of 104 °F, the oil viscosity is at its maximum of about 700 cP. However, the oil viscosity is reduced when the temperature is increasing as it reaches to 90 cP at a temperature of 176 °F.

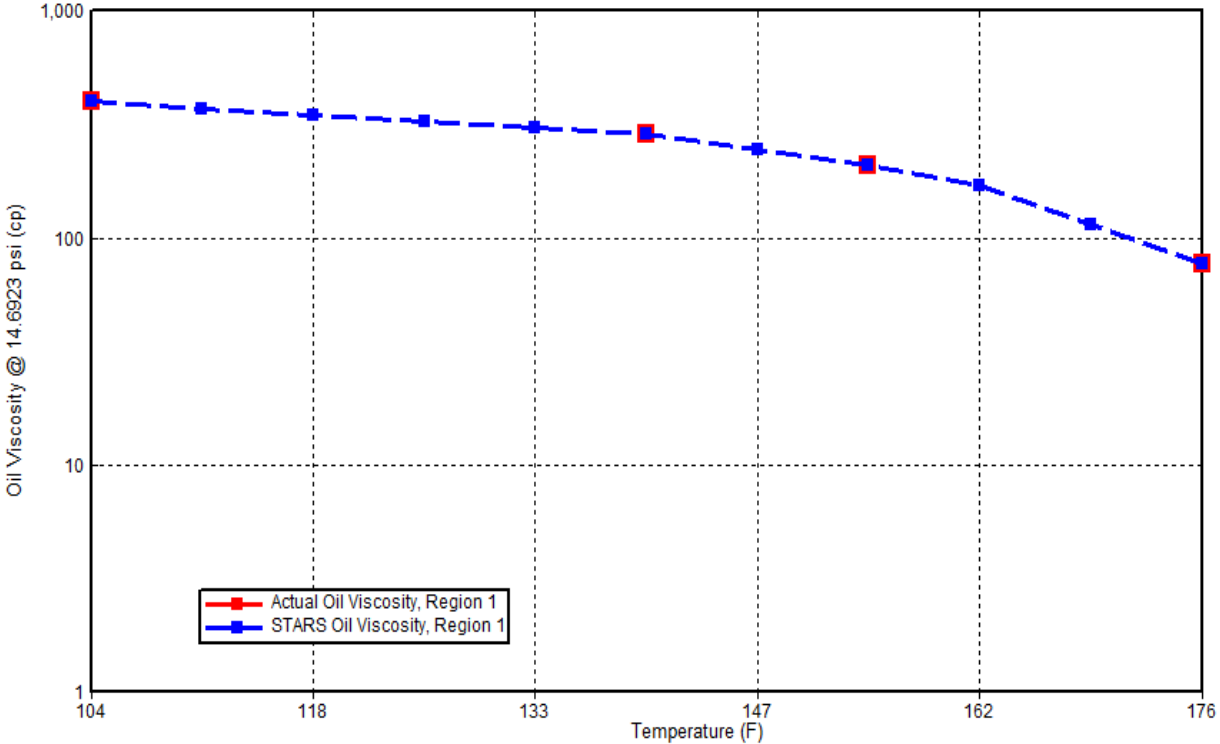


**Figure 3.7:** Oil viscosity versus temperature

Figure 3.8 shows the GOR versus pressure for the studied model. Based on the plot, the GOR is 0 at pressure of 15 psi and then increased when the pressure is increased as a GOR of 378 ft<sup>3</sup>/bbl at a pressure of 2300 psi. The result shows that the greater the pressure, the greater the gas oil ratio till it reaches a point where it no longer increases.

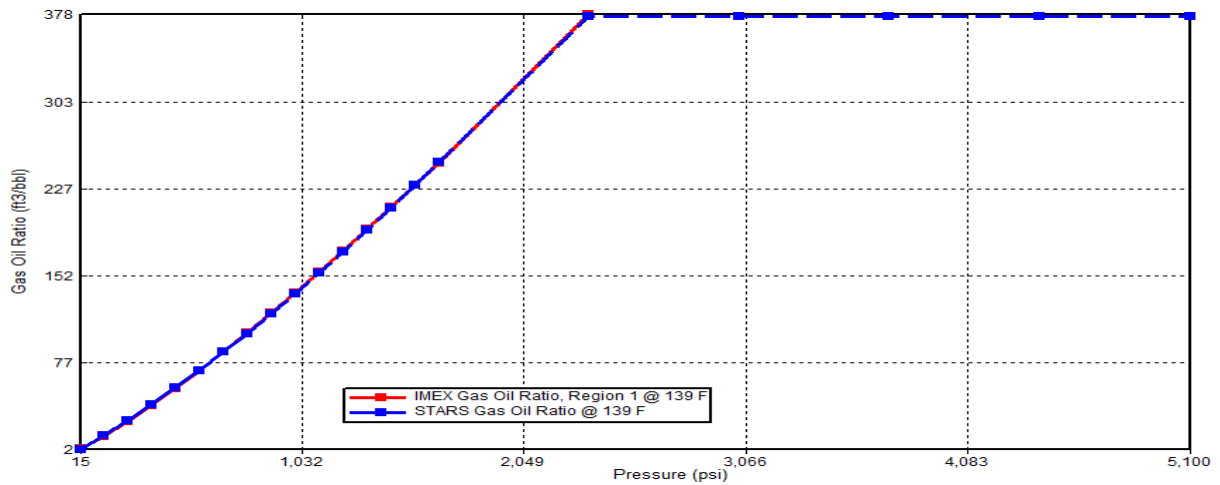


**Figure 3.8:** Gas oil ratio versus Pressure

### 3.5. Well Properties

In this study, one production and four injection wells were used. The producer is producing to maximum production rate of 15000 bpd, while the injection wells were designed to inject either hot water or CO<sub>2</sub>. In the injection wells three different bottom hole pressure (BHP) scenarios of 2400, 2700, 3000 psi were tested.

**Table 3.2:** Well Properties

Parameters	Value
Well Radius (ft)	0.28
Perforation Interval (layer)	Layer number (3 to 8)
Control Mode	Oil production rate
Production Rate (bpd)	15000
Injector control mode	Pressure
Injection pressure (psi)	2400, 2700, 3000

### 3.6 Case Studies

Three main cases were developed in this project.

1. Hot-WAG injection
2. CO<sub>2</sub> flooding
3. Hot-water flooding

Each case involved different scenarios, including different injection pressure, and different injection temperature.

#### 3.6.1 Hot WAG injection

Hot WAG injections effect on heavy oil recovery in a fractured carbonate reservoir was investigated. A total of 14 cases involved in this technique. Three different cycles were investigated, 1 month, 6 months, and 1 year. Each cycle has been run on a different injection pressure and injection temperature to observe the impact of injection pressure and temperature on well productivity, average water injection rate per well is 2150 bpd but average CO<sub>2</sub> as gas injection rate per well is 2.500e+7 ft<sup>3</sup>/d. Figure 3.9 shows the hot WAG average rate per day.

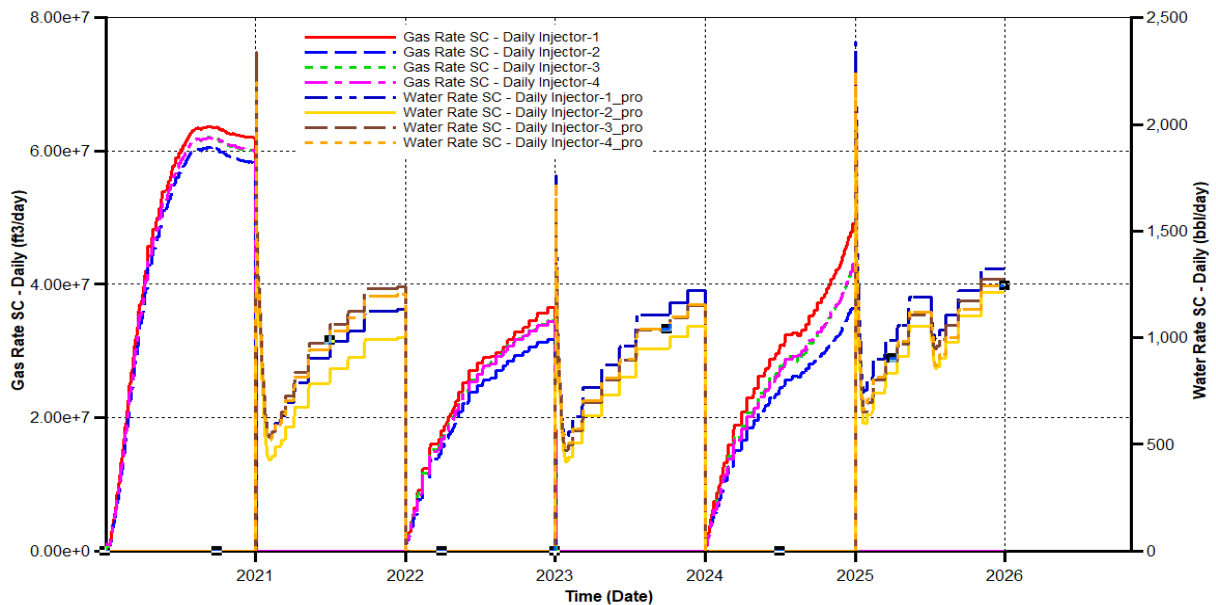


Figure 3.9: Hot WAG injection rate versus time for one-year hot WAG scenario

**Table 3.3:** Hot WAG injection scenario

Hot WAG Injection Cycle Scenarios	Injection pressure Scenarios (psi)	Injection Temperature Scenarios (°F)
1 Month Cycle	2400, 2700, 3000	190, 200, 211
6 Month Cycle	2400	190
1 Year Cycle	2400, 2700, 3000	190, 200, 211

### 3.6.2 CO<sub>2</sub> Flooding

In this scenario, CO<sub>2</sub> flooding was used for recovery of heavy oil. The injection process involves using three different injection pressures (2400psi, 2700psi, and 3000psi), all at 190 °F temperature. Results were analysed based on water-cut and cumulative oil production. The average CO<sub>2</sub> injection rate per well is 2.00e+8 ft<sup>3</sup>/d. Figure 3.10 shows the CO<sub>2</sub> injection rate per day versus time plot.

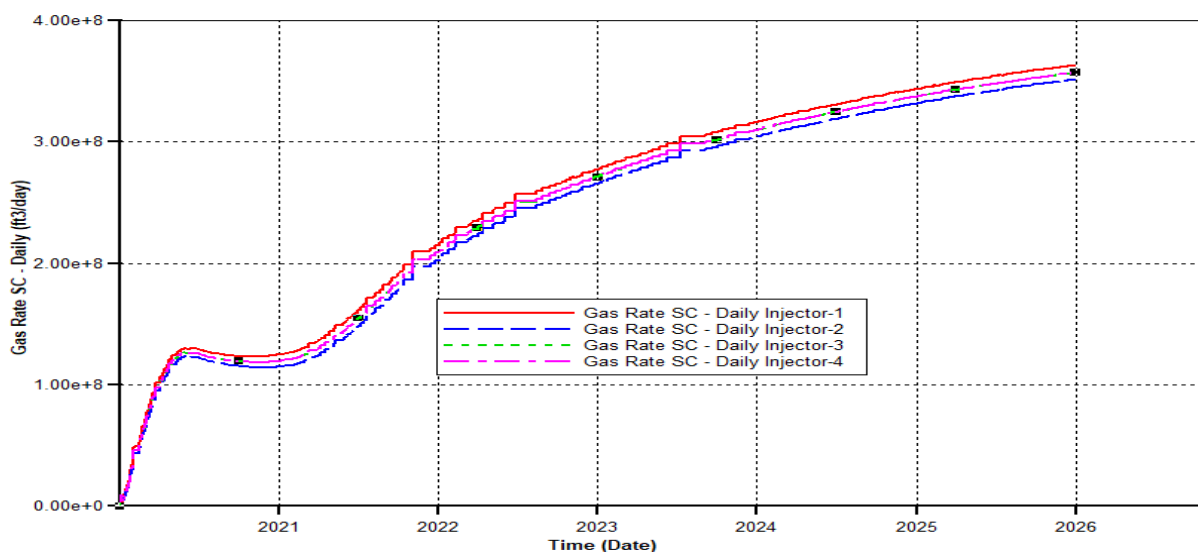


**Figure 3.10:** CO<sub>2</sub> gas injection rate versus time

### 3.5.3 Hot Water Flooding

Hot water flooding with an injection temperature of 190 °F was used to see if regular hot water will contribute to optimize oil recovery through upgrading the heavy oil. The injection process involves injecting hot water at three different injection pressures (2400 psi, 2700 psi, and 3000 psi), average hot water per well is 2750 bpd. Figure 3.11 shows the time versus average hot water injected per day.

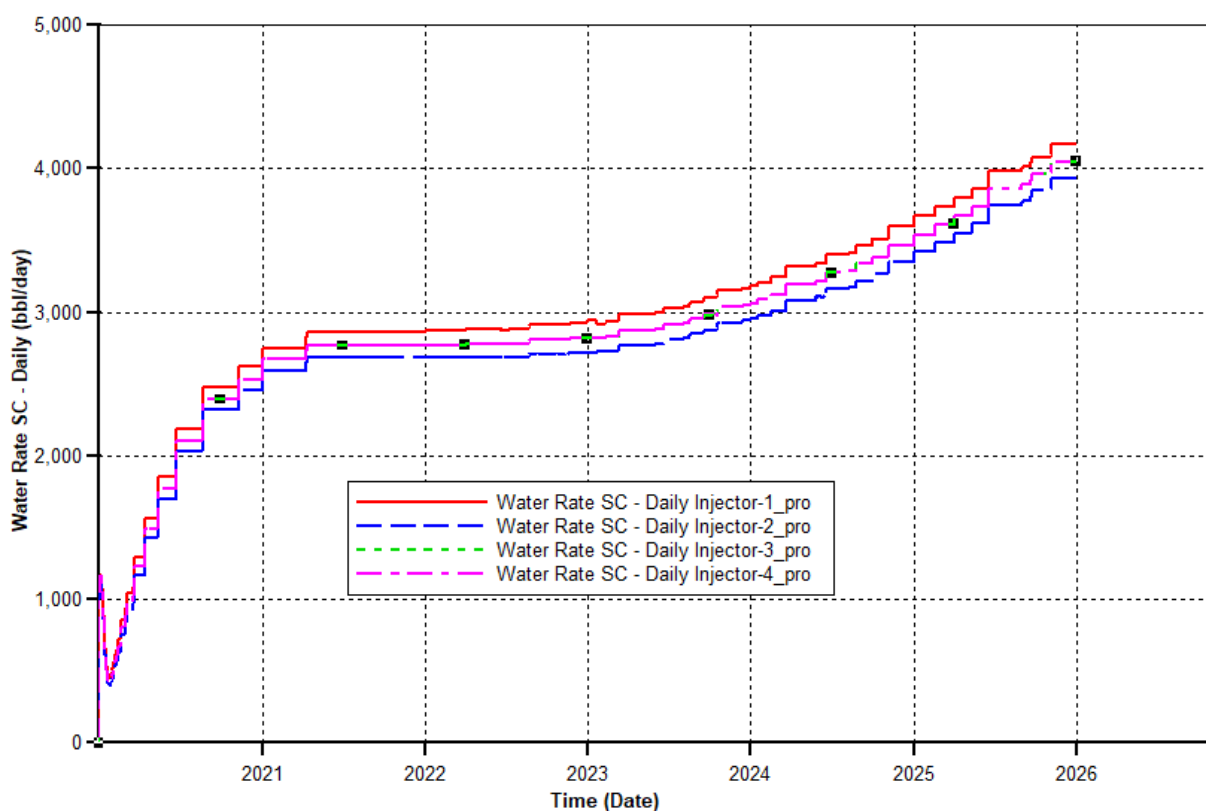


Figure 3.11: Hot water injection rate versus time

## **CHAPTER 4**

### **RESULTS AND DISCUSSIONS**

In this chapter, all the simulation outputs have been analysed and discussed based on several main factors; OPR oil production rate, WCT water cut, WOR water oil ratio, and cumulative-oil production. Additionally, a detailed discussion is provided to show the impact of Hot WAG on production performance in heavy oil recovery.

#### **4.1 Hot-Water Flooding Scenarios**

##### **4.1.1 Hot 190 °F-water flooding at 2400 psi**

In this study, one production well has been used to compare performances of different EOR methods based on WOR and cumulative oil production. Figure 4.1a shows the WOR, oil production rate and cumulative oil production against time for the hot water flooding method with an injection pressure of 2400 psi. According to simulation output, the water-oil ratio started to increase rapidly from the start which indicates the presence of fractures in the reservoir. The water production rate reached over 5000 bpd in 2026 and oil production declined from the beginning due to excessive water production and reached a production rate of 150 bpd in the beginning until the end of the simulation time. Additionally, cumulative oil production reached 198 011 barrels at the end of simulation time as shown in Figure 4.1b.

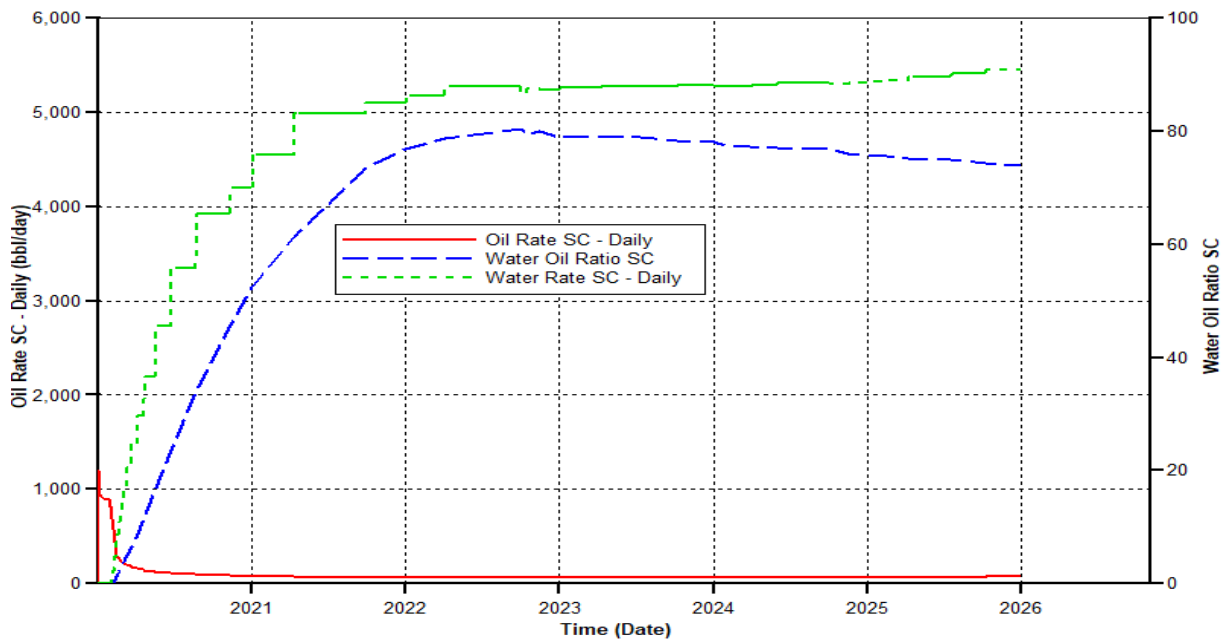


**Figure 4.1a:** OPR, WCT, and WOR versus time for hot 190 °F-water flooding at 2400 psi

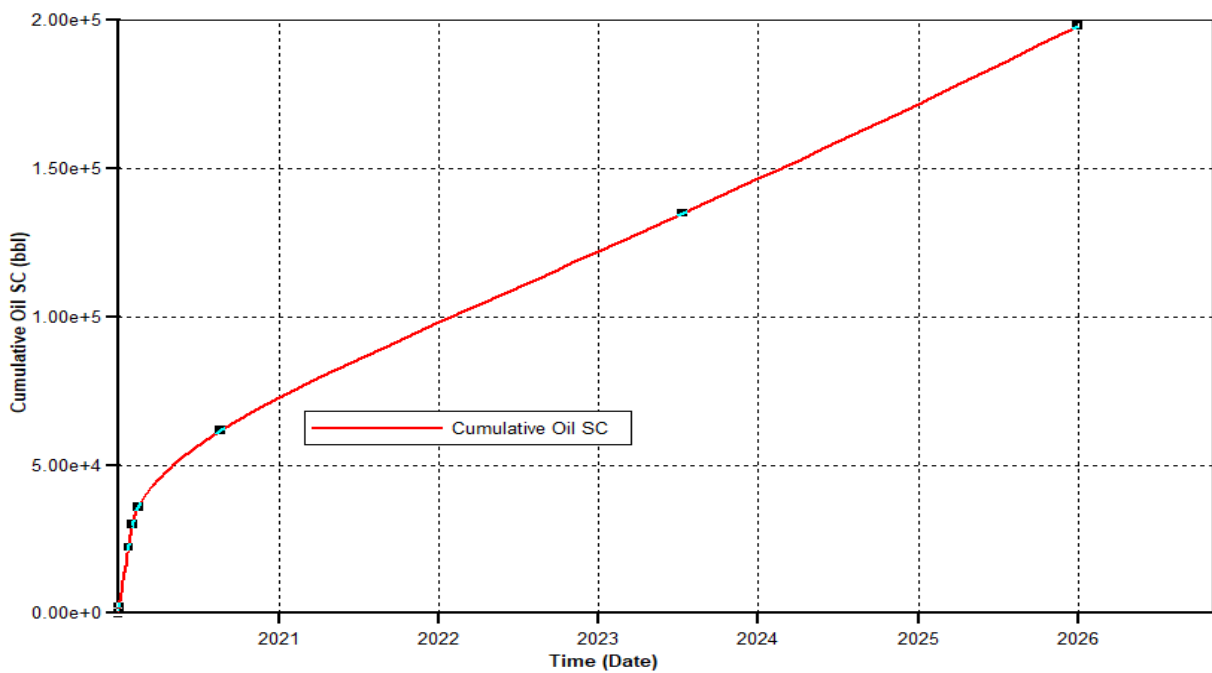


**Figure 4.1b:** Cumulative oil production versus time for hot 190 °F-water flooding at 2400 psi

#### 4.1.2 Hot 190 °F-water flooding at 2700 psi

Figure 4.2a shows hot water-flooding method with an injection pressure of 2700 psi. Production performance analysis is based on oil production rate, WOR, and cumulative oil production. Based on simulation result, the water production rate has reached over 9500 bpd and WOR of over 110 while the oil production is critically low, below 150 bpd. The cumulative oil production has reached 191832 barrel after 6 years of production as shown in Figure 4.2b. This result is due to the reservoir characteristics of the carbonate reservoir, where large fractures within the reservoir connected to a bottom water aquifer.

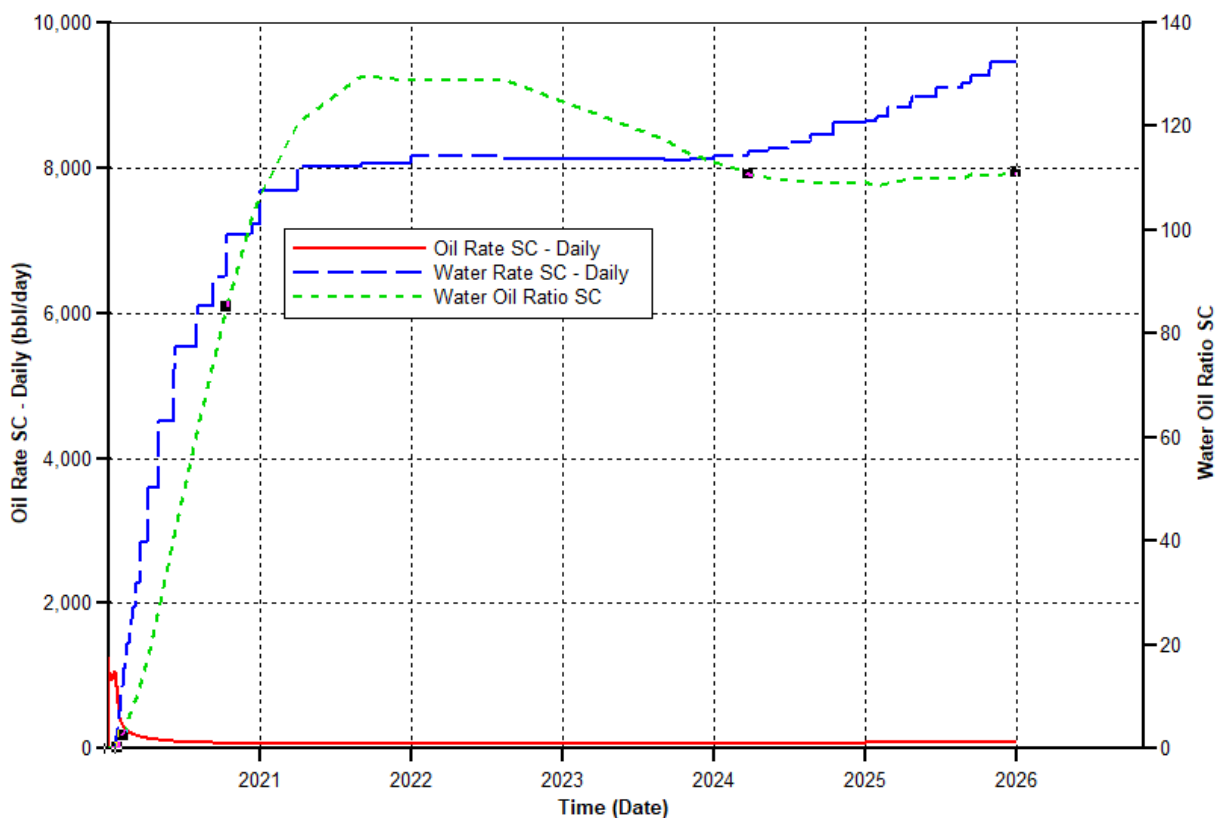
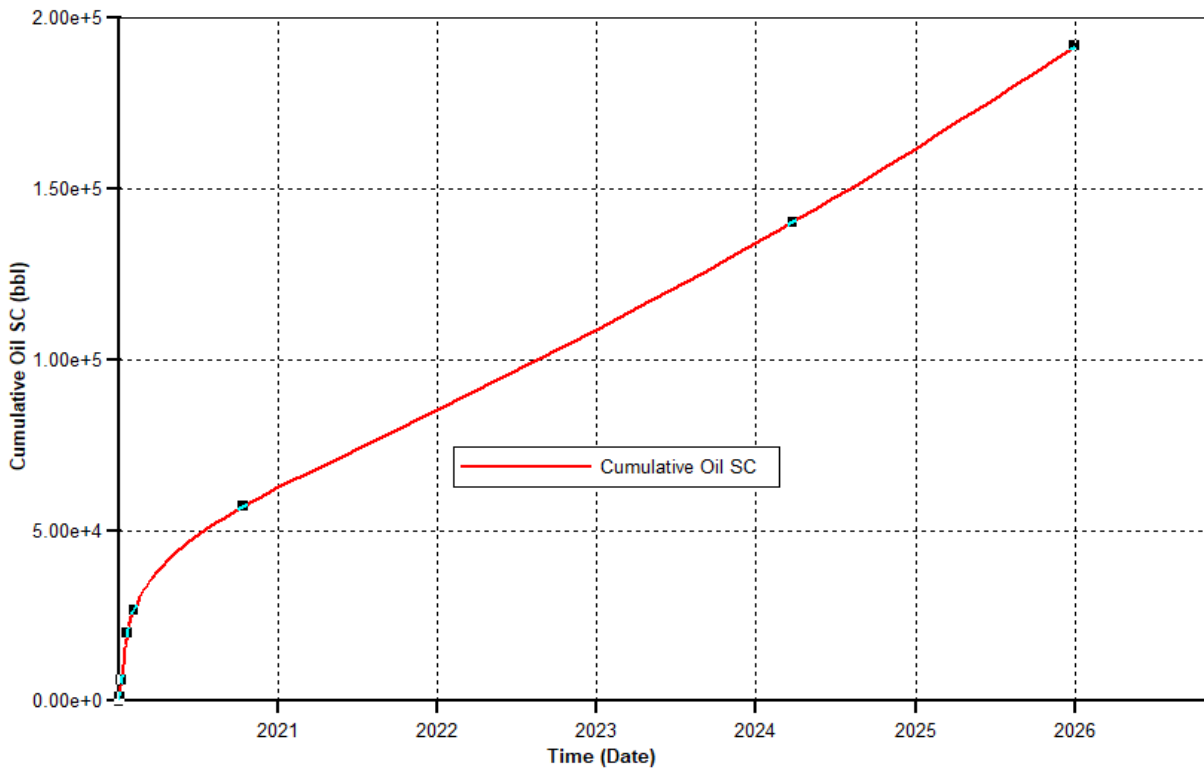


Figure 4.2a: OPR, WCT, and WOR versus time for hot 190 °F-water flooding at 2700 psi



**Figure 4.2b:** Cumulative oil production versus time for hot 190 °F-water flooding at 2700 psi

#### 4.1.3 Hot 190 °F-water flooding at 3000 psi

Water-flooding of injection pressure of 3000 psi and injection temperature of 190 °F has been examined to investigate its production performance. Plot of water production rate, WOR, and oil production rate versus time is shown in Figure 4.3a. The simulation result shows that water production rate has reached over 15000 bpd and WOR has reached 180 while the oil production rate has reached less than 80 bpd. The cumulative oil production has reached 194925 barrels after 6 years of production. The low oil production is due to the fact that the reservoir contains heavy oil and the reservoir type is fractured carbonate reservoir which allows the water to flow easily through the reservoir.

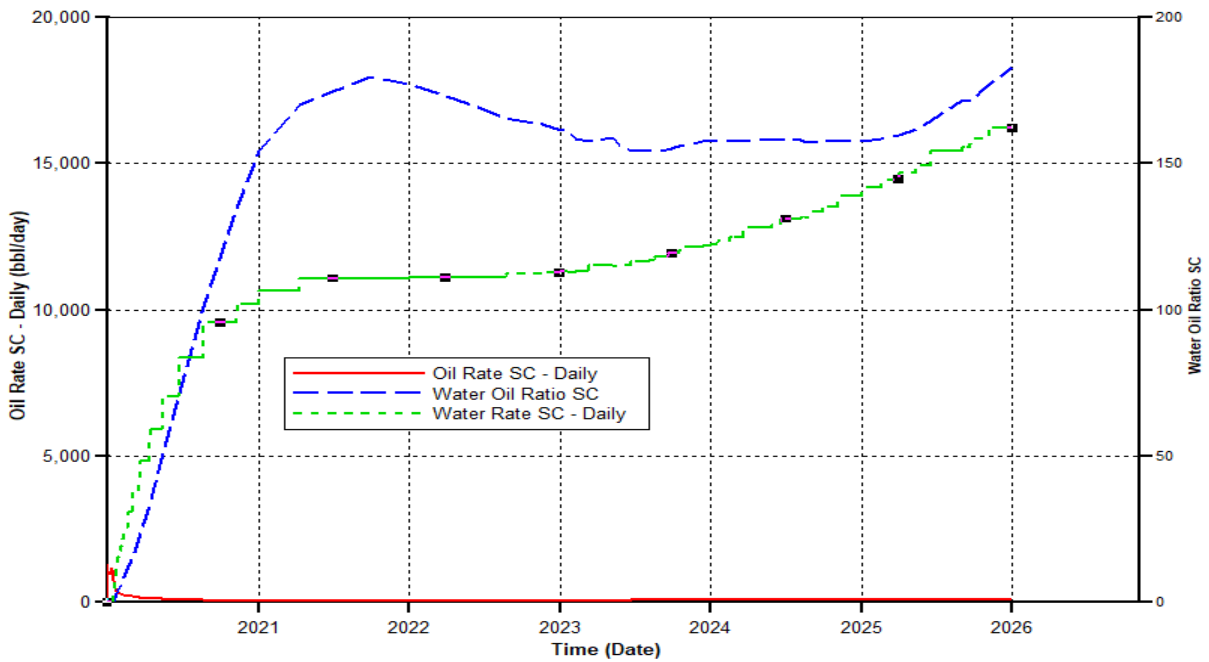


**Figure 4.3a:** OPR, WCT, and WOR versus time for hot 190 °F-water flooding at 3000 psi

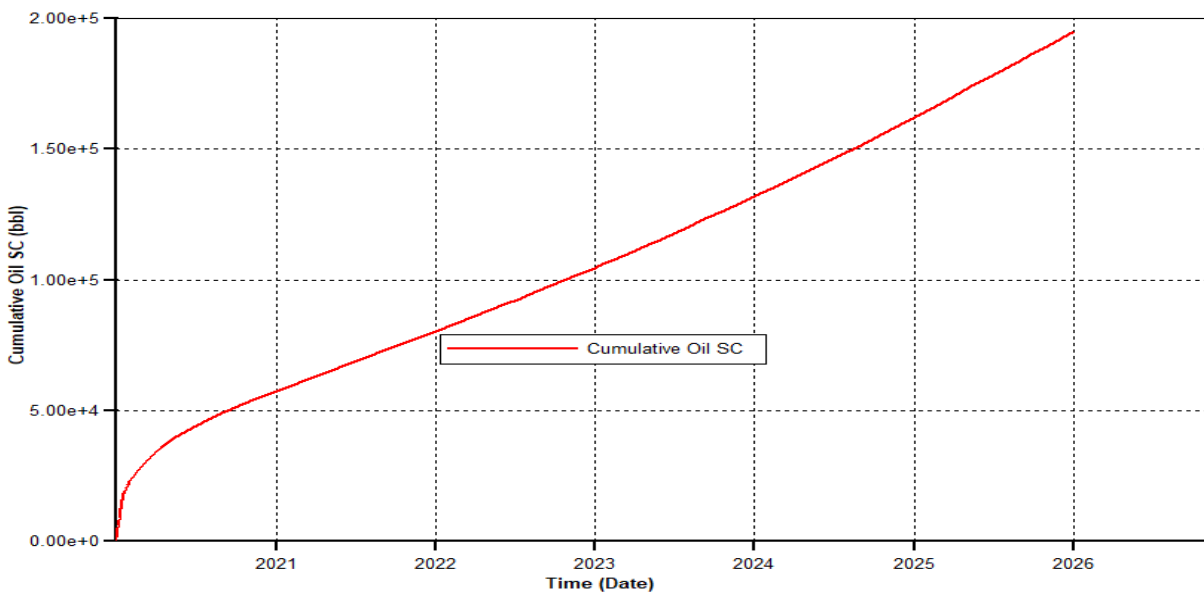


**Figure 4.3b:** Cumulative oil production versus time for hot 190 °F-water flooding at 3000 psi

In the hot water flooding case, water production rate was increased gradually but gas production rate was decreased if it compared to water cut because it had been injected the hot water in the injector wells, low heavy oil mobility, water can flow faster than heavy oil through the naturally fractured reservoir due to lower water viscosity and on other hand due to presences of effective naturally fractured reservoir in the studied model, Figure 4.3C. Shows the differences between water production and gas production rate per day.

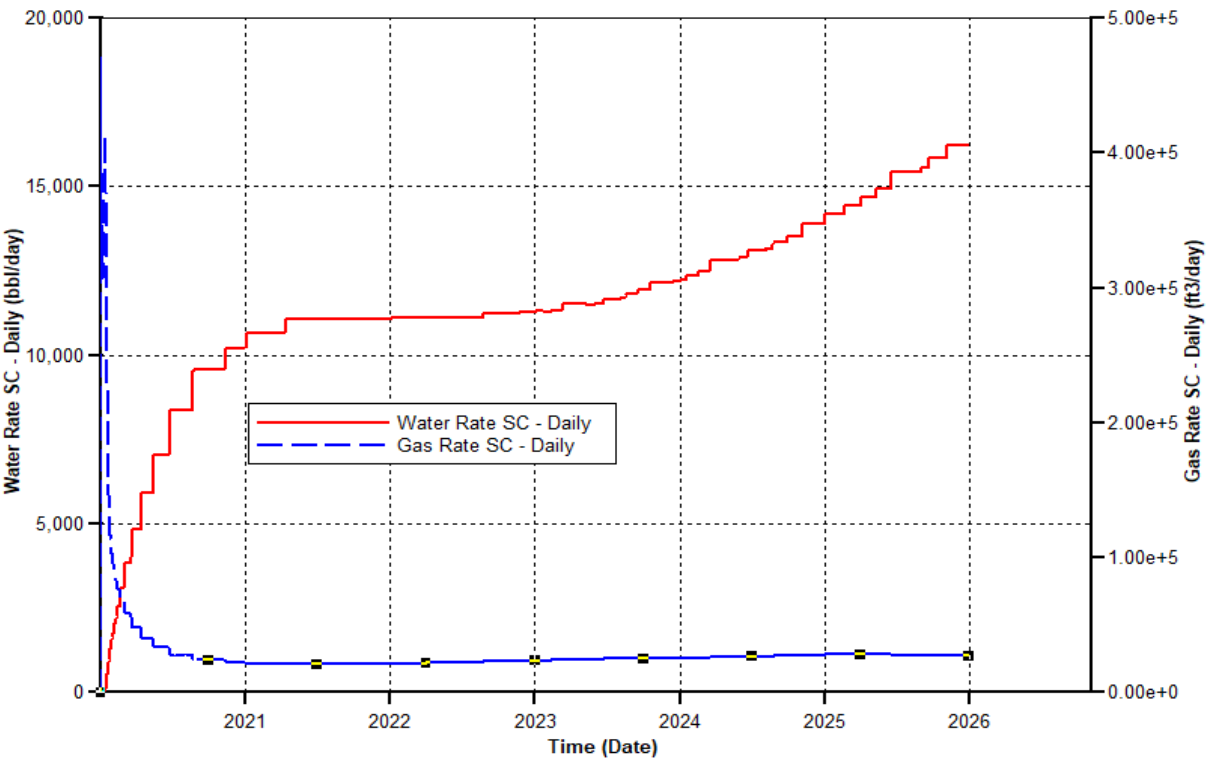


Figure 4.3C: Water and gas production rate versus time for hot 190 °F-water flooding at 3000 psi

**4.2 CO<sub>2</sub> Flooding Scenarios**

**4.2.1 CO<sub>2</sub> flooding at 2400 psi**

CO<sub>2</sub> injection with an injection pressure of 2400 psi has been investigated in this study to predict its impact on production performance. The investigation is based on observing water-oil ratio, production rate and cumulative oil production. Figure 4.4a shows the simulation result which is

clear that the oil production rate is 270 bpd and declined after 3 years of production as indicated in the red colour. WOR is 0.14 while the water production rate is almost zero. This result is due to the fact that CO<sub>2</sub> mixes with the heavy oil and upgrades it, which result in better oil production compared to water-flooding scenario. The cumulative oil production has reached over 464541 barrels in 2026 as seen in Figure 4.4b.

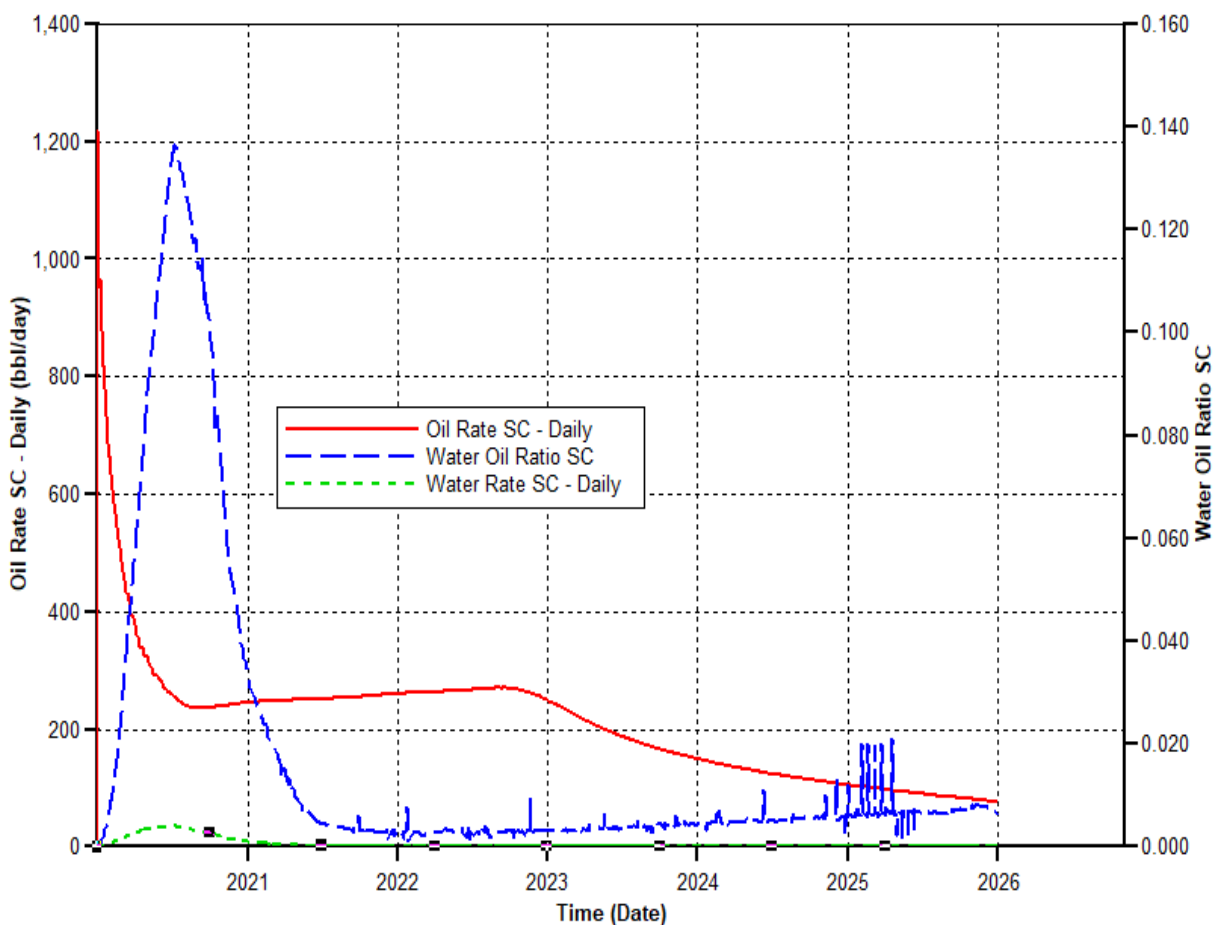


**Figure 4.4a:** OPR, WCT, and WOR versus time for CO<sub>2</sub> flooding at 2400 psi

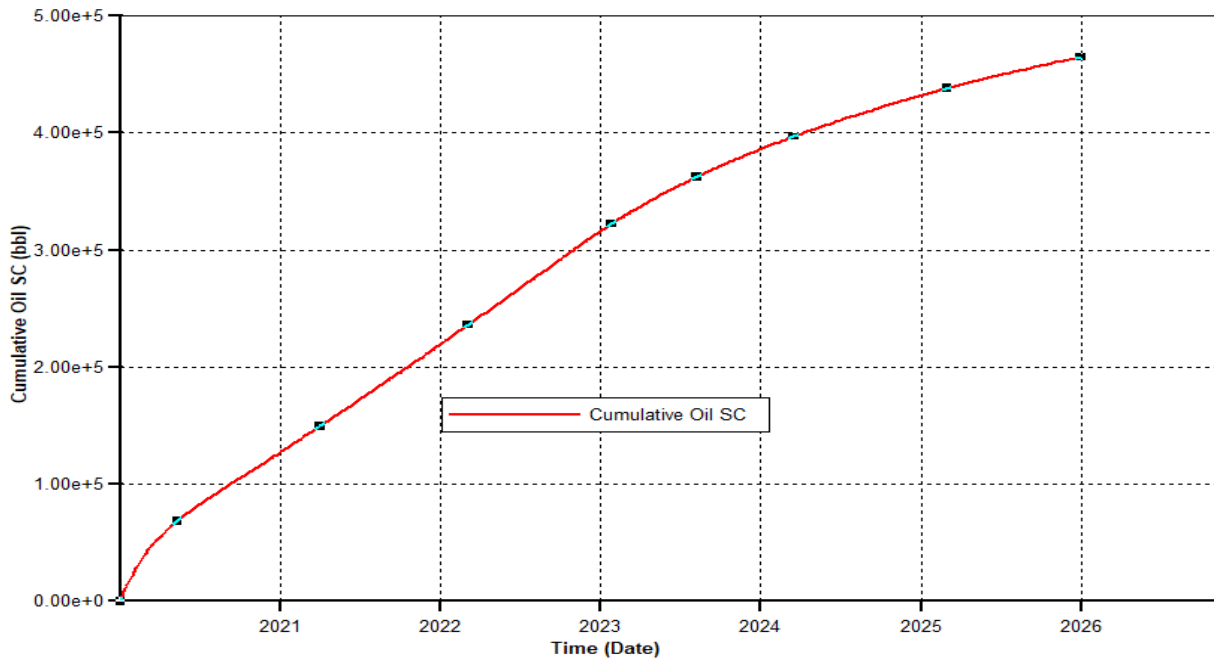


**Figure 4.4b:** Cumulative oil production versus time for CO<sub>2</sub> flooding at 2400 psi

#### 4.2.2 CO<sub>2</sub> flooding at 2700 psi

Figure 4.5a shows CO<sub>2</sub> flooding method has been used with an injection pressure of 2700 psi. Oil production rate, WOR, and cumulative oil production were analysed. Based on simulation results, the water production rate is around 10 bpd and WOR of 0.04 while the oil production is reduced from 240 bpd to 80 bpd. The cumulative oil production has reached 415839 after 6 years of production as shown in Figure 4.5b. This result is due to the reservoir characteristics of carbonate reservoir, and mainly the presence of large fractures and heavy oil within the reservoir.

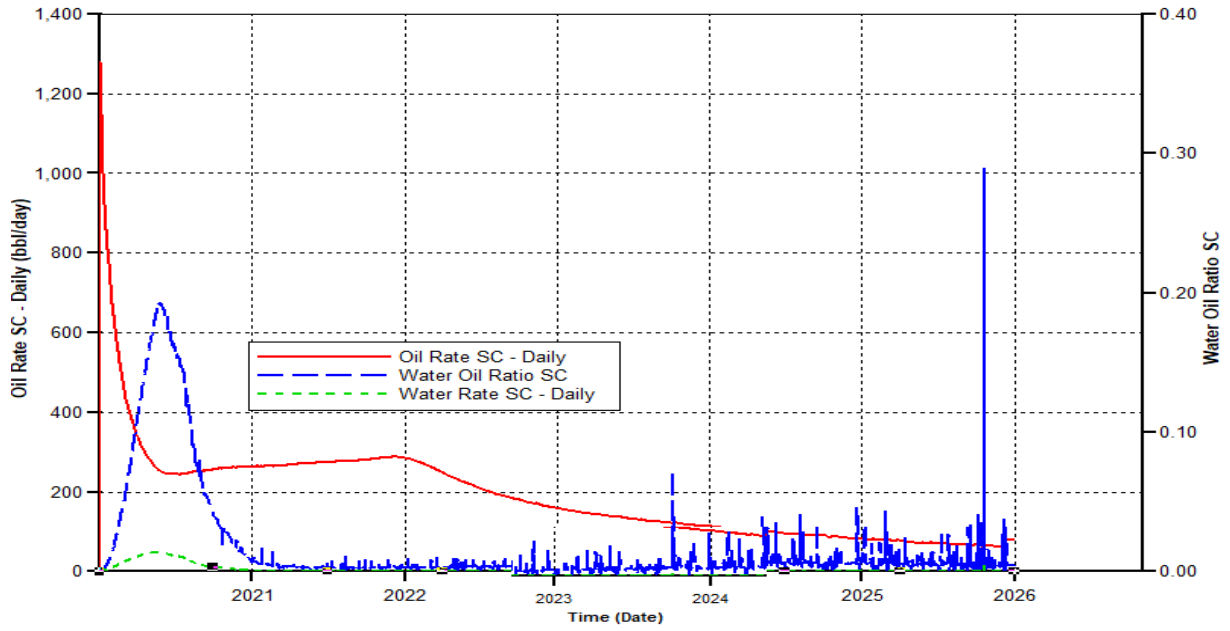


**Figure 4.5a:** OPR, WCT, and WOR versus time for CO<sub>2</sub> flooding at 2700 psi

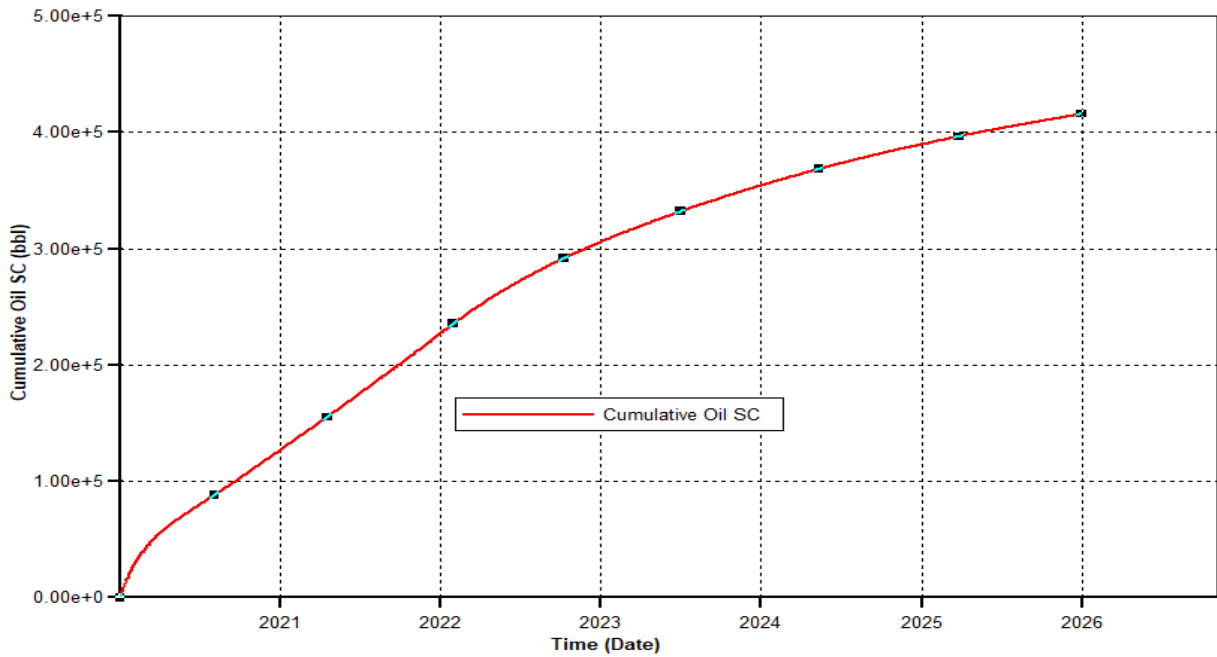


**Figure 4.5b:** Cumulative oil production versus time for CO<sub>2</sub> flooding at 2700 psi

### 4.2.3 CO<sub>2</sub> flooding at 3000 psi

CO<sub>2</sub> flooding at 3000 psi pressure and injection temperature of 190 °F has been examined. Plot of water production rate, WOR, and oil production rate versus time is shown in Figure 4.6a. The simulation result shows that water production rate and WOR is greater than previous scenarios of CO<sub>2</sub> flooding scenarios while the oil production rate drops less than 80 bpd. The cumulative oil production has reached 353564 barrels after 6 years of production as seen in Figure 4.6b. The low oil production is due to the fact that the reservoir contains heavy oil and the reservoir type is fractured carbonate reservoir which heavy oil is difficult to be extracted.

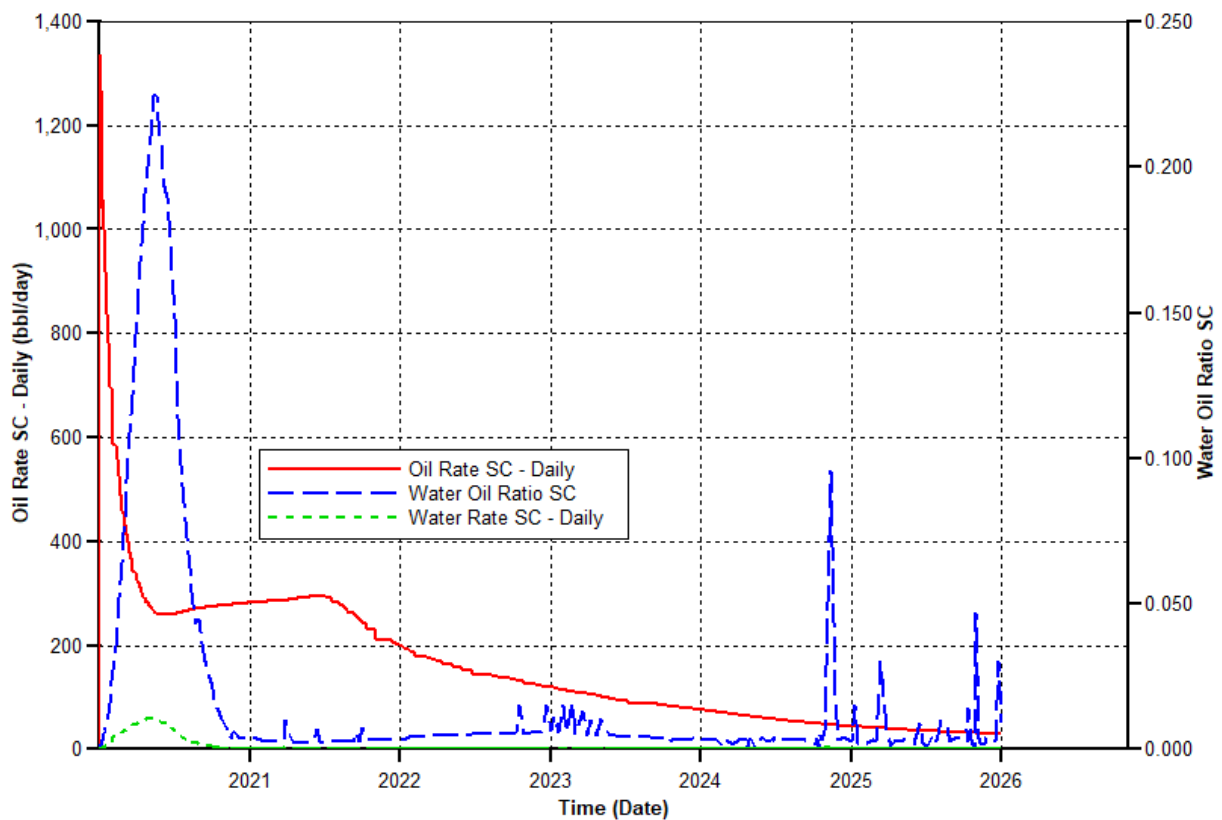


**Figure 4.6a:** OPR, WCT, and WOR versus time for CO<sub>2</sub> flooding at 3000 psi

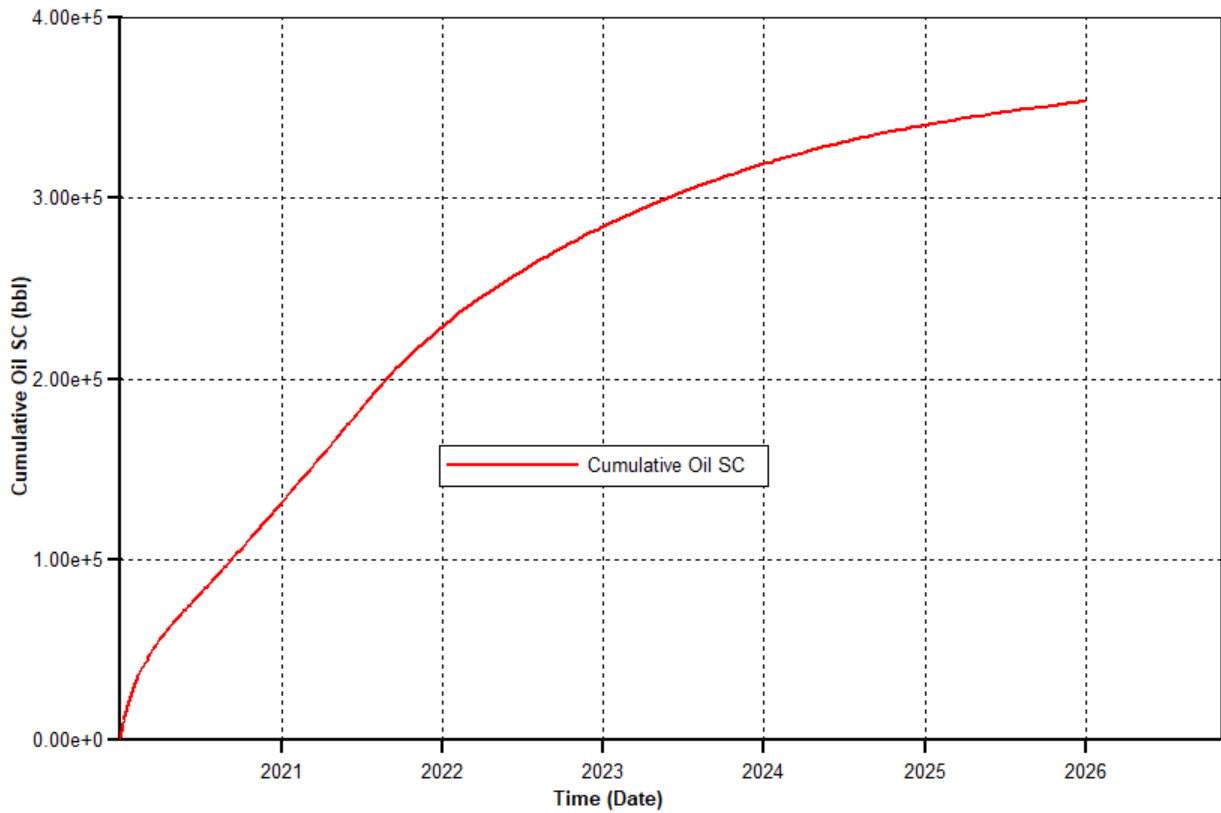


**Figure 4.6b:** Cumulative oil production versus time for CO<sub>2</sub> flooding at 3000 psi

In the CO<sub>2</sub> flooding scenario, gas production rate was  $5.00e+8$  ft<sup>3</sup>/d, while water production rate was 60 bbl/d at January 2020 as seen in Figure 4.6c. After implementing CO<sub>2</sub> injection, the gas production rate gradually increased to  $1.500e+9$  ft<sup>3</sup>/d but water production rate dropped to zero at the end simulation study. This is due to low viscosity of oil, presence of effective open natural fractures in the model.

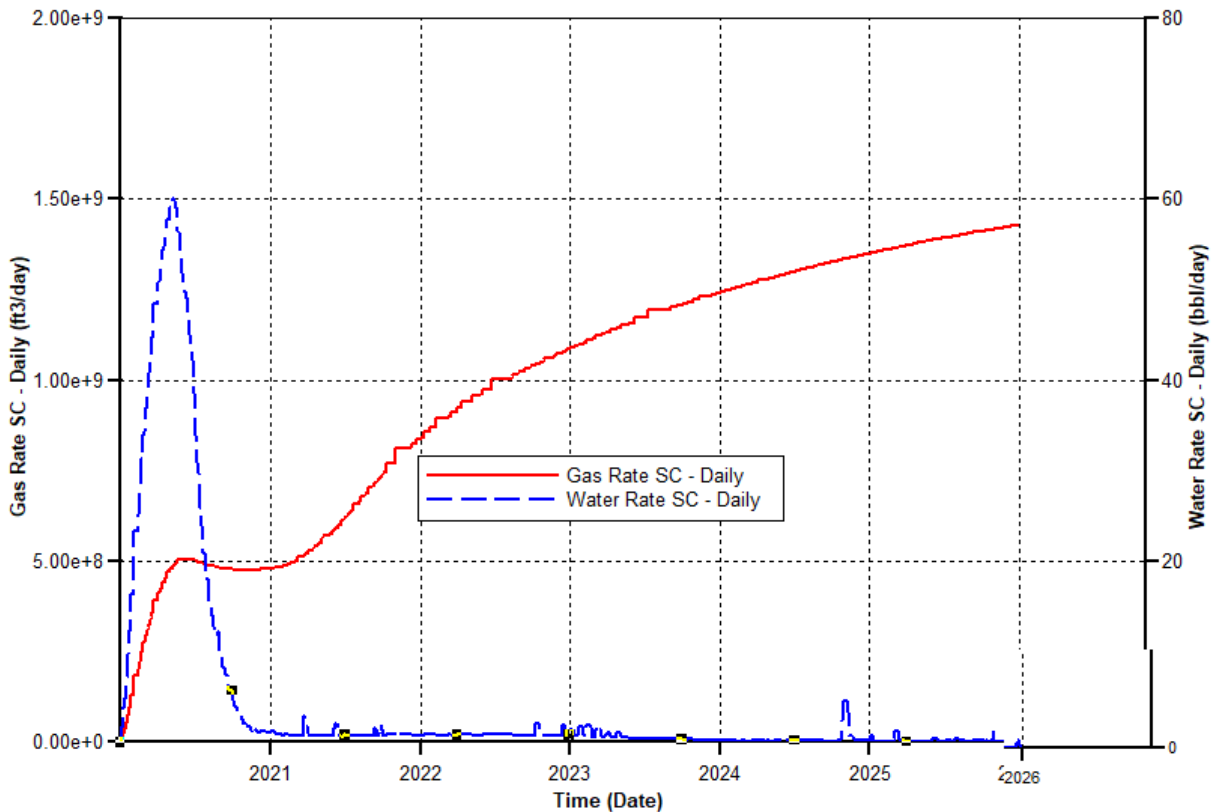


**Figure 4.6C:** Gas and water production rate versus time for CO<sub>2</sub> flooding at 3000 psi

### 4.3 Hot WAG Injection Scenarios

#### 4.3.1 Hot 190 °F WAG injection 1-month

Figure 4.7a represents the plot of daily oil production, water production rate and WOR for 1-month hot WAG injection cycle with an injection temperature of 190 °F. Based on the plot, water production rate has increased to 2500 bpd in 2023 and to 4300 bpd in 2026. Oil production rate has reduced from 1300 bpd to 350 bpd and maintained the same production with time. Based on Figure 4.7b, cumulative oil production has reached 568919 barrels at the end of simulation run. This result is different from the previous scenarios due to the fact that hot WAG injection helps to minimize oil viscosity through injecting the gas and at the same time helps to push the residual oil through injecting water.

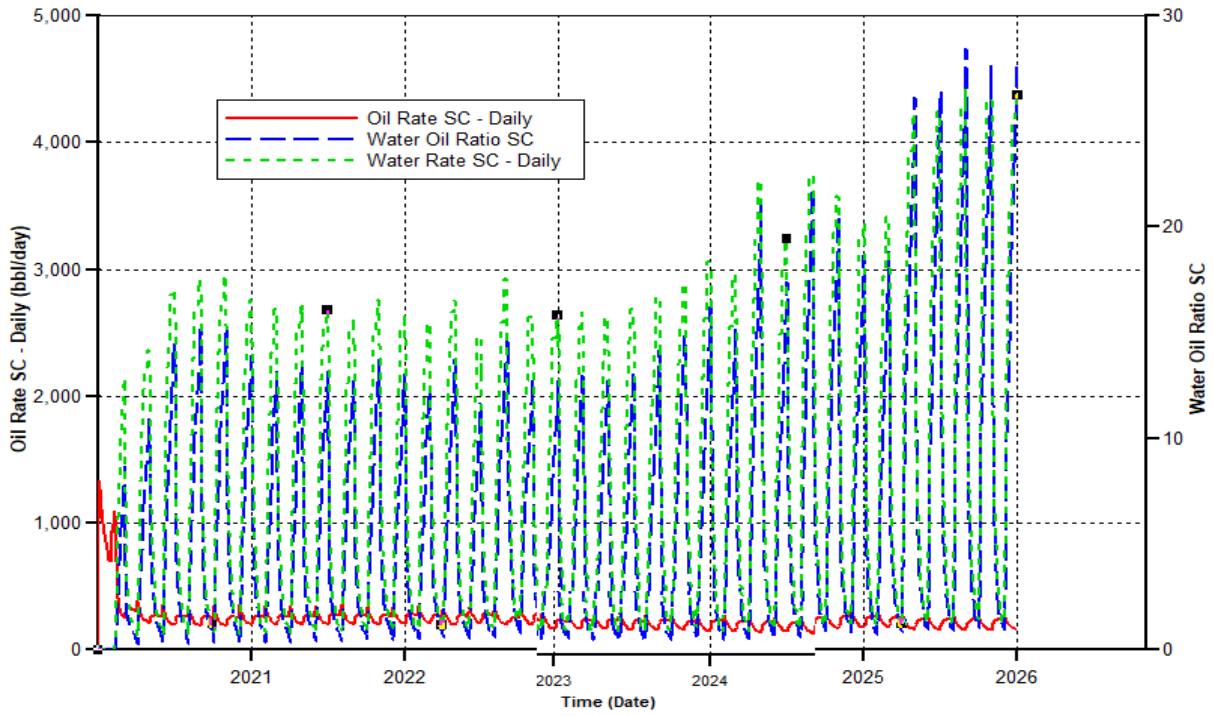


**Figure 4.7a:** OPR, WCT, and WOR versus time for hot 190 °F WAG injection 1-month

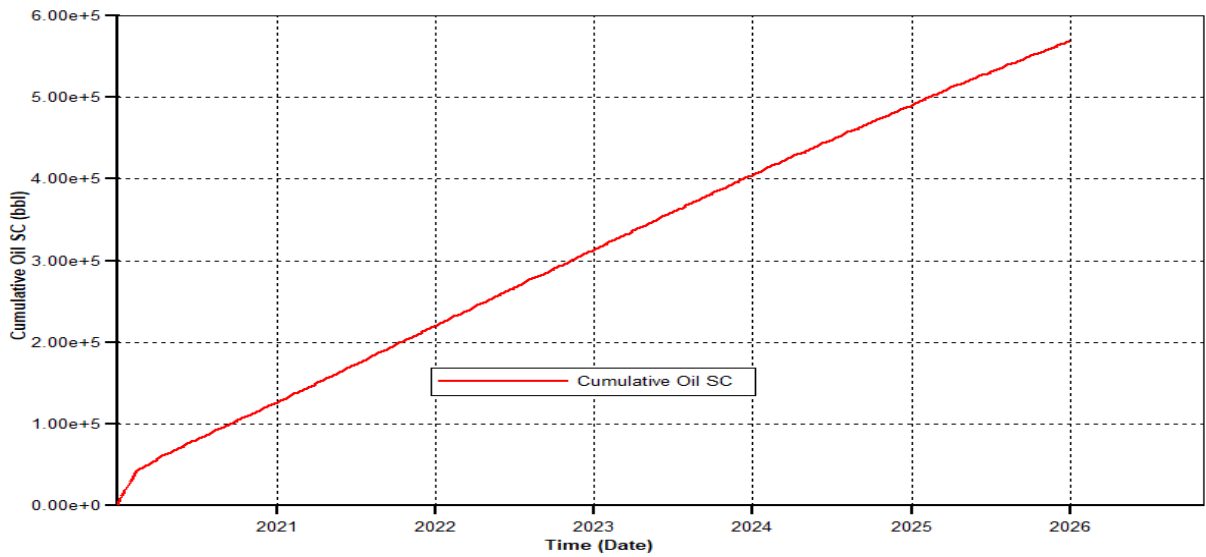


**Figure 4.7b:** Cumulative oil production versus time for hot 190 °F WAG injection 1-month

### 4.3.2 Hot 200 °F WAG injection 1-month

Figure 4.8a shows the plot of oil production rate, water production rate and WOR for 1-month hot WAG injection cycle with an injection temperature of 200 °F. Based on the plot, water production rate has increased with time to reach 4280 bpd. The WOR has reached around 34 while oil production rate has reduced from 1300 bpd to 340 bpd and maintained the same production with time. As seen in Figure 4.7b, cumulative oil production has reached 568951 barrels at the end of simulation run. This result is different than the previous scenarios due to the fact that hot WAG injection helps to minimize oil viscosity through injecting the miscible gas and the injected water help to push the oil

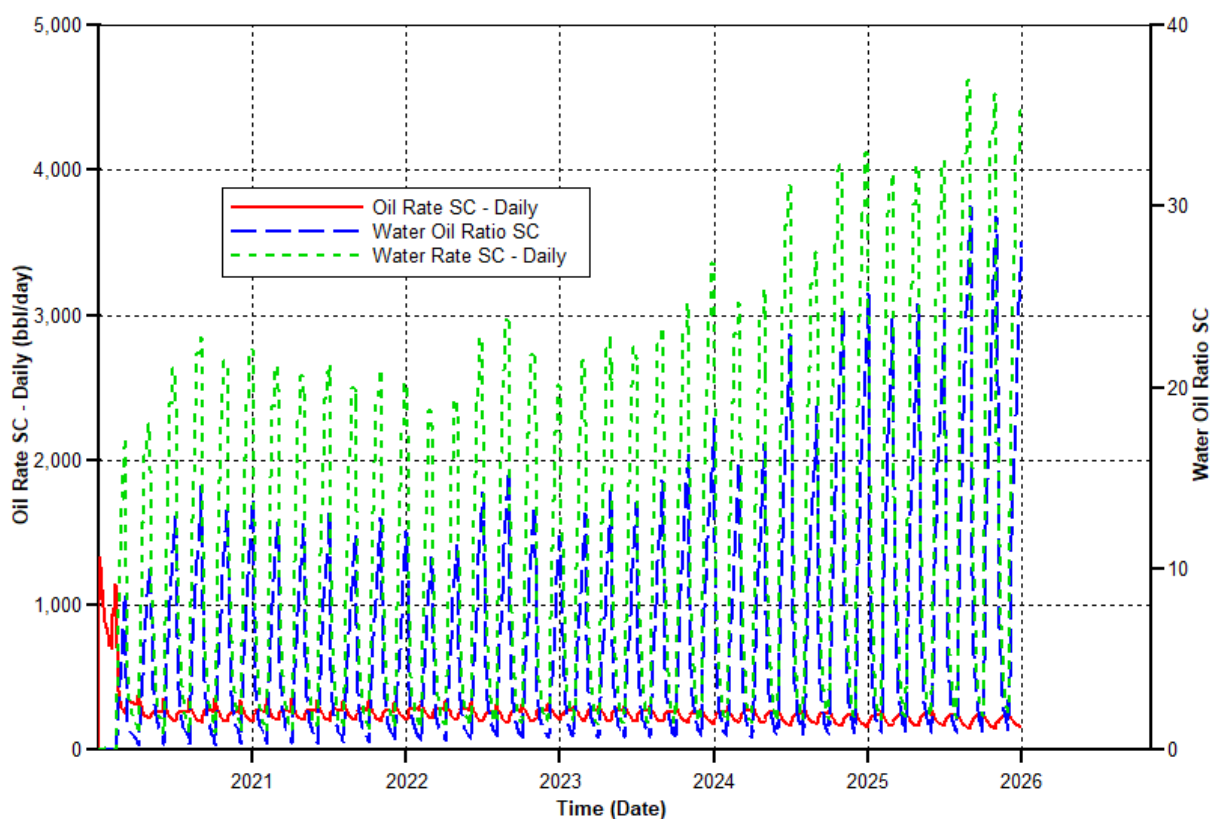


**Figure 4.8a:** OPR, WCT, and WOR versus time for hot 200 °F WAG injection 1-month

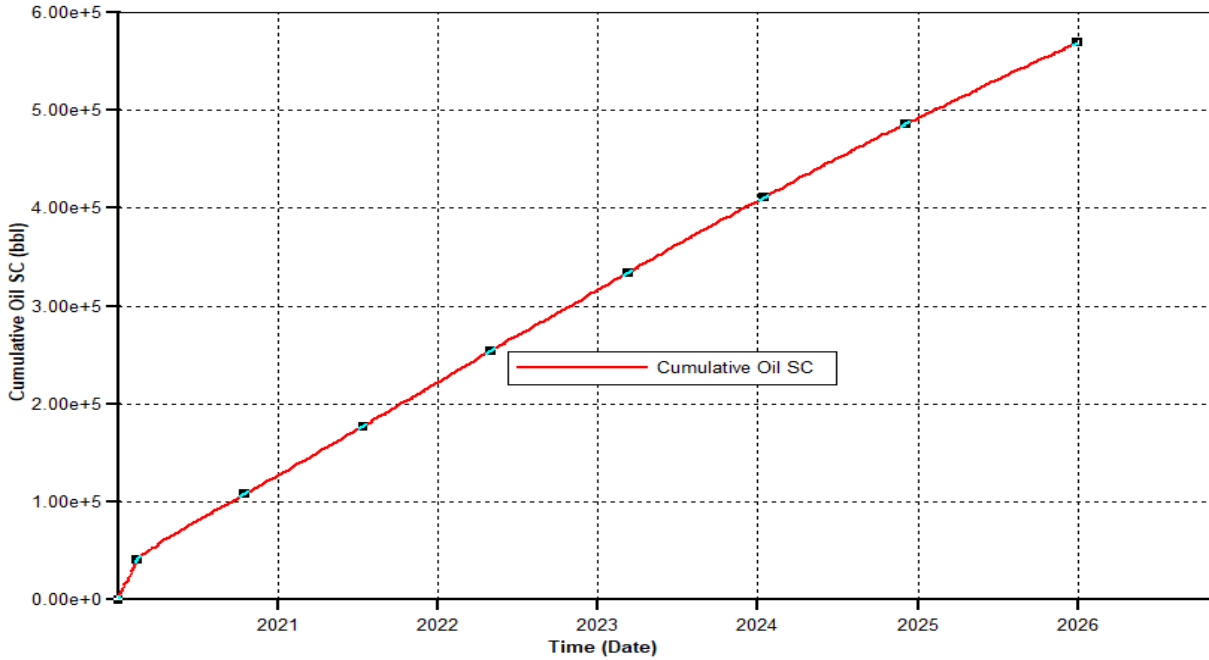


**Figure 4.8b:** Cumulative oil production versus time for hot 200 °F WAG injection 1-month

### 4.3.3 Hot 211°F WAG injection 1-month

Hot WAG injection with a one-month cycle and an injection temperature of 211°F has been used in this study to investigate the effect of hot WAG injection on production performance. Figure 4.9a shows the effect of this scenario on production performance based on analyzing the simulation output. As seen in Figures 4.9a and 4.9b oil production rate is around 290 bpd as indicated in green colour. The water production rate increased from 2300 bbl/day in 2021 to 4000 bbl/day in the end of the simulation study, because gas had been injected after water. The increase in water production is due to the presence of large fractures within the reservoir, which contribute to transport of water to the wellbore. The cumulative oil production is about 569130 barrels as shown in Figure 4.9b. Cumulative oil production is about 220 barrels more compared to previous scenario. This increase is due to the impact of temperature change from 200 °F to 211 °F.

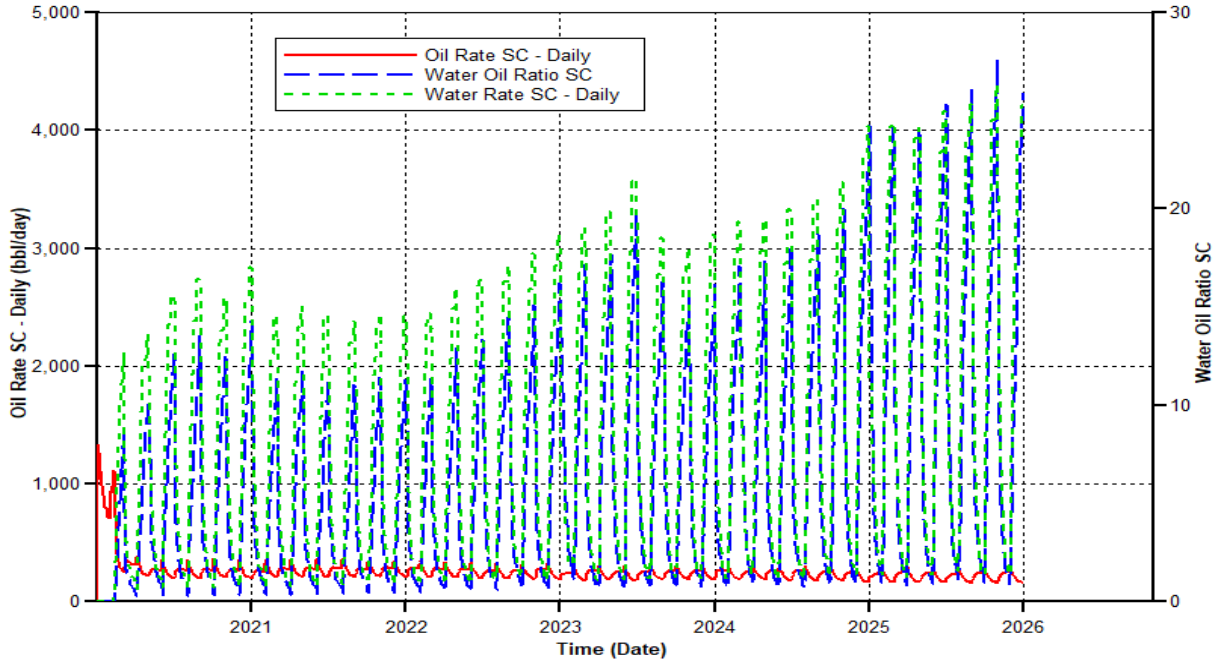


**Figure 4.9a:** OPR, WCT and WOR versus time for hot 211 °F WAG injection 1-month

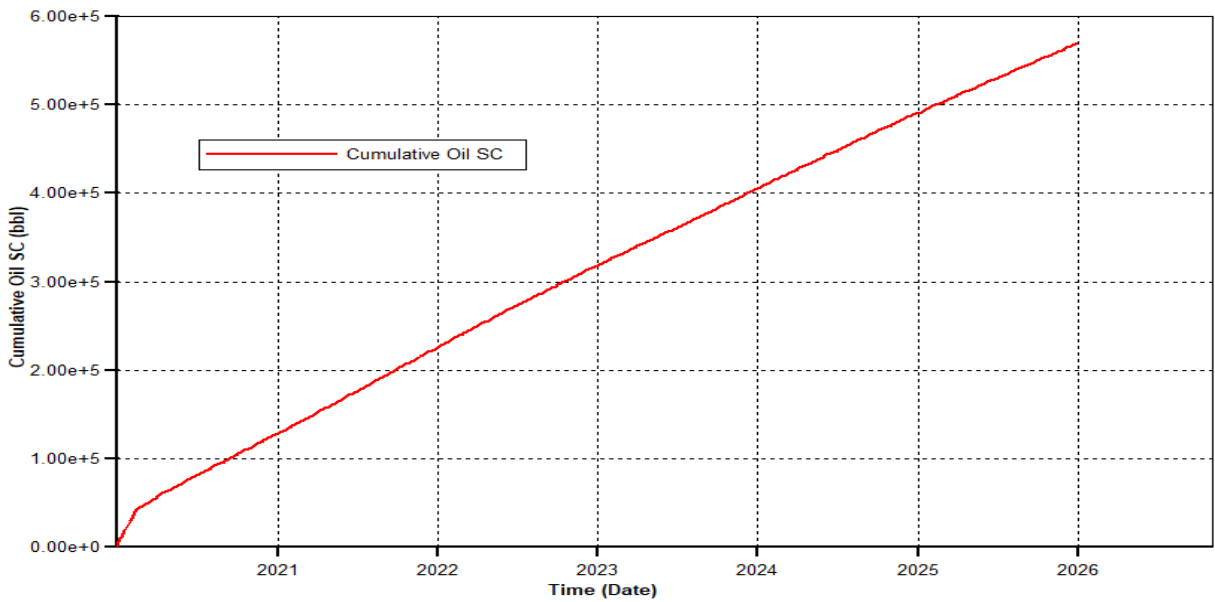


**Figure 4.9b:** Cumulative oil production versus time for hot 211 °F WAG injection 1-month

#### 4.3.4 Hot 190 °F WAG injection at 2700 psi 1-month

Additionally, 1-month cycle WAG injection scenario for an injection pressure of 2700 psi has been examined to see its impact on production performance by analyzing water production rate, oil rate and WOR as seen in Figure 4.10a. The result proves that water production rate is between 2100 bpd to 2550 bpd. The WOR is around 17.1 at the end of the simulation period, which means that water production is high. Additionally, the oil production rate is maintained around 200 bpd. Based on Figure 4.10b, the total oil production after 6 years of production has reached 494516 barrels.

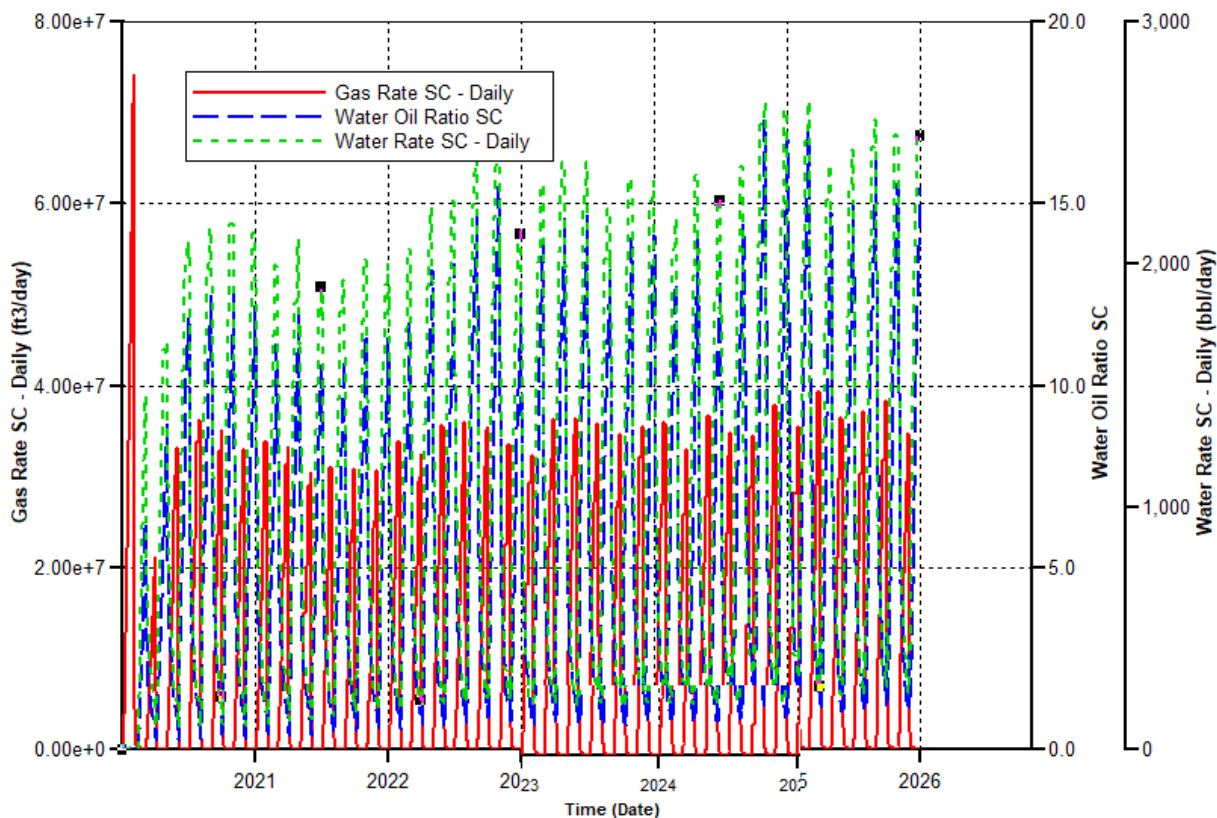


**Figure 4.10a:** OPR, WCT and WOR versus time for hot 190 °F WAG injection at 2700 psi 1-month

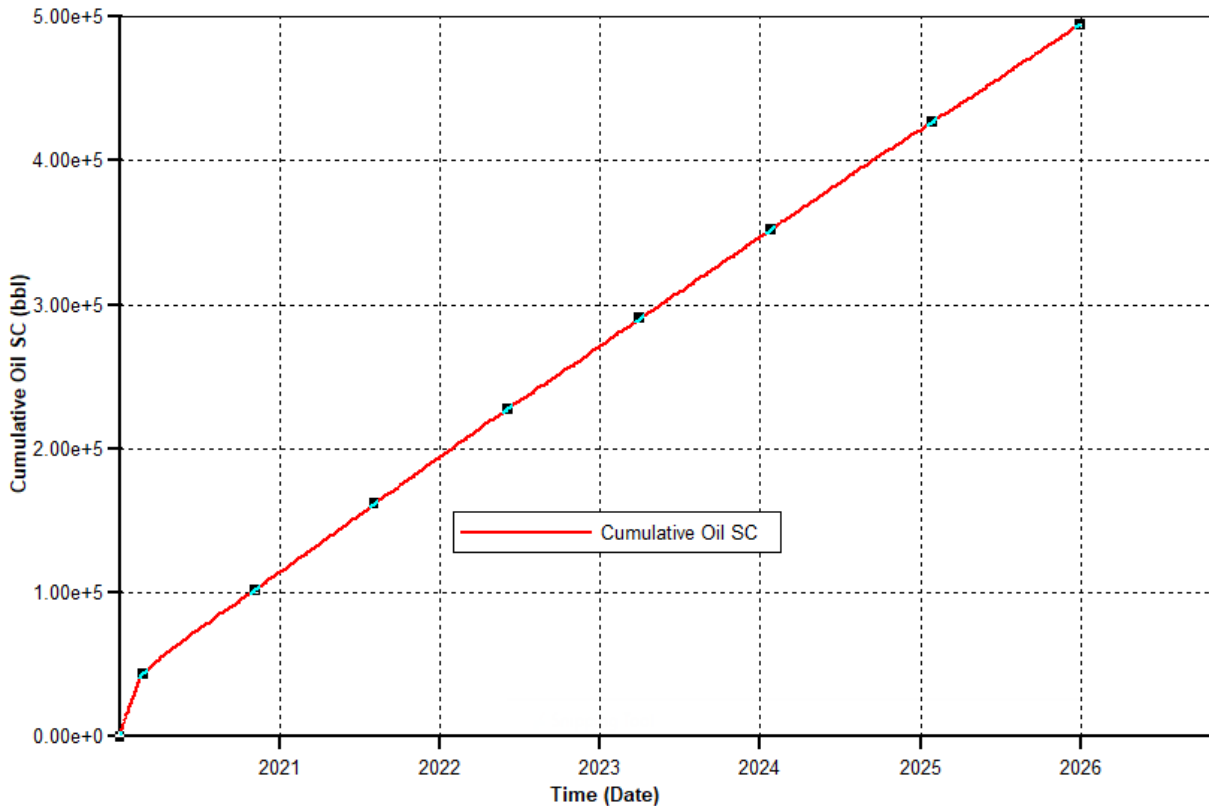


**Figure 4.10b:** Cumulative oil production versus time for hot 190 °F WAG injection at 2700 psi 1-month

#### 4.3.5 Hot 190 °F WAG injection 12-month

WAG injection cycles are considered as an important parameter of WAG design which affects oil production rate significantly. 1-year cycle has been investigated with an injection temperature of 190 °F. Figure 4.11 a shows the simulation result of this scenario, which it is clear that the production rate is low as indicated in red color. The water production rate increases over time as water is injected after gas injection in WAG injection process. The blue color represents water production rate, which in 2021, it is clear that water has been injected as the water production rate and WOR (green-line) shows a rapid increase over time. In 2022 the WOR and water production rate shows a decline to zero, which means that gas has been injected throughout this year. Cumulative oil production has reached 508024 barrels after 6 years of production as indicated in Figure 4.11 b.

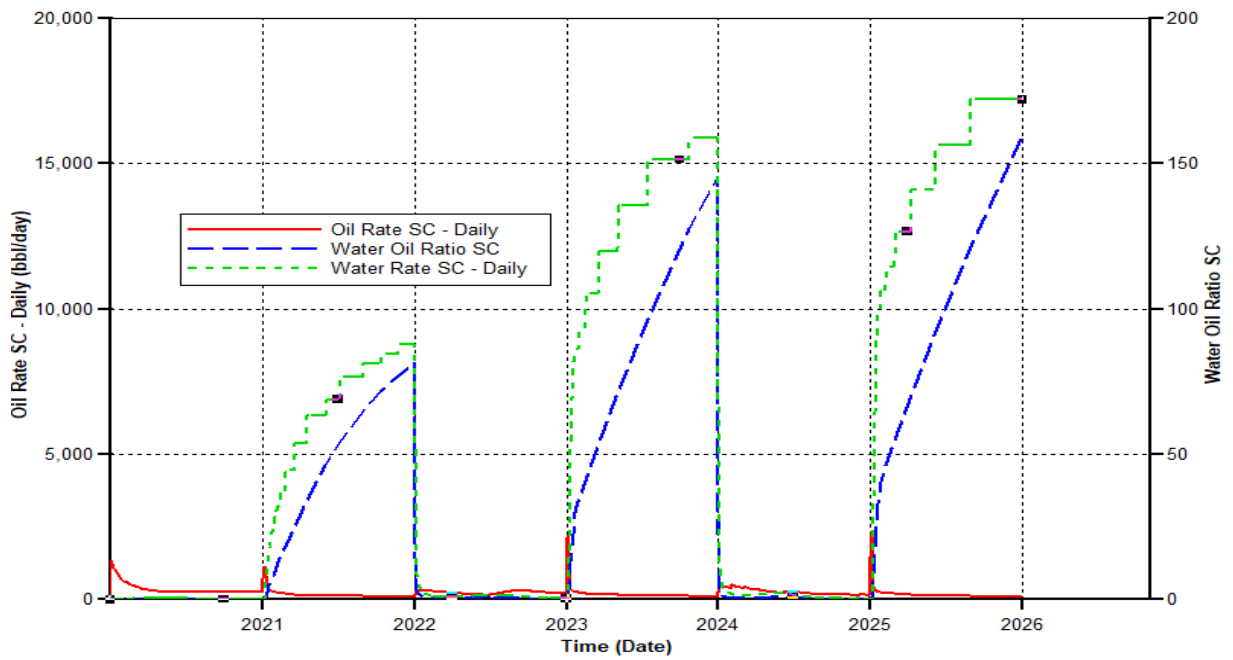


**Figure 4.11a:** OPR, WPR, and WOR versus time for hot 190 °F WAG injection 12-month

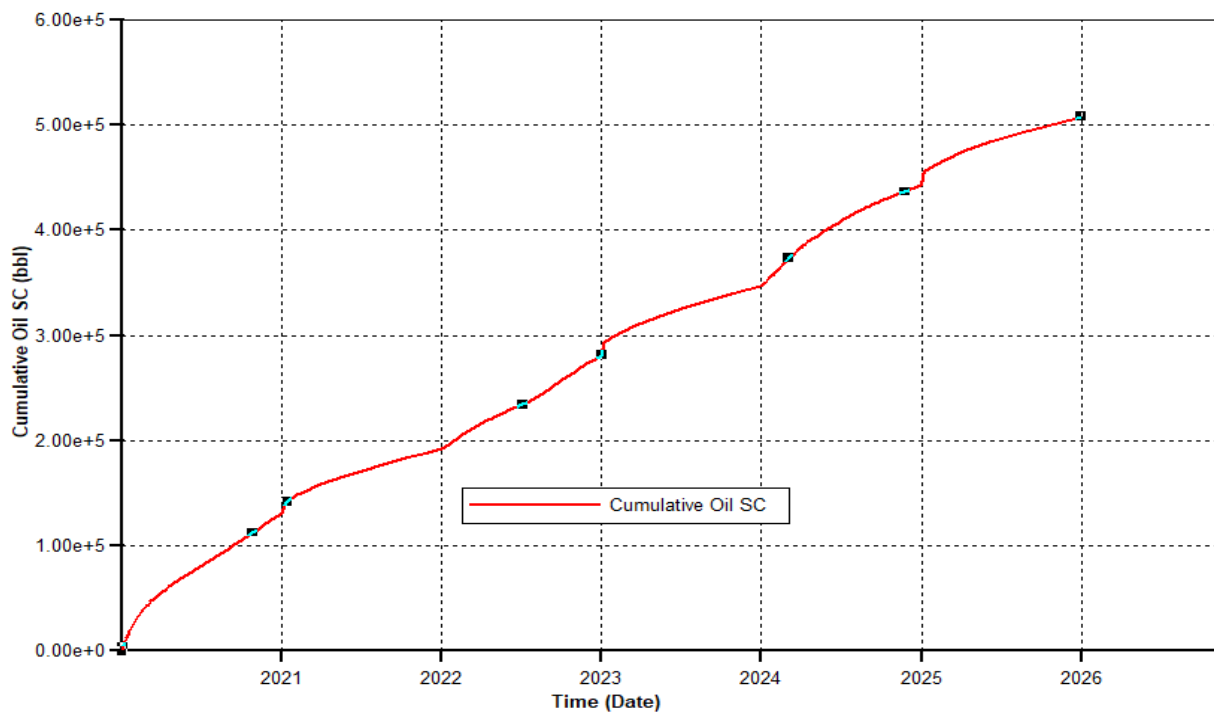


**Figure 4.11b:** Cumulative oil production versus time for hot 190 °F WAG injection 12-month

### 4.3.6 Hot 200 °F WAG injection 12-month

With an injection temperature of 200°F, a one-year period was investigated. Figure 4.12a depicts the simulation outcome for this case, showing that the output rate is modest, as shown by the red colour. As water is injected after gas injection in the WAG injection phase, the water output rate rises over time, and WOR (green-line) indicates a rapid growth over time. The WOR and water production levels also drop to zero in 2022, indicating that gas has been pumped for the whole year.

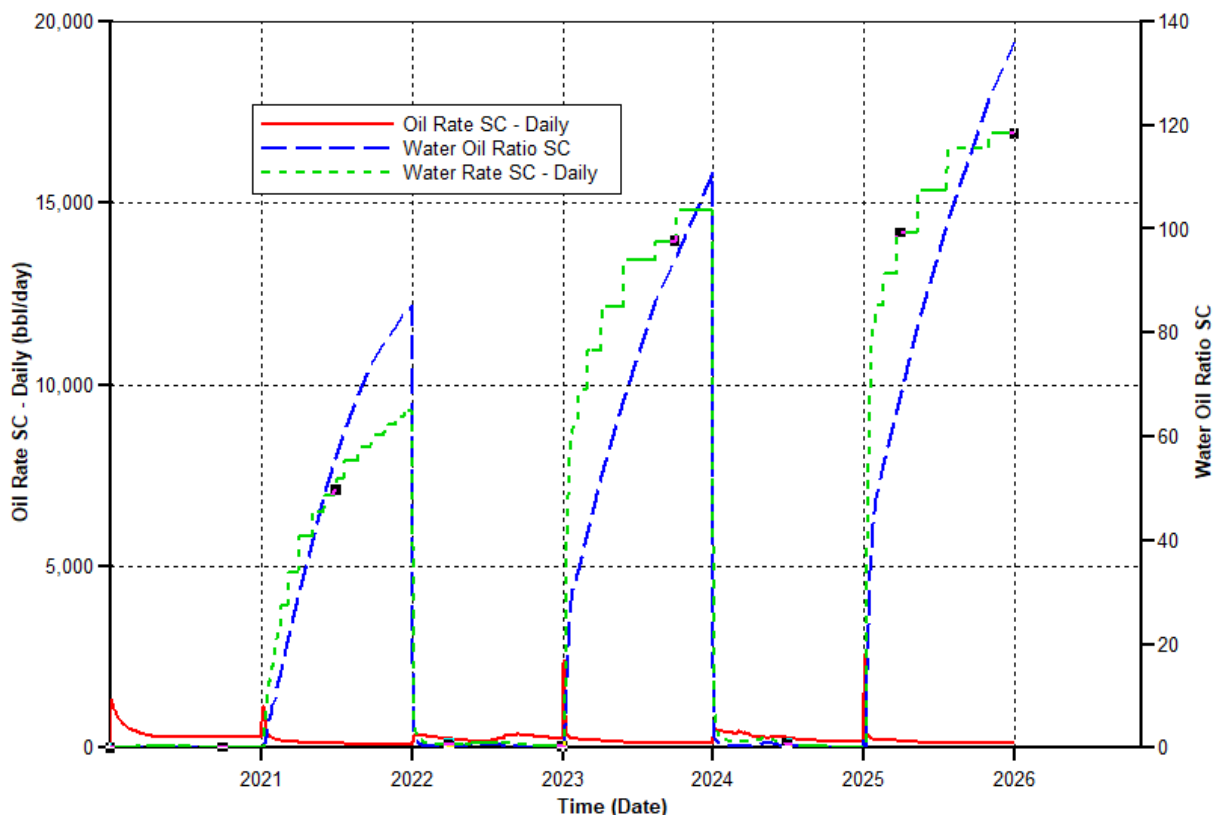


**Figure 4.12a:** OPR, WPR, and WOR versus time for hot 200 °F WAG injection 12-month

Figure 4.12b shows the cumulative oil production plot, which based on the simulation result, 553332 barrels of oil have been produced, which means more oil is produced with increasing temperature and cycle duration.

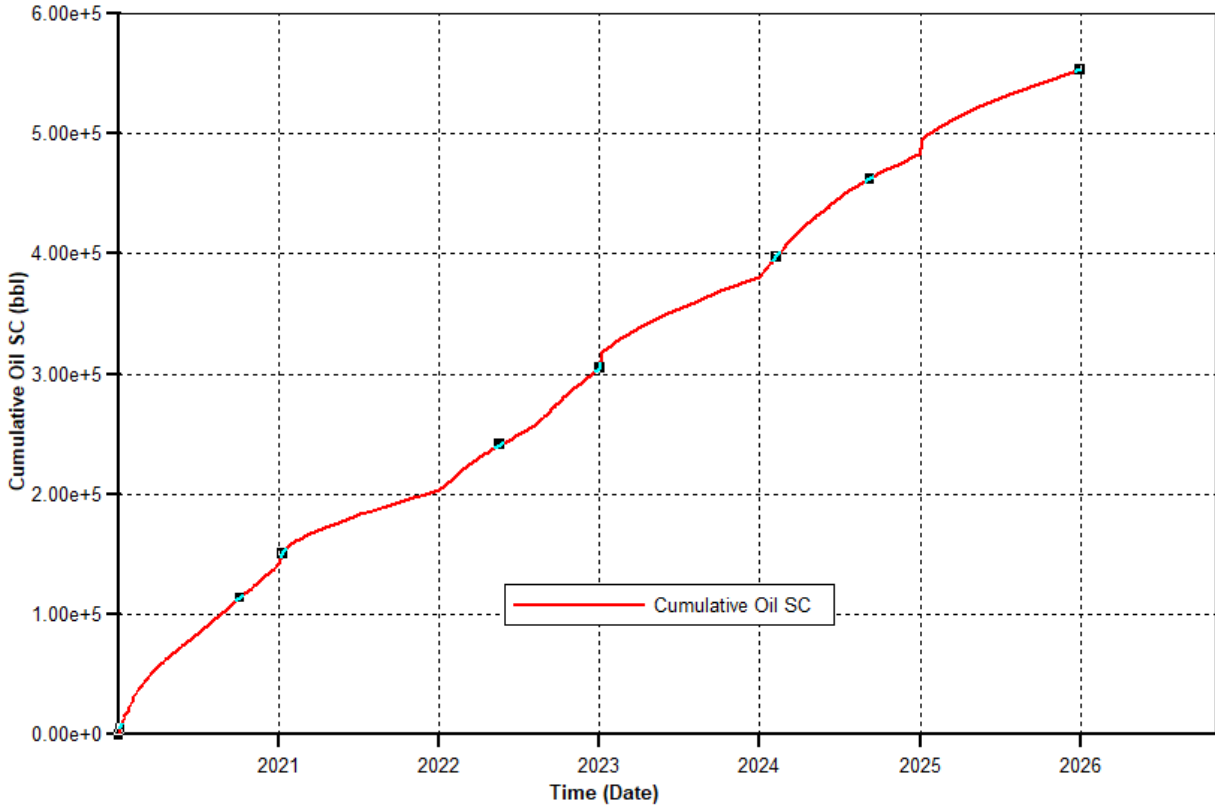


**Figure 4.12b:** Cumulative oil production versus time for hot 200 °F WAG injection 12-month

#### 4.3.7 Hot 211 °F WAG injection 12-month

Hot WAG injection with a one-year cycle and an injection temperature of 211 °F has been used in this study to investigate the effect of Hot WAG injection on production performance. Figure 4.12a shows the effect of this scenario on production performance based on analyzing the simulation output as seen in Figure 4.13a and 4.13b. oil production rate is around 320 bpd as indicated in red colour. The water production rate increased in years 2021 to 2022, 2023 to 2024, and 2025 to 2026, this increase is due to the water-alternating gas cycle which gas is injected then water. The water production rate has increased to 7000 bpd and declines when gas is injected. The increase in water production is due to the presence of large fractures within the reservoir, which contribute to transport the water to the wellbore. The cumulative oil production is about 591325 barrels as shown in Figure 4.13b.

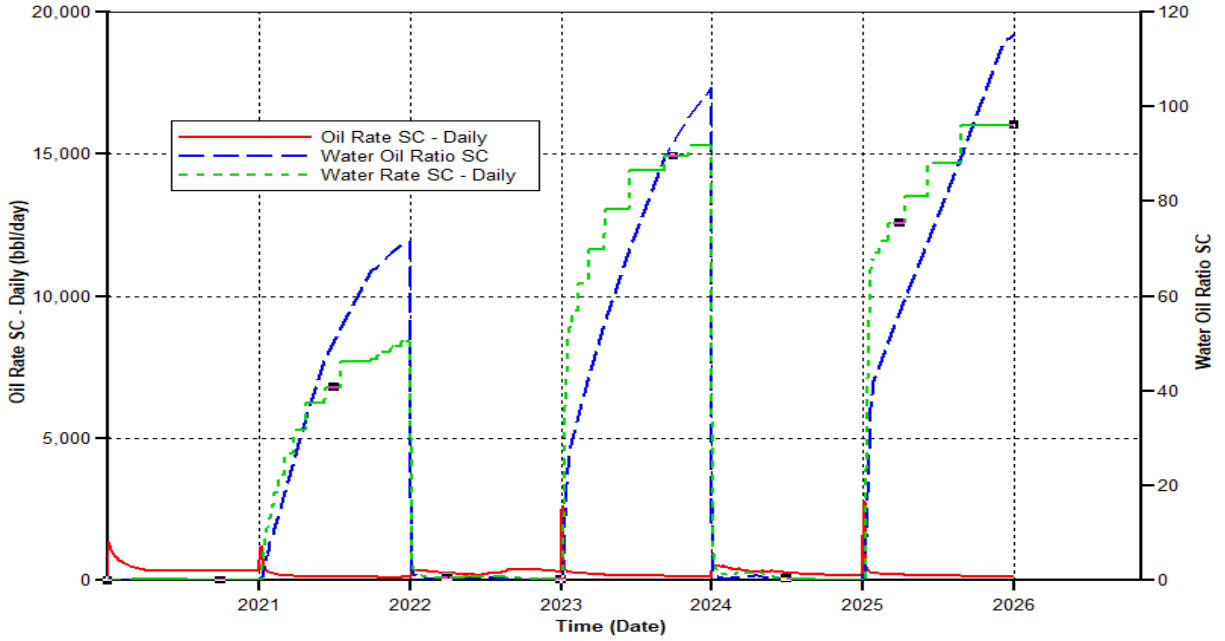


**Figure 4.13a:** OPR, water production rate, and WOR versus time for hot 211 °F WAG injection 12-month

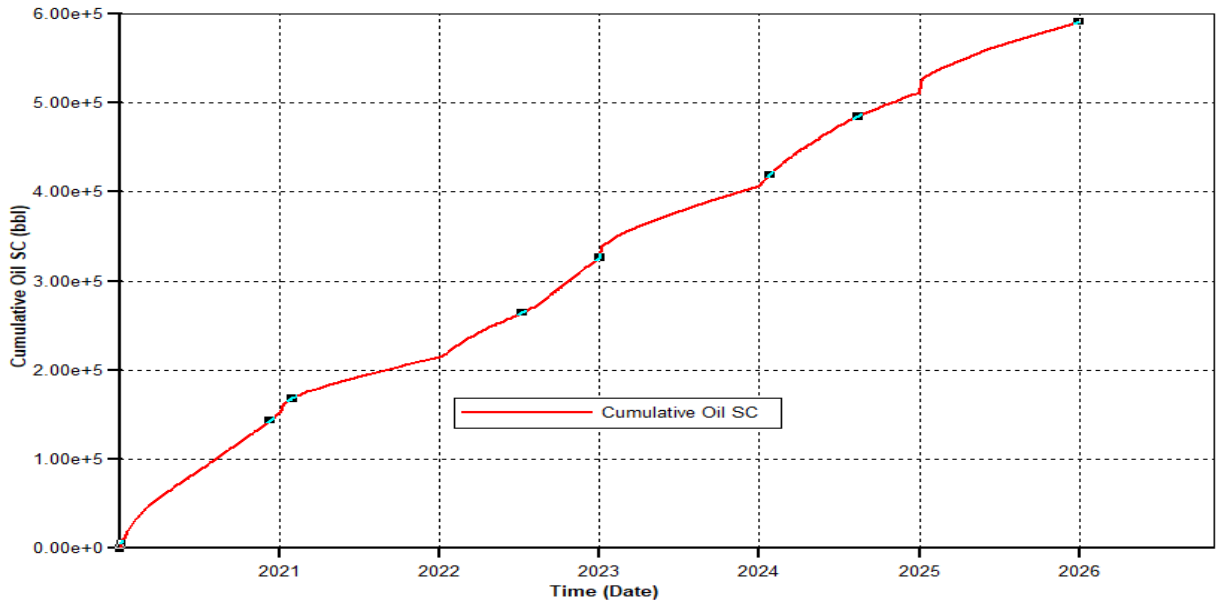


**Figure 4.13b:** Cumulative oil production versus time for hot 211 °F WAG injection 12-month

### 4.3.8 Hot 190 °F WAG injection at 2700 psi 12-month

Figure 4.14a shows the plot of water production rate, WOR and oil production rate versus time for hot WAG injection (2700 psi) for a 12-month scenario. Based on the simulation result, the oil production rate is around 200 bpd while water production rate in 2021 started to increase from 2021 to a maximum of 6000 bpd in 2022. In 2023, the water production rate increased from 0 to 7600 bpd in 2024, and in 2025, the water production rate has increased from 0 to a maximum of 11600 bpd. The total oil production has reached 464170 barrels for this scenario as seen in Figure 4.14b. This result is due to the fact that in this scenario, higher injection pressure of 2700 psi has been used which affects the production performance negatively with the presence of fractures compared to previous cases.

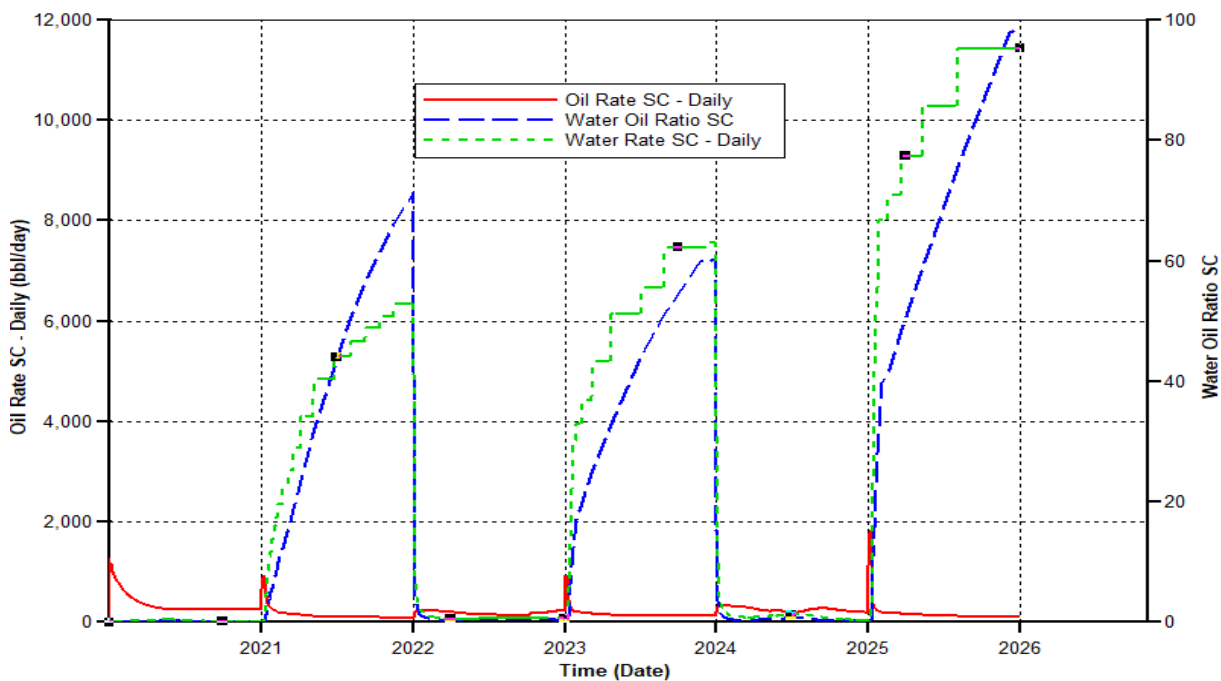


**Figure 4.14a:** OPR, WCT, and WOR versus time for hot 190 °F WAG injection at 2700 psi 12-month

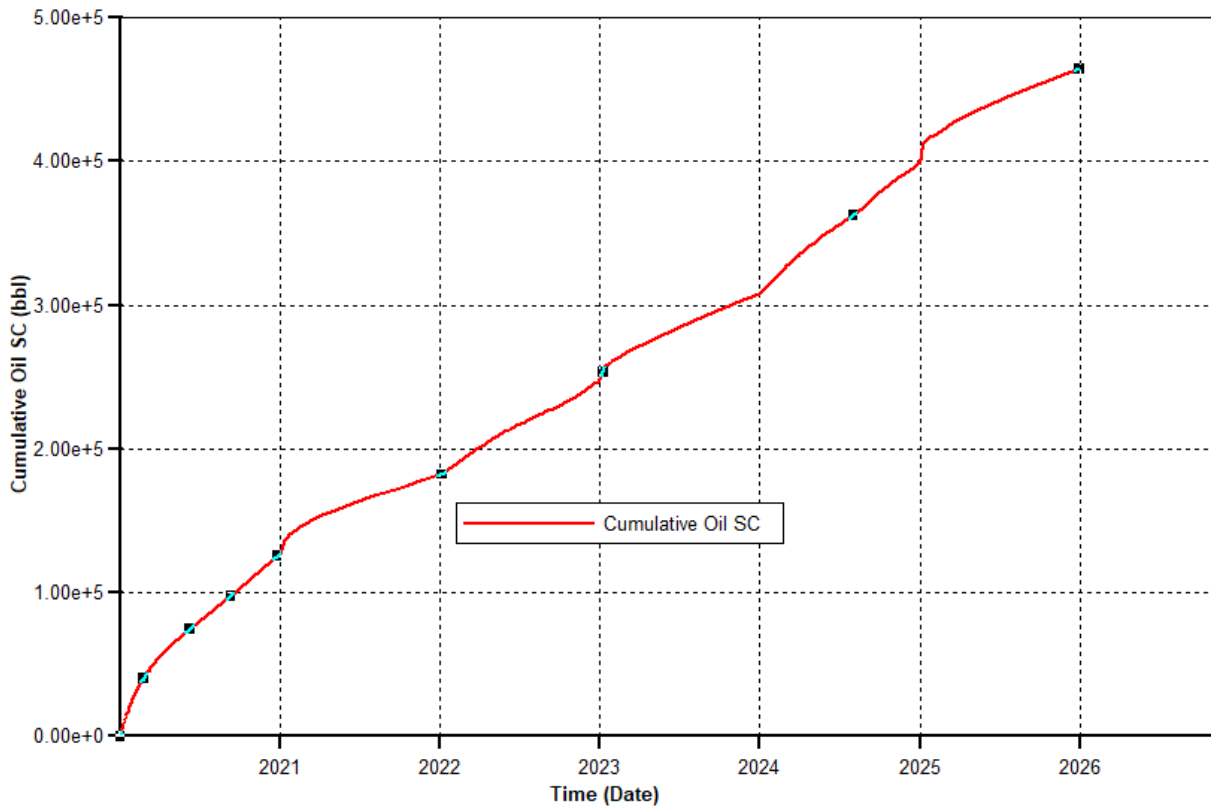


**Figure 4.14b:** Cumulative oil production versus time for hot 190°F WAG injection at 2700 psi 12-month

#### 4.3.9 Hot 190°F WAG injection at 2400 psi 6-month

In this scenario, Hot-WAG injection with an injection pressure of 2400 psi and a cycle of 6-month has been used. Figures 4.15a and 4.15b show the production performance after using Hot-WAG injection with a 6-month cycles. Based on Figure 4.15a, the red color represents the oil production rate which around 140 bpd and the water production rate is between 3000 bpd to 3500 bpd while the WOR is between 30 to 40. The cumulative oil production is shown in Figure 4.15b, which around 389809 barrels has been produced.

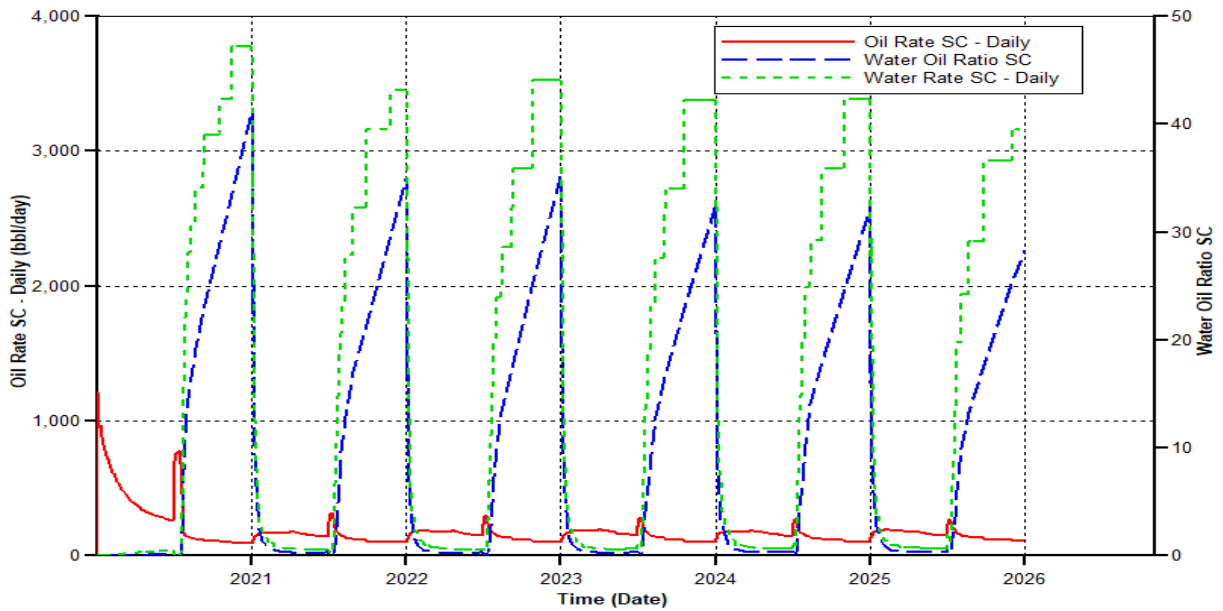


**Figure 4.15a:** OPR, WCT, and WOR versus time for hot 190°F WAG injection at 2400 psi 6-month

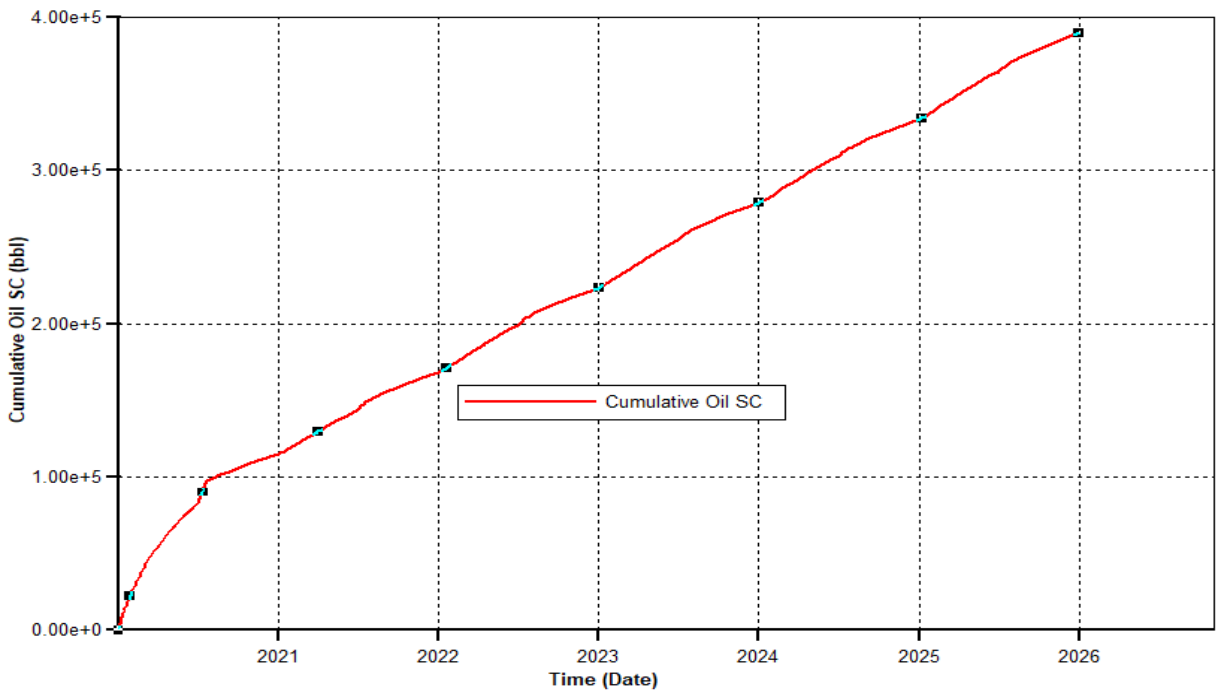
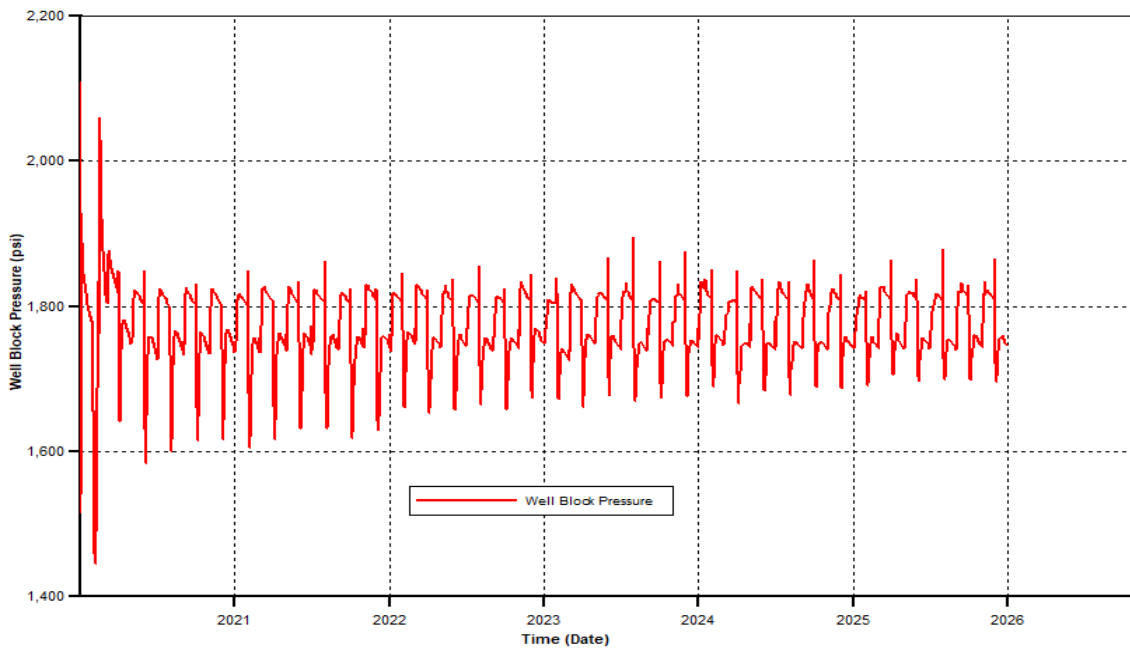


**Figure 4.15b:** Cumulative oil production versus time for hot 190°F WAG injection at 2400 psi 6-month

#### 4.4 Discussions

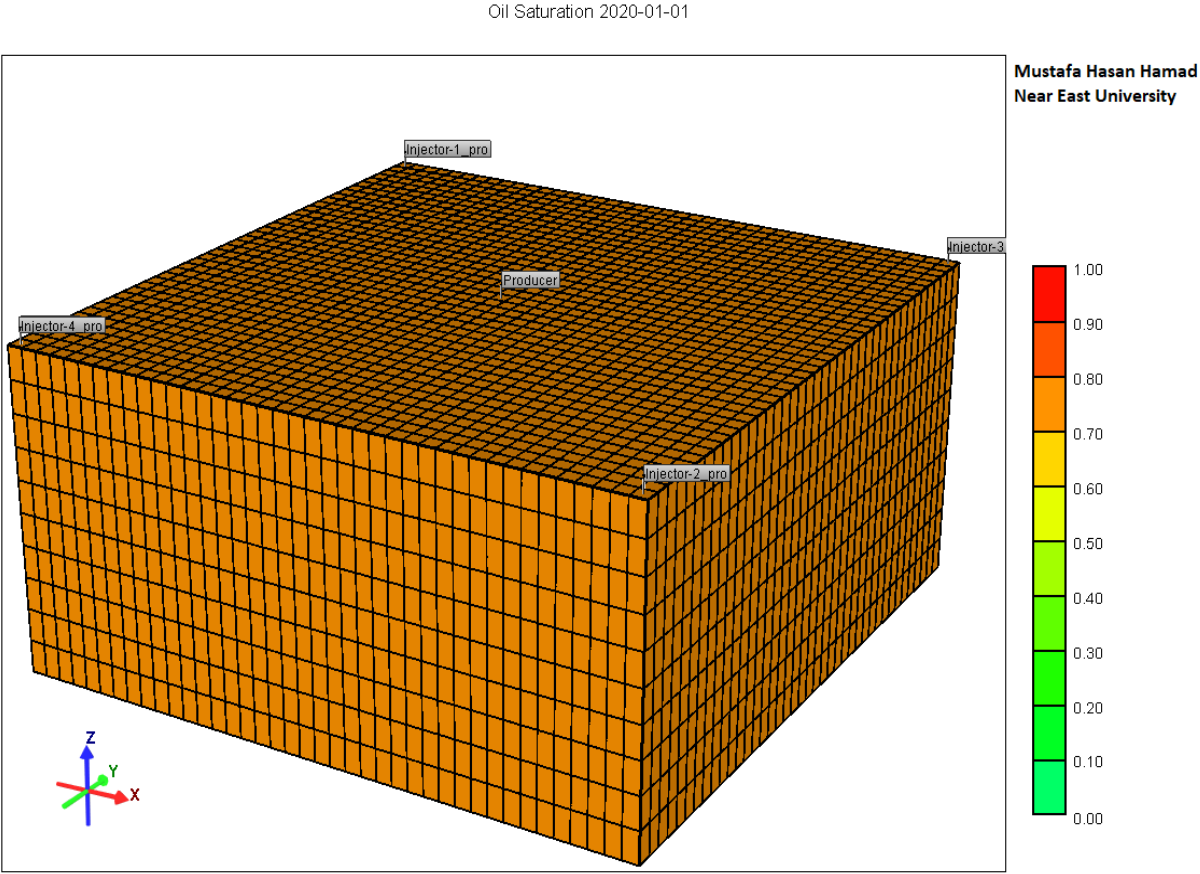
One of the main functions of EOR is to increase or maintain pressure after pressure depletion occurs. Figure 4.16 shows the well block pressure Versus time which the simulation result shows that there is a reduction and increase in well pressure as hot-WAG is injected. This result proves that hot-WAG maintains and increases the field pressure which in turn results in an increase of heavy oil recovery.

Fractured carbonate heavy oil reservoir is a complex reservoir because most of EOR methods cannot be used as excessive water production issues results in most cases or not successful production optimization. Therefore, knowing what method to use is indeed important to maximize the overall oil production. In this study, hot-WAG injection, water flooding and CO<sub>2</sub> flooding has been used to maximize oil recovery. From the water flooding result, excessive water production is resulted which affected the production negatively. CO<sub>2</sub> flooding was successful but not as successful as hot-WAG injection which results in greater heavy oil recovery due to the fact that injecting miscible gas into heavy oil helps to upgrade it, while injecting the water afterward the gas pushes the oil toward the wellbore.

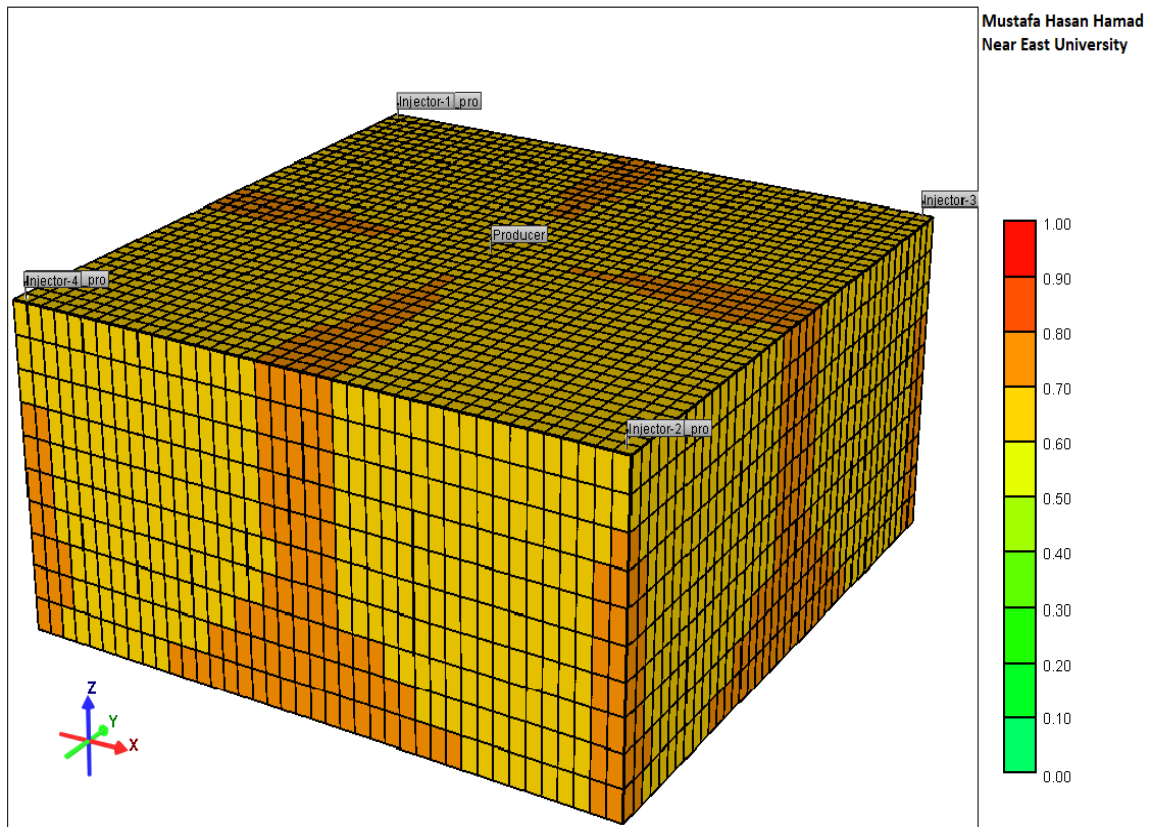


**Figure 4.16:** Well pressure versus time for hot WAG injection scenario

Figure 4.17a shows the 3D model of the base case, while Figure 4.17b shows the 3D model after implementing Hot-WAG injection. As seen in the Figure, the plot represents the oil saturation, which is around 80% as indicated in orange color. After implementing Hot-WAG injection, the heavy oil saturation has reduced significantly to between 60% to 65%. This result proves that Hot-WAG injection contributed to recover heavy oil.

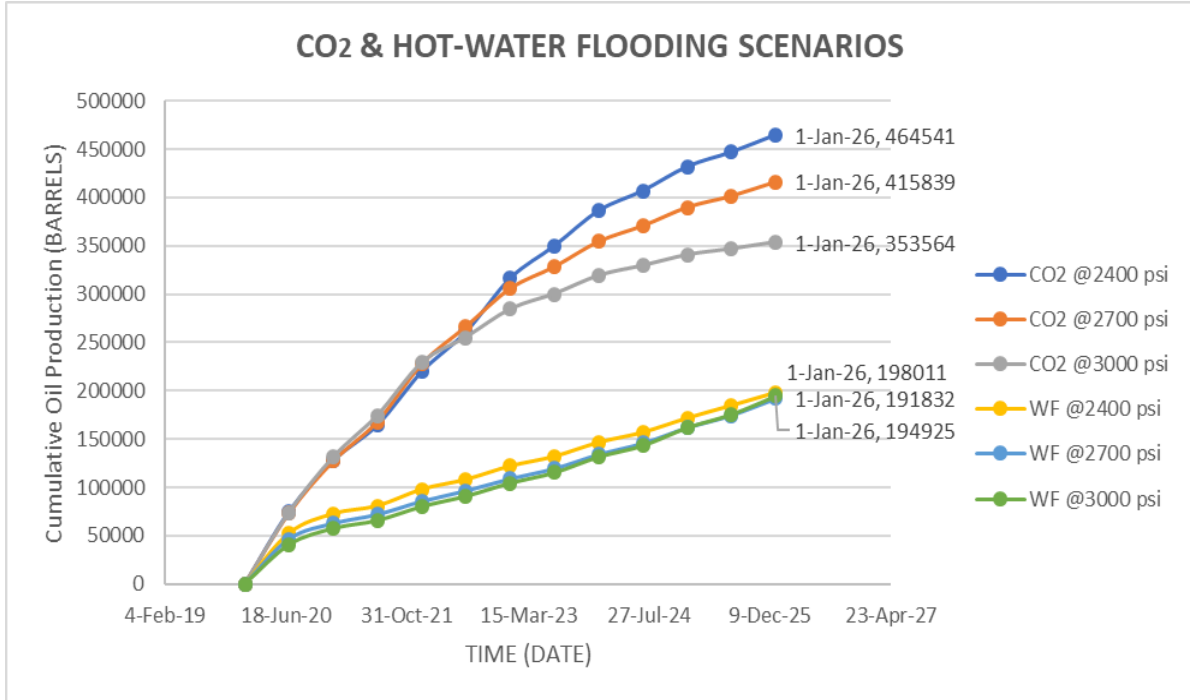


**Figure 4.17a:** 3D model for hot WAG injection scenario (Base-Case)



**Figure 4.17b:** 3D model for hot WAG injection scenario (after implementing hot WAG injection)

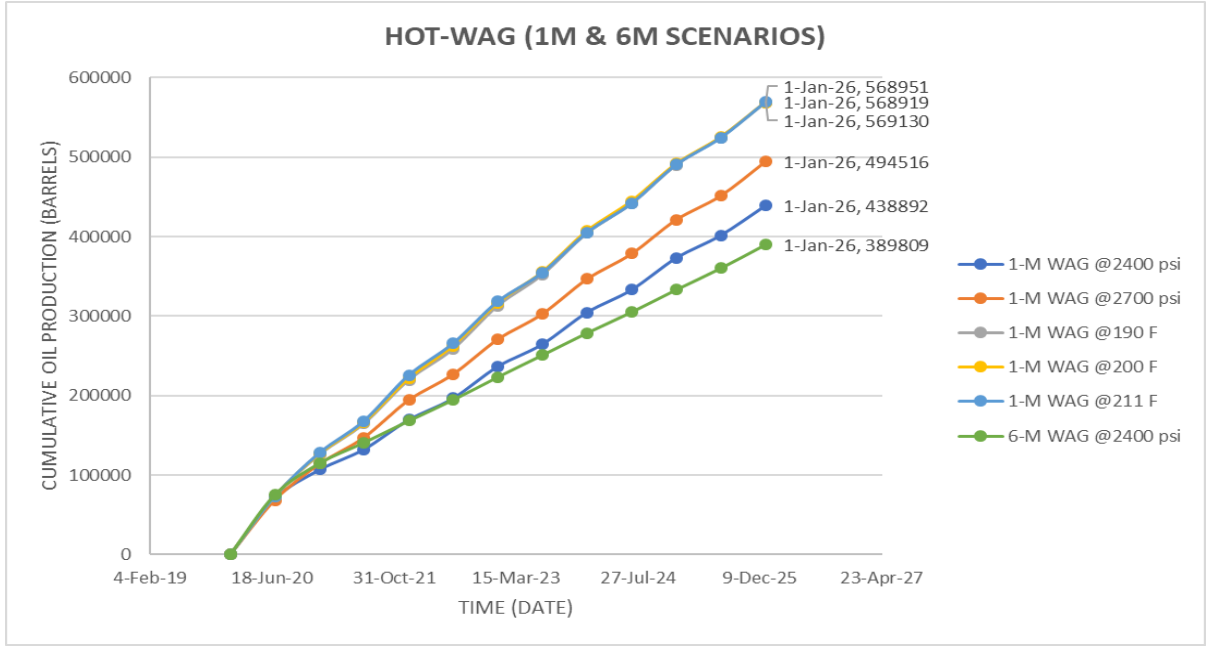
Additionally, Figure 4.18 shows the plot of cumulative oil production for CO<sub>2</sub> flooding and hot water-flooding cases in this study. Based on the result, injecting CO<sub>2</sub> with an injection pressure of 2400 psi results in the greatest cumulative oil production of 464541 barrels compared to other CO<sub>2</sub> flooding scenarios and hot water-flooding cases. Meanwhile the hot water flooding scenarios provide the lowest cumulative oil production due to the presence of fractures within the reservoir and the fact that the oil is heavy.



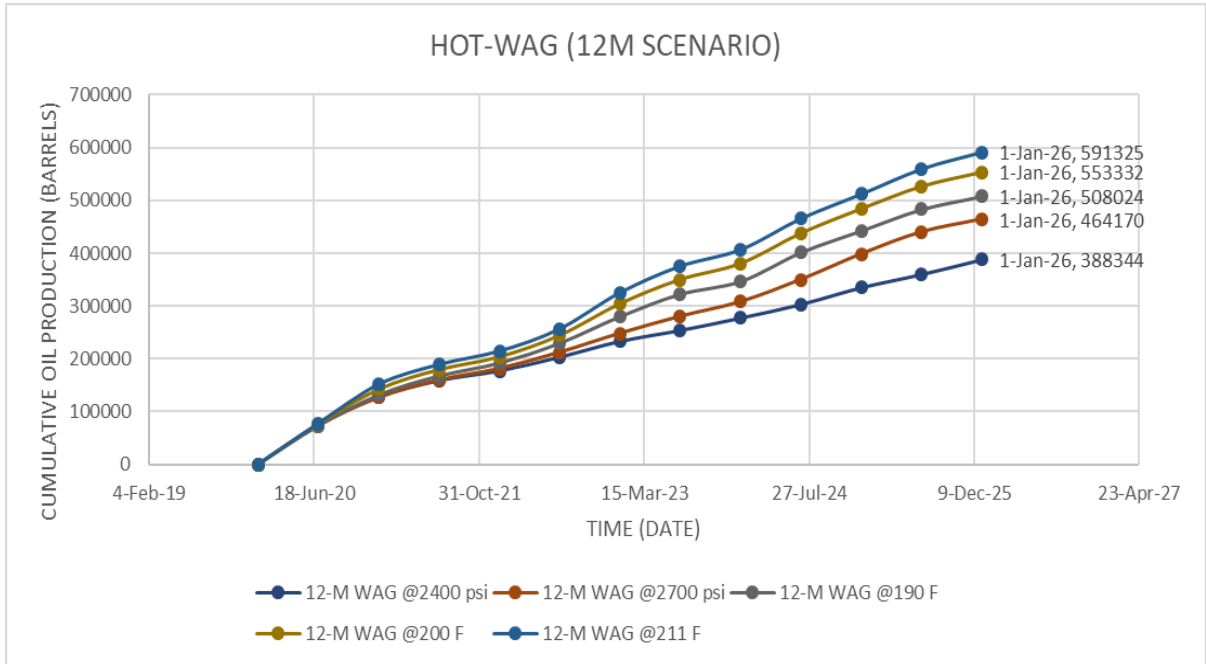
**Figure 4.18:** Cumulative oil production for different CO2 and hot Water-Flooding scenarios

Figure 4.19 shows the total oil production for one month and six-month hot WAG scenarios. The result proves that one-month WAG injection at an injection temperature of 211 °F produces the highest amount of oil with an amount of 569130 barrels. While six-month WAG injection with an injection pressure of 2400 psi produces the lowest amount of oil.

Figure 4.20 illustrates the simulation result for 12-month WAG injection at different injection pressure and temperature. The result is analyzed based on cumulative oil production as seen in Figure 4.20 the result proves that 12-Month Hot-WAG 211 °F case scenario provides the greater cumulative oil production of 591325 barrels. However, Hot 190 °F WAG at 2400 psi for 12-Month injection results in the lowest amount of oil compared to other 12-month WAG injection scenarios.



**Figure 4.19:** Cumulative oil production for one month and six-month WAG scenarios



**Figure 4.20:** Cumulative oil production for twelve-month WAG scenarios

## CHAPTER 5

### CONCLUSIONS AND RECOMMENDATIONS

#### 5.1 Conclusions

In this chapter, conclusions of the study have been discussed and summarized.

The following are the main conclusive remarks of this project:

1. Hot water-flooding scenarios have shown that excessive water production is resulted due to the presence of fractures, high water mobility and high oil viscosity.
2. Based on the simulation result, CO<sub>2</sub> is an efficient EOR technique to extract hydrocarbon in fractured carbonate reservoirs, with no water production problems.
3. Hot WAG injection method has shown that oil can be extracted in case of using both; gas to upgrade the oil and reducing its viscosity, and injecting water afterward to push the remaining oil.
4. The 1-month, 6-month and 12-month injection cycle, injection temperature 190, 200 and 211 °F and injection pressure 2400, 2700 and 3000 psi are the main factors that affected oil recovery, in which 12-month cycle and higher injection temperature are desirable and effective for higher oil recovery in heavy oil fractured carbonate reservoirs.
5. The result proves that a 12-month cycle WAG injection with an injection temperature of 211 °F produces the greatest oil amount, therefore it has been selected as the best scenario for this study.

## **5.2 Recommendations**

In this study, hot WAG flooding has been used and compared with hot water flooding and CO<sub>2</sub> flooding. Different parameters have been investigated, including injection pressure, injection temperature, and injection cycle. Based on our result, the best method is HOT-WAG injection with high pressure to optimize heavy oil production. Unfortunately, less study has been made to examine the effect of other factors on WAG performance, including wettability, relative permeability, heterogeneity and injection pattern. Therefore, I recommend further study to be made on the effect of certain factors on WAG injection performance in heavy oil fractured carbonate reservoir.

## REFERENCES

- Adjoutah, L. (2019). The Project Process “WAG”. *Society of Petroleum Engineers*.
- Aguilera, R. (1998). Geologic aspects of naturally fractured reservoirs. *The Leading Edge*, 17(12), 1667–1670. <https://doi.org/10.1190/1.1437912>
- Alajmi, A. F., Gharbi, R., and Algharaib, M. (2009). Investigating the performance of hot water injection in geostatistically generated permeable media. *Journal of Petroleum Science and Engineering*, 66(3–4), 143–155.
- Alvarez, J, M., and Han, S. (2013). Current overview of cyclic steam injection process, *Journal of Petroleum Science Research*.
- Ancheyta, J., and Speight, J.G. (2007). Hydro processing of Heavy Oils and Residual. Florida: CRC-Taylor and Francis Group, Boca Raton, Florida.
- Arshad, Aziz, Al-Majed, Abdulaziz A., Menouar, Habib, Muhammadain, Abdulrahim M., and Bechir Mtawaa. (2009). Carbon Dioxide (CO<sub>2</sub>) Miscible Flooding in Tight Oil Reservoirs: A Case Study. *Paper presented at the Kuwait International Petroleum Conference and Exhibition, Kuwait City, Kuwait*,
- Ashrafi, M., Souraki, Y., Karimaie, H., Torsaeter, O., and Bjorkvik, B. J. (2011). Experimental PVT property analyses for Athabasca bitumen. *Society of Petroleum Engineers. Presented at Canadian Unconventional Resources Conference*.
- Ashrafi, M., Souraki, Y., Karimaie, H., Torsaeter, O., and Bjorkvik, B. J. A. (2011). Experimental PVT Property Analyses for Athabasca Bitumen. *Paper CSUG/SPE 147064 presented at the Canadian Unconventional Resources Conference held in Calgary, Alberta, Canada*.
- Barenblatt, G., Zheltov, I., and Kochina, I. (1960). Basic concepts in the theory of seepage of homogeneous liquids in fissured rocks [strata]. *Journal of Applied Mathematics and Mechanics*, 24(5): 1286–1303.
- Batzle, M., Zadler, B., Hofmann, R., and Han, D. (2005). Heavy oils - Seismic properties. *67th EAGE Conference and Exhibition*.
- Bourbiaux, B. (2010). Fractured Reservoir Simulation: a Challenging and Rewarding Issue. *Oil & Gas Science and Technology-revue De L Institut Francais Du Petrole*, 65, 227-238.

- Bratton, T., Canh, D., Que, N., Duc, N.V., Gillespie, P., Hunt, D., Li, B., Marcinew, R., Ray, S., Montaron, B., Nelson, R., Schoderbeck, D., and Sonnerland, L. (2006). The nature of naturally fractured reservoirs. *Oilfield Review*. 18. 4-23.
- Butler, R. M. (1991). Thermal recovery of oil and bitumen. Prentice Hall.
- Chen, Z. (1989). Transient flow of slightly compressible fluids through double porosity, double-permeability systems - a state-of-the-art review. *Journal of Transport in Porous Media*, 4(2):147–184.
- Curtis, C., R. Kopper, E. Decoster, A. G. Garcia, C. Huggins, L. Knauer, M. Minner, N. Kupsch, L. M. Linares, H. Rough, and M. Waite. (2002). Heavy-oil reservoirs. *Oilfield Review*, 14, 30-51.
- Dorostkar, M. J., Mohebbi, A., Sarrafi, A., and Soltani, A. (2009). A laboratory study of hot WAG injection into fractured and conventional sand packs. *Petroleum Science*, 6(4), 400-404.
- Ebadati, A., Akbari, E., and Davarpanah, A. (2018). An experimental study of alternative hot water alternating gas injection in a fractured model. *Energy Exploration and Exploitation*, 37(3), 945–959.
- Foroozanfar M., and Aminshahidy, B. (2013) Efficiency evaluation of immiscible water alternating gas(IWAG) process in one of Iranian oil reservoirs. *Global Journal of Science (GJSET) publishing, Engineering and Technology*, 14: 76-81
- Gai, P. Y., Yin, F. H., Hao, T. T., and Zhang, Z. P. (2012). Experimental research on hot water flooding of different rhythm heavy oil reservoir after the steam injection. *Advanced Materials Research*, 550-553, 2878-2882.
- Gringarten, A. C. (1984). Interpretation of tests in fissured and Multilayered reservoirs with double-porosity behavior: Theory and practice. *Journal of Petroleum Technology*, 36(04), 549-564.
- Gringarten, A. C. (1987). How to recognize "double-porosity" Systems from well tests. *Journal of Petroleum Technology*, 39(06), 631-633.
- Hite, J. and Bondor, Paul. (2004). Planning EOR Projects. 10.2118/92006-MS.
- IEA. (2005). Resources to Reserves: Oil and Gas Technologies for the Energy Markets of the Future. Paris, France: International Energy Agency.
- Kamali, F., and Cinar, Y. (2013). Optimizing Enhanced Oil Recovery and CO<sub>2</sub> Storage by Simultaneous Water and CO<sub>2</sub> Injection. *Energy Exploration and Exploitation*.

- Lake, L. W. (2010). Enhanced oil recovery. Richardson, Tex.: *Society of Petroleum Engineers*.
- Lee Y, Park H, Lee J, et al. (2018) Enhanced oil recovery efficiency of low-salinity water flooding in oil reservoirs including Fe<sup>2</sup> ions. *Energy Exploration and Exploitation*. 3(1).
- Lei, H., Yang, S., Zu, L., Wang, Z., and Li, Y. (2016). Oil recovery performance and CO<sub>2</sub> storage potential of CO<sub>2</sub> water-Alternating-Gas injection after continuous CO<sub>2</sub> injection in a Multilayer formation. *Journal of Energy and Fuels*, 30(11), 8922-8931.
- Lemonnier, P. and Bourbiaux, B. (2010b). Simulation of naturally fractured reservoirs. state of the art - part 2 - matrix-fracture transfers and typical features of numerical studies. *Oil and Gas Science and Technology*, 65(2):263–286.
- Mari Albrigtsen. (2015). EOR Opportunities on the Gyda Field, a WAG Injection Simulation Study. *Semantic Scholar*.
- Meyer, R. F. (1997). Heavy Crude Oil Resources. Presented at the 15th World Petroleum Congress. Beijing, China.
- Moench, A. F. (1984). Double-porosity models for a fissured groundwater reservoir with fracture skin. *Water Resources Research*, 20(07):831–846.
- Person, M., Wilson, J., and Morrow, N. (2017). Continental-shelf freshwater water resources and improved oil recovery by low-salinity waterflooding. *AAPG Bulletin* 101: 1–18.
- Petrowiki.org. (2015). Relative Permeability Models. Retrieved from [petrowiki.org/Relative\\_permeability\\_models#cite\\_note-r2-1](http://petrowiki.org/Relative_permeability_models#cite_note-r2-1)
- Pinerez, P., Puntervold, T, and Strand S. (2016). Experimental study of the response time of the low-salinity enhanced oil recovery effect during secondary and tertiary low-salinity waterflooding. *Energy and Fuels*. 30: 4733–4739.
- Saniere, A., Hénaut, I., and Argillier, J. F. (2004). Pipeline transportation of heavy oils, a strategic, economic and technological challenge. *Oil and Gas Science and Technology*, 59(5), 455-466.
- Sheng, J. J. (2013). Enhanced Oil Recovery - Field Case Studies: Elsevier.
- Slb.com. (2014c). Sweep efficiency. Retrieved 09/11/2014, from [http://www.glossary.oilfield.slb.com/en/Terms/a/areal\\_sweep\\_efficiency.aspx](http://www.glossary.oilfield.slb.com/en/Terms/a/areal_sweep_efficiency.aspx)
- Speight, J. (2013). Enhanced recovery methods for heavy oil and tar sands. *Elsevier*.
- Speight, J. (2016). Introduction to enhanced recovery methods for heavy oil and tar sands. New York: *Elsevier*.

- Spence, G. H. and Finch, E. (2014). Influences of nodular chert rhythmites on natural fracture networks in carbonates: an outcrop and two-dimensional discrete element modelling study.
- Spence, G. H., Redfern, J., Aguilera, R., Bevan, T. G., Cosgrove, J. W., Couples, G. D. and Daniel, J. M. (2014). Advances in the study of fractured reservoirs. *Geological Society*, London, Special Publications, 374, 211– 249.
- Taber, J. J., Martin, F. D., and Seright, R. S. (1997). EOR Screening criteria revisited—part 2: applications and impact of oil prices. *SPE*, 39234-PA.
- Taber, J., Martin, F., and Seright, R. (1997). EOR screening criteria revisited - Part 1: Introduction to screening criteria and enhanced recovery Field projects. *SPE Reservoir Engineering*, 12(03), 189-198.
- Terry, R. E. (2001). Enhanced oil recovery. Retrieved 08/12/2014, from [http://www.firp.ula.ve/archivos/cuadernos/01\\_Chap\\_Terry\\_EOR.pdf](http://www.firp.ula.ve/archivos/cuadernos/01_Chap_Terry_EOR.pdf)
- Venkatesan, V.N., and W.R. Shu. (1986). Alteration in heavy oil characteristics during thermal recovery." *J Can Pet Technol*: No Pagination Specified.
- Warren, J. E. and Root, P. J. (1963). The behavior of naturally fractured reservoirs. *Society of Petroleum Engineers Journal*, 3(03):245–255.
- Xuezhong, W., Yuanliang, Y., and Weijun, X (2016) Microbial enhanced oil recovery of oil-water tran-sitional zone in thin-shallow extra heavy oil reservoirs: A case study of Chunfeng Oilfield in westernmargin of Junggar Basin, NW China. *Petroleum Exploration and Development* 43: 689–694.
- Zerafat, M. M., Ayatollahi, Sh., Mehranbod, N., and D. (2011). Barzegari. "Bayesian Network Analysis as a Tool for Efficient EOR Screening. Paper presented at the *SPE Enhanced Oil Recovery Conference*, Kuala Lumpur, Malaysia.
- Zhao, David W., and Ian D. Gates. (2013). Stochastic Optimization of Hot Water Flooding Strategy in Thin Heavy Oil Reservoirs. Paper presented at the *SPE Heavy Oil Conference-Canada*, Calgary, Alberta, Canada.

## **APPENDICES**

**Appendix 1**  
**Hot-Water-Flooding CMG-STARS Data**

INUNIT FIELD  
WSRF WELL 1  
WSRF GRID TIME  
WSRF SECTOR TIME  
OUTSRF GRID PRES SG SO SW TEMP  
OUTSRF WELL LAYER NONE  
WPRN GRID 0  
OUTPRN GRID NONE  
OUTPRN RES NONE

\*\* Distance units: ft  
RESULTS XOFFSET       0.0000  
RESULTS YOFFSET       0.0000

\*\* (DEGREES)  
\*\* (DEGREES)  
RESULTS ROTATION       0.0000 \*\* (DEGREES)  
RESULTS AXES-DIRECTIONS 1.0 -1.0 1.0

\*\*  
\*\*\*\*\*

\*\* Definition of fundamental cartesian grid  
\*\*

\*\*\*\*\*

GRID VARI 40 40 10  
KDIR DOWN  
DI IVAR  
40\*41  
DJ JVAR  
40\*41  
DK ALL  
16000\*10  
DTOP  
1600\*4500  
DUALPOR  
SHAPE GK

\*\* 0 = null block, 1 = active block

```

NULL *MATRIX CON      1
** 0 = null block, 1 = active block
NULL *FRACTURE CON    1
DIFRAC CON      0.001
PERMJ MATRIX EQUALSI
PERMJ FRACTURE EQUALSI
PERMK *MATRIX KVAR
0.3 2*0.31 0.33 0.29 0.3 0.33 0.35 0.32 0.3
PERMK *FRACTURE CON    150
** 0 = pinched block, 1 = active block
PINCHOUTARRAY CON    1
DJFRAC EQUALSI
DKFRAC KVAR
0 7*0.001 2*0
POR *FRACTURE KVAR
0.004 0.0042 0.0045 0.0028 0.0035 0.0048 0.0027 0.0032 0.003 0.0031
POR *MATRIX KVAR
0.12 0.125 0.13 0.14 0.135 0.138 0.128 0.126 0.14 0.123
PERMI *FRACTURE KVAR
1830 1750 1850 1645 1570 2100 1950 1320 1290 1120
PERMI *MATRIX KVAR
30 2*31 33 29 30 33 35 32 30
END-GRID
ROCKTYPE 1
PRPOR 2100
CPOR 6e-6
** Model and number of components
** Model and number of components
** Model and number of components
MODEL 4 4 4 1
COMPNAME 'Water' 'Dead_Oil' 'Soln_Gas' 'CO2'
CMM
0 314.824 24.3927 44.01
PCRIT
0 0 655.035 1069.8
TCRIT
0 0 -40.3276 87.89
KV1
0 0 54415.5 0
KV2
0 0 0.00226612 0
KV3
0 0 2.45478 0
KV4

```

0 0 -1583.98 0  
 KV5  
 0 0 -446.782 0  
 PRSR 14.6488  
 TEMR 139  
 PSURF 14.6488  
 TSURF 62.33  
 MASSDEN  
 64.9423 57.6721 24.1393 24.1393  
 CP  
 2.96889e-006 3.73926e-006 3.73926e-006 3.73926e-006

CT1  
 0.000210377 0.000404861 0.000404861 0.000404861

AVG  
 0 0 2.61316e-005 0

BVG  
 0 0 1 0

VISCTABLE

**	temp					
41	1.66863	3770.48	6.07323	6.07323	** Live oil visc (P=2346.82) = 169.287	
59	1.24688	1866.63	4.6228	4.6228	** Live oil visc (P=2346.82) = 103.143	
77	0.97902	980.24	3.59999	3.59999	** Live oil visc (P=2346.82) = 65.5071	
95	0.791124	542.808	2.86164	2.86164	** Live oil visc (P=2346.82) = 43.1881	
104	0.717503	411.345	2.56942	2.56942	** Live oil visc (P=2346.82) = 35.5197	
139	0.521154	295.264	3.41459	3.41459	** Live oil visc (P=2346.82) = 34.3207	
140	0.516908	292.586	3.44137	3.44137	** Live oil visc (P=2346.82) = 34.2884	
160	0.439822	189.91	3.03998	3.03998	** Live oil visc (P=2346.82) = 25.8243	
176	0.391444	78.6042	1.57904	1.57904	** Live oil visc (P=2346.82) = 11.9267	
248	0.256148	17.8446	0.856286	0.856286	** Live oil visc (P=2346.82) = 4.1216	
320	0.19014	6.02724	0.546907	0.546907	** Live oil visc (P=2346.82) = 1.89319	
392	0.152884	2.6796	0.391196	0.391196	** Live oil visc (P=2346.82) = 1.05879	
464	0.127359	1.44702	0.303186	0.303186	** Live oil visc (P=2346.82) = 0.680662	
536	0.107844	0.899242	0.248999	0.248999	** Live oil visc (P=2346.82) = 0.48391	
608	0.0937713	0.619632	0.213409	0.213409	** Live oil visc (P=2346.82) = 0.370465	
680	0.0823501	0.461228	0.188834	0.188834	** Live oil visc (P=2346.82) = 0.299752	
752	0.07344	0.364015	0.171182	0.171182	** Live oil visc (P=2346.82) = 0.252932	
824	0.0660552	0.300509	0.158095	0.158095	** Live oil visc (P=2346.82) = 0.220421	
896	0.0598572	0.256913	0.148137	0.148137	** Live oil visc (P=2346.82) = 0.196968	
968	0.0545812	0.225764	0.140397	0.140397	** Live oil visc (P=2346.82) = 0.179516	
1040	0.0500357	0.202772	0.13427	0.13427	** Live oil visc (P=2346.82) = 0.166194	
1112	0.0460789	0.185336	0.129344	0.129344	** Live oil visc (P=2346.82) = 0.155804	
1184	0.0426033	0.171811	0.125333	0.125333	** Live oil visc (P=2346.82) = 0.147553	
1256	0.0395261	0.16112	0.122028	0.122028	** Live oil visc (P=2346.82) = 0.140899	
1328	0.0367827	0.152529	0.119277	0.119277	** Live oil visc (P=2346.82) = 0.135462	

1400 0.0343214 0.145528 0.116966 0.116966 \*\* Live oil visc (P=2346.82) = 0.130966  
 1472 0.0321009 0.139753 0.115011 0.115011 \*\* Live oil visc (P=2346.82) = 0.127211  
 1544 0.0300875 0.134939 0.113343 0.113343 \*\* Live oil visc (P=2346.82) = 0.124047  
 VSMIXCOMP 'Soln\_Gas'  
 VSMIXENDP 0.00680369 0.49  
 VSMIXFUNC 0.00680369 0.0649184 0.119184 0.170503 0.219362 0.266376 0.312057  
 0.356805 0.401034 0.445197 0.48936  
 ROCKFLUID  
 RPT 1 WATWET  
 \*\* Sw krw krow  
 SWT  
 5.200000E-02 0.00000 0.300000  
 5.353000E-02 0.00000 0.297640  
 6.424000E-02 0.00000 0.281473  
 7.495000E-02 0.00000 0.265910  
 8.566000E-02 0.00000 0.250941  
 9.637000E-02 0.00000 0.236552  
 0.107080 0.00000 0.222731  
 0.117790 0.00000 0.209468  
 0.128500 0.00000 0.196750  
 0.139210 0.00000 0.184564  
 0.149920 0.00000 0.172900  
 0.160630 0.00000 0.161745  
 0.171340 0.00000 0.151087  
 0.182050 0.00000 0.140915  
 0.192760 0.00000 0.131216  
 0.194290 6.042947E-07 0.129869  
 0.205000 6.015733E-06 0.120697  
 0.215710 2.307301E-05 0.111974  
 0.226420 5.988640E-05 0.103688  
 0.237130 1.254947E-04 9.582704E-02  
 0.247840 2.296910E-04 8.837941E-02  
 0.258550 3.829133E-04 8.133356E-02  
 0.269260 5.961670E-04 7.467789E-02  
 0.279970 8.809674E-04 6.840081E-02  
 0.290680 1.249295E-03 6.249076E-02  
 0.301390 1.713558E-03 5.693622E-02  
 0.312100 2.286566E-03 5.172569E-02  
 0.322810 2.981498E-03 4.684771E-02  
 0.333520 3.811889E-03 4.229085E-02  
 0.344230 4.791602E-03 3.804372E-02  
 0.354940 5.934821E-03 3.409495E-02  
 0.365650 7.256029E-03 3.043322E-02  
 0.376360 8.769999E-03 2.704725E-02

0.387070	1.049178E-02	2.392579E-02
0.397780	1.243669E-02	2.105762E-02
0.408490	1.462029E-02	1.843159E-02
0.419200	1.705841E-02	1.603656E-02
0.429910	1.976711E-02	1.386147E-02
0.440620	2.276268E-02	1.189527E-02
0.451330	2.606164E-02	1.012699E-02
0.462040	2.968071E-02	8.545694E-03
0.472750	3.363685E-02	7.140500E-03
0.483460	3.794722E-02	5.900587E-03
0.494170	4.262916E-02	4.815191E-03
0.504880	4.770023E-02	3.873612E-03
0.515590	5.317818E-02	3.065215E-03
0.526300	5.908093E-02	2.379437E-03
0.537010	6.542661E-02	1.805790E-03
0.547720	7.223351E-02	1.333868E-03
0.558430	7.952010E-02	9.533553E-04
0.569140	8.730503E-02	6.540310E-04
0.579850	9.560709E-02	4.257830E-04
0.590560	0.104445	2.586189E-04
0.601270	0.113839	1.426824E-04
0.611980	0.123807	6.827563E-05
0.622690	0.134369	2.588991E-05
0.633400	0.145544	6.253676E-06
0.644110	0.157354	0.00000
0.650230	0.164394	0.00000
0.660940	0.177238	0.00000
0.671650	0.190768	0.00000
0.682360	0.205003	0.00000
0.693070	0.219963	0.00000
0.704000	0.236000	0.00000

\*\*      Sl            krg            krog

SLT

0.152000	0.250000	0.00000
0.161531	0.241431	0.00000
0.175189	0.229492	0.00000
0.182017	0.223671	1.840344E-06
0.195674	0.212322	1.393535E-05
0.209331	0.201358	4.554367E-05
0.222988	0.190773	1.055205E-04
0.236645	0.180560	2.024800E-04
0.250302	0.170713	3.448632E-04
0.263959	0.161226	5.409766E-04
0.277616	0.152092	7.990163E-04

0.291273	0.143305	1.127086E-03
0.304930	0.134858	1.533207E-03
0.318587	0.126745	2.025334E-03
0.332245	0.118960	2.611354E-03
0.345902	0.111495	3.299100E-03
0.359559	0.104346	4.096352E-03
0.373216	9.750387E-02	5.010845E-03
0.386873	9.096372E-02	6.050266E-03
0.400530	8.471866E-02	7.222266E-03
0.414187	7.876216E-02	8.534454E-03
0.427844	7.308770E-02	9.994407E-03
0.441501	6.768871E-02	1.160967E-02
0.455158	6.255865E-02	1.338774E-02
0.468815	5.769093E-02	1.533612E-02
0.482472	5.307897E-02	1.746224E-02
0.496129	4.871615E-02	1.977355E-02
0.509786	4.459585E-02	2.227743E-02
0.523443	4.071145E-02	2.498126E-02
0.537100	3.705626E-02	2.789240E-02
0.550757	3.362363E-02	3.101817E-02
0.564414	3.040686E-02	3.436589E-02
0.578071	2.739924E-02	3.794284E-02
0.591728	2.459403E-02	4.175629E-02
0.605385	2.198449E-02	4.581349E-02
0.619042	1.956383E-02	5.012167E-02
0.632699	1.732527E-02	5.468804E-02
0.646357	1.526198E-02	5.951979E-02
0.660014	1.336711E-02	6.462412E-02
0.673671	1.163381E-02	7.000816E-02
0.687328	1.005516E-02	7.567909E-02
0.700985	8.624252E-03	8.164402E-02
0.714642	7.334123E-03	8.791006E-02
0.728299	6.177789E-03	9.448433E-02
0.741956	5.148228E-03	0.101374
0.755613	4.238385E-03	0.108586
0.769270	3.441164E-03	0.116127
0.782927	2.749429E-03	0.124005
0.796584	2.156000E-03	0.132227
0.810241	1.653647E-03	0.140799
0.823898	1.235088E-03	0.149728
0.837555	8.929818E-04	0.159022
0.851212	6.199220E-04	0.168688
0.864869	4.084278E-04	0.178732
0.878526	2.509339E-04	0.189162

0.892183	1.397757E-04	0.199984
0.905840	6.716902E-05	0.211205
0.919497	2.518044E-05	0.222833
0.933154	5.677509E-06	0.234874
0.946811	0.00000	0.247335
0.953640	0.00000	0.253726
0.967297	0.00000	0.266830
0.980954	0.00000	0.280372
1.00000	0.00000	0.300000

BSWIRG \*MATRIX CON 0.24  
INITIAL  
VERTICAL DEPTH\_AVE  
  
INITREGION 1  
REFPRES 2100  
REFDEPTH 4500  
DWOC 4600  
TEMP \*MATRIX CON 139  
SW \*MATRIX CON 0.2  
SO \*MATRIX CON 0.8  
MFRAC\_OIL 'Soln\_Gas' \*FRACTURE CON 0.482558  
MFRAC\_OIL 'Soln\_Gas' \*MATRIX CON 0.482558  
MFRAC\_OIL 'Dead\_Oil' \*FRACTURE CON 0.517442  
MFRAC\_OIL 'Dead\_Oil' \*MATRIX CON 0.517442  
NUMERICAL  
RUN  
DATE 2020 1 1  
DTWELL 0.001  
\*\*  
WELL 'Producer'  
PRODUCER 'Producer'  
OPERATE MAX STO 15000.0 CONT  
\*\* rad geofac wfrac skin  
GEOMETRY I 0.28 0.249 1.0 0.0  
PERF GEOA 'Producer'  
\*\* UBA ff Status Connection  
20 20 3 1.0 OPEN FLOW-TO 'SURFACE' REFLAYER  
20 20 4 1.0 OPEN FLOW-TO 1  
20 20 5 1.0 OPEN FLOW-TO 2  
20 20 6 1.0 OPEN FLOW-TO 3  
20 20 7 1.0 OPEN FLOW-TO 4  
20 20 8 1.0 OPEN FLOW-TO 5  
\*\*  
WELL 'Injector-1\_pro'

```

INJECTOR MOBWEIGHT EXPLICIT 'Injector-1_pro'
INCOMP WATER 1.0 0.0 0.0 0.0
TINJW 190.0
OPERATE MAX BHP 3000.0 CONT
**      rad geofac wfrac skin
GEOMETRY K 0.28 0.249 1.0 0.0
  PERF  GEOA 'Injector-1_pro'
** UBA      ff      Status Connection
  1 1 8    1.0 OPEN  FLOW-FROM 'SURFACE' REFLAYER
  1 1 7    1.0 OPEN  FLOW-FROM 1
  1 1 6    1.0 OPEN  FLOW-FROM 2
  1 1 5    1.0 OPEN  FLOW-FROM 3
  1 1 4    1.0 OPEN  FLOW-FROM 4
**
WELL 'Injector-2_pro'
INJECTOR MOBWEIGHT EXPLICIT 'Injector-2_pro'
INCOMP WATER 1.0 0.0 0.0 0.0
TINJW 190.0
OPERATE MAX BHP 3000.0 CONT
**      rad geofac wfrac skin
GEOMETRY K 0.28 0.249 1.0 0.0
  PERF  GEOA 'Injector-2_pro'
** UBA      ff      Status Connection
  40 40 8  1.0 OPEN  FLOW-FROM 'SURFACE' REFLAYER
  40 40 7  1.0 OPEN  FLOW-FROM 1
  40 40 6  1.0 OPEN  FLOW-FROM 2
  40 40 5  1.0 OPEN  FLOW-FROM 3
  40 40 4  1.0 OPEN  FLOW-FROM 4
**
WELL 'Injector-3_pro'
INJECTOR MOBWEIGHT EXPLICIT 'Injector-3_pro'
INCOMP WATER 1.0 0.0 0.0 0.0
TINJW 190.0
OPERATE MAX BHP 3000.0 CONT
**      rad geofac wfrac skin
GEOMETRY K 0.28 0.249 1.0 0.0
  PERF  GEOA 'Injector-3_pro'
** UBA      ff      Status Connection
  40 1 8   1.0 OPEN  FLOW-FROM 'SURFACE' REFLAYER
  40 1 7   1.0 OPEN  FLOW-FROM 1
  40 1 6   1.0 OPEN  FLOW-FROM 2
  40 1 5   1.0 OPEN  FLOW-FROM 3
  40 1 4   1.0 OPEN  FLOW-FROM 4
**

```

WELL 'Injector-4\_pro'  
INJECTOR MOBWEIGHT EXPLICIT 'Injector-4\_pro'  
INCOMP WATER 1.0 0.0 0.0 0.0  
TINJW 190.0  
OPERATE MAX BHP 3000.0 CONT  
\*\* rad geofac wfrac skin  
GEOMETRY K 0.28 0.249 1.0 0.0  
PERF GEOA 'Injector-4\_pro'  
\*\* UBA ff Status Connection  
1 40 8 1.0 OPEN FLOW-FROM 'SURFACE' REFLAYER  
1 40 7 1.0 OPEN FLOW-FROM 1  
1 40 6 1.0 OPEN FLOW-FROM 2  
1 40 5 1.0 OPEN FLOW-FROM 3  
1 40 4 1.0 OPEN FLOW-FROM 4  
DATE 2021 1 1.00000  
DATE 2022 1 1.00000  
DATE 2023 1 1.00000  
DATE 2024 1 1.00000  
DATE 2025 1 1.00000  
DATE 2026 1 1.00000  
STOP  
DATE 2030 1 1.00000  
RESULTS PVTIMEX VISCREGION 1  
RESULTS PVTIMEX PVTREGION 1 FALSE  
RESULTS PVTIMEX TABLECOLS P RS BO BG VISO VISG DENOIL DENGAS CO  
RESULTS PVTIMEX TABLE 101.325 0.494257 1.03545 1.14531 290.001 0.0112108 919.81  
0.898526 4.35113e-006  
RESULTS PVTIMEX TABLE 856.908 2.41232 1.03957 0.132898 252.319 0.011334 918.063  
7.74349 4.35113e-006  
RESULTS PVTIMEX TABLE 1612.5 4.67483 1.04449 0.0692796 217.432 0.0115038 915.968  
14.8542 4.35113e-006  
RESULTS PVTIMEX TABLE 2368.08 7.14796 1.04994 0.0462608 187.74 0.0117083 913.637  
22.2454 4.35113e-006  
RESULTS PVTIMEX TABLE 3123.67 9.77841 1.05582 0.0343814 163.03 0.011945 911.113  
29.9317 4.35113e-006  
RESULTS PVTIMEX TABLE 3879.25 12.5362 1.06205 0.0271347 142.571 0.0122143  
908.441 37.9253 4.35113e-006  
RESULTS PVTIMEX TABLE 4634.83 15.4019 1.06861 0.0222572 125.598 0.0125174  
905.624 46.2363 4.35113e-006  
RESULTS PVTIMEX TABLE 5390.42 18.3616 1.07546 0.0187549 111.447 0.0128562  
902.687 54.8707 4.35113e-006  
RESULTS PVTIMEX TABLE 6146.01 21.405 1.08259 0.0161229 99.5689 0.0132329 899.635  
63.8279 4.35113e-006

RESULTS PVTIMEX TABLE 6901.58 24.524 1.08999 0.014078 89.529 0.0136498 896.472  
73.0994 4.35113e-006  
RESULTS PVTIMEX TABLE 7657.18 27.7121 1.09762 0.0124489 80.9821 0.0141091 893.23  
82.6654 3.92446e-006  
RESULTS PVTIMEX TABLE 8412.78 30.9638 1.1055 0.011126 73.6535 0.0146124 889.89  
92.4941 3.47136e-006  
RESULTS PVTIMEX TABLE 9168.37 34.2748 1.1136 0.0100361 67.3286 0.0151608 886.477  
102.539 3.10345e-006  
RESULTS PVTIMEX TABLE 9923.97 37.6411 1.12192 0.00912782 61.8334 0.015754 882.99  
112.742 2.79943e-006  
RESULTS PVTIMEX TABLE 10679.5 41.0595 1.13045 0.00836441 57.031 0.016391 879.44  
123.032 2.54453e-006  
RESULTS PVTIMEX TABLE 11435.1 44.5269 1.13918 0.00771831 52.8097 0.0170692  
875.832 133.331 2.32807e-006  
RESULTS PVTIMEX TABLE 16180.8 67.2871 1.19834 0.00531106 35.0573 0.0219857  
852.14 193.764 1.48308e-006  
RESULTS PVTIMEX TABLE 20926.3 91.4595 1.19233 0.00427286 35.0573 0.0271885  
856.436 240.844 1.06238e-006  
RESULTS PVTIMEX TABLE 25672 116.78 1.18914 0.00373772 35.0573 0.031992 858.732  
275.326 8.15134e-007  
RESULTS PVTIMEX TABLE 30417.6 143.077 1.18728 0.0034179 35.0573 0.0362549  
860.078 301.089 6.54336e-007  
RESULTS PVTIMEX TABLE 35163.3 170.225 1.18613 0.00320443 35.0573 0.0400412  
860.912 321.146 5.42334e-007  
RESULTS PVTIMEX TABLEDO 40 440  
RESULTS PVTIMEX TABLEDO 60 315  
RESULTS PVTIMEX TABLEDO 71.1111 205  
RESULTS PVTIMEX TABLEDO 80 85  
RESULTS PVTIMEX TRES 59.4444  
RESULTS PVTIMEX BPP 16  
RESULTS PVTIMEX BWI 1.00979  
RESULTS PVTIMEX DENSITYWATER 1046.81  
RESULTS PVTIMEX VISCOSITYWATER 0.521154  
RESULTS PVTIMEX WATERCVW 0  
RESULTS PVTIMEX DENSITYOIL 951.908  
RESULTS PVTIMEX GASGRAVITY 0.842  
RESULTS PVTIMEX WATERCOMP 4.30601e-007  
RESULTS PVTIMEX REFPW 14823.7  
RESULTS PVTIMEX CVO 0  
RESULTS PVTIMEX RATIODEADPVT 0.912433  
RESULTS PVTIMEX VISC PRESSURE 101.3  
RESULTS PVTIMEX COMPOSITION 2 0.517442 0.482558  
RESULTS PVTIMEX KVALUETEMP FALSE 400 -99999 0 0.264  
RESULTS PVTIMEX END

RESULTS PVTIMEX VISCREGION 1  
 RESULTS PVTIMEX PVTREGION 1 FALSE  
 RESULTS PVTIMEX TABLECOLS P RS BO BG VISO VISG DENOIL DENGAS CO  
 RESULTS PVTIMEX TABLE 101.325 0.494257 1.03545 1.14531 290.001 0.0112108 919.81  
 0.898526 4.35113e-006  
 RESULTS PVTIMEX TABLE 856.908 2.41232 1.03957 0.132898 252.319 0.011334 918.063  
 7.74349 4.35113e-006  
 RESULTS PVTIMEX TABLE 1612.5 4.67483 1.04449 0.0692796 217.432 0.0115038 915.968  
 14.8542 4.35113e-006  
 RESULTS PVTIMEX TABLE 2368.08 7.14796 1.04994 0.0462608 187.74 0.0117083 913.637  
 22.2454 4.35113e-006  
 RESULTS PVTIMEX TABLE 3123.67 9.77841 1.05582 0.0343814 163.03 0.011945 911.113  
 29.9317 4.35113e-006  
 RESULTS PVTIMEX TABLE 3879.25 12.5362 1.06205 0.0271347 142.571 0.0122143  
 908.441 37.9253 4.35113e-006  
 RESULTS PVTIMEX TABLE 4634.83 15.4019 1.06861 0.0222572 125.598 0.0125174  
 905.624 46.2363 4.35113e-006  
 RESULTS PVTIMEX TABLE 5390.42 18.3616 1.07546 0.0187549 111.447 0.0128562  
 902.687 54.8707 4.35113e-006  
 RESULTS PVTIMEX TABLE 6146.01 21.405 1.08259 0.0161229 99.5689 0.0132329 899.635  
 63.8279 4.35113e-006  
 RESULTS PVTIMEX TABLE 6901.58 24.524 1.08999 0.014078 89.529 0.0136498 896.472  
 73.0994 4.35113e-006  
 RESULTS PVTIMEX TABLE 7657.18 27.7121 1.09762 0.0124489 80.9821 0.0141091 893.23  
 82.6654 3.92446e-006  
 RESULTS PVTIMEX TABLE 8412.78 30.9638 1.1055 0.011126 73.6535 0.0146124 889.89  
 92.4941 3.47136e-006  
 RESULTS PVTIMEX TABLE 9168.37 34.2748 1.1136 0.0100361 67.3286 0.0151608 886.477  
 102.539 3.10345e-006  
 RESULTS PVTIMEX TABLE 9923.97 37.6411 1.12192 0.00912782 61.8334 0.015754 882.99  
 112.742 2.79943e-006  
 RESULTS PVTIMEX TABLE 10679.5 41.0595 1.13045 0.00836441 57.031 0.016391 879.44  
 123.032 2.54453e-006  
 RESULTS PVTIMEX TABLE 11435.1 44.5269 1.13918 0.00771831 52.8097 0.0170692  
 875.832 133.331 2.32807e-006  
 RESULTS PVTIMEX TABLE 16180.8 67.2871 1.19834 0.00531106 35.0573 0.0219857  
 852.14 193.764 1.48308e-006  
 RESULTS PVTIMEX TABLE 20926.3 91.4595 1.19233 0.00427286 35.0573 0.0271885  
 856.436 240.844 1.06238e-006  
 RESULTS PVTIMEX TABLE 25672 116.78 1.18914 0.00373772 35.0573 0.031992 858.732  
 275.326 8.15134e-007  
 RESULTS PVTIMEX TABLE 30417.6 143.077 1.18728 0.0034179 35.0573 0.0362549  
 860.078 301.089 6.54336e-007

RESULTS PVTIMEX TABLE 35163.3 170.225 1.18613 0.00320443 35.0573 0.0400412  
 860.912 321.146 5.42334e-007  
 RESULTS PVTIMEX TABLEDO 40 440  
 RESULTS PVTIMEX TABLEDO 60 315  
 RESULTS PVTIMEX TABLEDO 71.1111 205  
 RESULTS PVTIMEX TABLEDO 80 85  
 RESULTS PVTIMEX TRES 59.4444  
 RESULTS PVTIMEX BPP 16  
 RESULTS PVTIMEX BWI 1.00979  
 RESULTS PVTIMEX DENSITYWATER 1046.81  
 RESULTS PVTIMEX VISCOSITYWATER 0.521154  
 RESULTS PVTIMEX WATERCVW 0  
 RESULTS PVTIMEX DENSITYOIL 951.908  
 RESULTS PVTIMEX GASGRAVITY 0.842  
 RESULTS PVTIMEX WATERCOMP 4.30601e-007  
 RESULTS PVTIMEX REFPW 14823.7  
 RESULTS PVTIMEX CVO 0  
 RESULTS PVTIMEX RATIODEADPVT 0.912433  
 RESULTS PVTIMEX VISCPRESSURE 101.3  
 RESULTS PVTIMEX COMPOSITION 2 0.517442 0.482558  
 RESULTS PVTIMEX KVALUETEMP FALSE 400 -99999 0 0.264  
 RESULTS PVTIMEX END  
 RESULTS PROCESSWIZ PROCESS -1  
 RESULTS PROCESSWIZ FOAMYOILMODEL -1  
 RESULTS PROCESSWIZ SGC 0.15  
 RESULTS PROCESSWIZ KRGCW 0.0001  
 RESULTS PROCESSWIZ COALESCENCE -14503.6 FALSE  
 RESULTS PROCESSWIZ BUBBLEPT -14503.6  
 RESULTS PROCESSWIZ MINPRESSURE -14503.6 FALSE  
 RESULTS PROCESSWIZ NUMSETSFOAMY 2  
 RESULTS PROCESSWIZ PRODTIME 1  
 RESULTS PROCESSWIZ FOAMYREACTIONS 1 1 1 1 1  
 RESULTS PROCESSWIZ VELOCITYFOAMY TRUE  
 RESULTS PROCESSWIZ CHEMMODEL -1  
 RESULTS PROCESSWIZ CHEMDATA1 TRUE FALSE TRUE TRUE FALSE 0 3 FALSE  
 FALSE  
 RESULTS PROCESSWIZ CHEMDATA2 0.1 -99999 0 1 0 5 0.9 180 -99999 0 0  
 RESULTS PROCESSWIZ CHEMDATA3 2.65 0 0.1 0.1 0.1 0.1  
 RESULTS PROCESSWIZ FOAMDATA FALSE TRUE FALSE 80 14.6923 62.06 1.386 0.693  
 693 13.86 0 0.02 0.35  
 RESULTS PROCESSWIZ TABLEFOAMVISC 0 0.02 0 1 0.1 20 0.2 40 0.3 45 0.4 48 0.5 49  
 0.6 15 0.7 10 0.8 5 0.9 2 1 0.02  
 RESULTS PROCESSWIZ TABLEFOAMVISC 0 0.1 0 1 0.1 160 0.2 170 0.3 180 0.4 205 0.5  
 210 0.6 220 0.7 150 0.8 48 0.9 20 1 15

RESULTS PROCESSWIZ TABLEFOAMVISC 0 0.2 0 1 0.1 235 0.2 255 0.3 345 0.4 380 0.5  
 415 0.6 335 0.7 255 0.8 180 0.9 125 1 40  
 RESULTS PROCESSWIZ FOAMVISCWEIGHT 1 0.1 0.4 1  
 RESULTS PROCESSWIZ TABLEIFT 0 18.2  
 RESULTS PROCESSWIZ TABLEIFT 0.05 0.5  
 RESULTS PROCESSWIZ TABLEIFT 0.1 0.028  
 RESULTS PROCESSWIZ TABLEIFT 0.2 0.028  
 RESULTS PROCESSWIZ TABLEIFT 0.4 0.0057  
 RESULTS PROCESSWIZ TABLEIFT 0.6 0.00121  
 RESULTS PROCESSWIZ TABLEIFT 0.8 0.00037  
 RESULTS PROCESSWIZ TABLEIFT 1 0.5  
 RESULTS PROCESSWIZ IFTSURFACTANT TRUE 8  
 RESULTS PROCESSWIZ SURFACTCONC 0 0.05  
 RESULTS PROCESSWIZ TABLEIFTS 0 23.4  
 RESULTS PROCESSWIZ TABLEIFTS 0.5 5.163  
 RESULTS PROCESSWIZ TABLEIFTS 0.75 4.356  
 RESULTS PROCESSWIZ TABLEIFTS 1 3.715  
 RESULTS PROCESSWIZ TABLEIFTS 1.25 4.102  
 RESULTS PROCESSWIZ TABLEIFTS 1.5 3.805  
 RESULTS PROCESSWIZ TABLEIFTS 1.75 3.521  
 RESULTS PROCESSWIZ TABLEIFTS 2 2.953  
 RESULTS PROCESSWIZ TABLEIFTS 0 0.17  
 RESULTS PROCESSWIZ TABLEIFTS 0.5 0.011  
 RESULTS PROCESSWIZ TABLEIFTS 0.75 0.005  
 RESULTS PROCESSWIZ TABLEIFTS 1 0.007  
 RESULTS PROCESSWIZ TABLEIFTS 1.25 0.007  
 RESULTS PROCESSWIZ TABLEIFTS 1.5 0.056  
 RESULTS PROCESSWIZ TABLEIFTS 1.75 0.097  
 RESULTS PROCESSWIZ TABLEIFTS 2 0.098  
 RESULTS PROCESSWIZ IFTSURFACTANTSALINITY TRUE 8  
 RESULTS PROCESSWIZ SURFACTSALINITYCONC 0 0.05  
 RESULTS PROCESSWIZ TABLEIFTSSALINITY 0 23.4  
 RESULTS PROCESSWIZ TABLEIFTSSALINITY 15000 5.163  
 RESULTS PROCESSWIZ TABLEIFTSSALINITY 22500 4.356  
 RESULTS PROCESSWIZ TABLEIFTSSALINITY 30000 3.715  
 RESULTS PROCESSWIZ TABLEIFTSSALINITY 37500 4.102  
 RESULTS PROCESSWIZ TABLEIFTSSALINITY 45000 3.805  
 RESULTS PROCESSWIZ TABLEIFTSSALINITY 52500 3.521  
 RESULTS PROCESSWIZ TABLEIFTSSALINITY 60000 2.953  
 RESULTS PROCESSWIZ TABLEIFTSSALINITY 0 0.17  
 RESULTS PROCESSWIZ TABLEIFTSSALINITY 15000 0.011  
 RESULTS PROCESSWIZ TABLEIFTSSALINITY 22500 0.005  
 RESULTS PROCESSWIZ TABLEIFTSSALINITY 30000 0.007  
 RESULTS PROCESSWIZ TABLEIFTSSALINITY 37500 0.007

RESULTS PROCESSWIZ TABLEIFTSSALINITY 45000 0.056  
 RESULTS PROCESSWIZ TABLEIFTSSALINITY 52500 0.097  
 RESULTS PROCESSWIZ TABLEIFTSSALINITY 60000 0.098  
 RESULTS PROCESSWIZ ADSORPTION TRUE TRUE FALSE TRUE 2 TRUE  
 RESULTS PROCESSWIZ ADSPOR 0.2494 0.2494 0.2494  
 RESULTS PROCESSWIZ ADSSURF 0 0  
 RESULTS PROCESSWIZ ADSSURF 0.1 27.5  
 RESULTS PROCESSWIZ ADSALK 0 0  
 RESULTS PROCESSWIZ ADSALK 0.1 50  
 RESULTS PROCESSWIZ ADSPOLYMER 0 0  
 RESULTS PROCESSWIZ ADSPOLYMER 0.1 50  
 RESULTS PROCESSWIZ ALKALINECONC 0 0.3 0.6  
 RESULTS PROCESSWIZ ADSSURF2 0 0  
 RESULTS PROCESSWIZ ADSSURF2 0.1 27.5  
 RESULTS PROCESSWIZ ADSSURF2 0 0  
 RESULTS PROCESSWIZ ADSSURF2 0.1 39.5  
 RESULTS PROCESSWIZ ADSSURF2 0 0  
 RESULTS PROCESSWIZ ADSSURF2 0.1 51  
 RESULTS PROCESSWIZ SALINITYPPM 0 30000 60000  
 RESULTS PROCESSWIZ ADSSURF3 0 0  
 RESULTS PROCESSWIZ ADSSURF3 0.1 27.5  
 RESULTS PROCESSWIZ ADSSURF3 0 0  
 RESULTS PROCESSWIZ ADSSURF3 0.1 39.5  
 RESULTS PROCESSWIZ ADSSURF3 0 0  
 RESULTS PROCESSWIZ ADSSURF3 0.1 51  
 RESULTS PROCESSWIZ VELOCITY 0.0328084  
 RESULTS PROCESSWIZ SALINITY 1000  
 RESULTS PROCESSWIZ COMPPOLY 0 0.03 0.05 0.075  
 RESULTS PROCESSWIZ POLYVISC 1 3.5 5.2 10.8  
 RESULTS PROCESSWIZ COMPSALINITY 0 0.03 0.05 0.075  
 RESULTS PROCESSWIZ SALINITYVISC 1 3.5 5.2 10.8  
 RESULTS PROCESSWIZ SALINITY\_INITIAL -99999  
 RESULTS PROCESSWIZ FINES 10000 8000 -179966 15000 500 50 10 5000 0.0001  
 0.0624279 FALSE  
 RESULTS PROCESSWIZ LSWI 50 0.19 0.5 0 2 2 'Ca-X2'  
 RESULTS PROCESSWIZ LSWIREACT FALSE TRUE TRUE TRUE TRUE TRUE TRUE  
 FALSE FALSE FALSE FALSE FALSE FALSE 0.9999  
 RESULTS PROCESSWIZ LSWIREACTAQ  
 RESULTS PROCESSWIZ LSWIREACTMIN  
 RESULTS PROCESSWIZ LSWIREACTAQMINTEQ  
 RESULTS PROCESSWIZ LSWIREACTMINMINTEQ  
 RESULTS PROCESSWIZ LSWIRPT 0.6 0.7  
 RESULTS PROCESSWIZ LSWIRPTCHG TRUE 0.001 2 4  
 RESULTS PROCESSWIZ LSWIAQINJ

RESULTS PROCESSWIZ LSWIAQINIT  
RESULTS PROCESSWIZ LSWIMIN  
RESULTS PROCESSWIZ ISCMODEL -1 FALSE FALSE FALSE FALSE FALSE FALSE  
FALSE  
RESULTS PROCESSWIZ ISCDATA 4.29923 500 144.166 150.574 0.065 0.708108 0.065  
0.708108  
RESULTS PROCESSWIZ REACTO2  
RESULTS PROCESSWIZ BURN  
RESULTS PROCESSWIZ CRACK  
RESULTS PROCESSWIZ COMPNAMES  
RESULTS PROCESSWIZ BLOCKAGE FALSE 4  
RESULTS PROCESSWIZ END

RESULTS SPEC 'Irreducible Water Sat G-W ST' MATRIX  
RESULTS SPEC SPECNOTCALCVAL -99999  
RESULTS SPEC REGION 'All Layers (Whole Grid)'  
RESULTS SPEC REGIONTYPE 'REGION\_WHOLEGRID'  
RESULTS SPEC LAYERNUMB 0  
RESULTS SPEC PORTYPE 1  
RESULTS SPEC CON 0.24  
RESULTS SPEC SPECKEEMOD 'YES'  
RESULTS SPEC STOP

RESULTS SPEC 'Fracture Spacing I'  
RESULTS SPEC SPECNOTCALCVAL -99999  
RESULTS SPEC REGION 'All Layers (Whole Grid)'  
RESULTS SPEC REGIONTYPE 'REGION\_WHOLEGRID'  
RESULTS SPEC LAYERNUMB 0  
RESULTS SPEC PORTYPE 1  
RESULTS SPEC CON 0.001  
RESULTS SPEC SPECKEEMOD 'YES'  
RESULTS SPEC STOP

RESULTS SPEC 'Fracture Spacing K'  
RESULTS SPEC SPECNOTCALCVAL -99999  
RESULTS SPEC REGION 'Layer 1 - Whole layer'  
RESULTS SPEC REGIONTYPE 'REGION\_LAYER'  
RESULTS SPEC LAYERNUMB 1  
RESULTS SPEC PORTYPE 1  
RESULTS SPEC CON 0  
RESULTS SPEC REGION 'Layer 10 - Whole layer'  
RESULTS SPEC REGIONTYPE 'REGION\_LAYER'

RESULTS SPEC LAYERNUMB 10  
RESULTS SPEC PORTYPE 1  
RESULTS SPEC CON 0  
RESULTS SPEC REGION 'Layer 9 - Whole layer'  
RESULTS SPEC REGIONTYPE 'REGION\_LAYER'  
RESULTS SPEC LAYERNUMB 9  
RESULTS SPEC PORTYPE 1  
RESULTS SPEC CON 0  
RESULTS SPEC REGION 'Layer 2 - Whole layer'  
RESULTS SPEC REGIONTYPE 'REGION\_LAYER'  
RESULTS SPEC LAYERNUMB 2  
RESULTS SPEC PORTYPE 1  
RESULTS SPEC CON 0.001  
RESULTS SPEC REGION 'Layer 3 - Whole layer'  
RESULTS SPEC REGIONTYPE 'REGION\_LAYER'  
RESULTS SPEC LAYERNUMB 3  
RESULTS SPEC PORTYPE 1  
RESULTS SPEC CON 0.001  
RESULTS SPEC REGION 'Layer 4 - Whole layer'  
RESULTS SPEC REGIONTYPE 'REGION\_LAYER'  
RESULTS SPEC LAYERNUMB 4  
RESULTS SPEC PORTYPE 1  
RESULTS SPEC CON 0.001  
RESULTS SPEC REGION 'Layer 5 - Whole layer'  
RESULTS SPEC REGIONTYPE 'REGION\_LAYER'  
RESULTS SPEC LAYERNUMB 5  
RESULTS SPEC PORTYPE 1  
RESULTS SPEC CON 0.001  
RESULTS SPEC REGION 'Layer 6 - Whole layer'  
RESULTS SPEC REGIONTYPE 'REGION\_LAYER'  
RESULTS SPEC LAYERNUMB 6  
RESULTS SPEC PORTYPE 1  
RESULTS SPEC CON 0.001  
RESULTS SPEC REGION 'Layer 7 - Whole layer'  
RESULTS SPEC REGIONTYPE 'REGION\_LAYER'  
RESULTS SPEC LAYERNUMB 7  
RESULTS SPEC PORTYPE 1  
RESULTS SPEC CON 0.001  
RESULTS SPEC REGION 'Layer 8 - Whole layer'  
RESULTS SPEC REGIONTYPE 'REGION\_LAYER'  
RESULTS SPEC LAYERNUMB 8  
RESULTS SPEC PORTYPE 1  
RESULTS SPEC CON 0.001  
RESULTS SPEC SPECKEEMOD 'YES'

RESULTS SPEC STOP

RESULTS SPEC 'Fracture Spacing J'  
RESULTS SPEC SPECNOTCALCVAL -99999  
RESULTS SPEC REGION 'All Layers (Whole Grid)'  
RESULTS SPEC REGIONTYPE 'REGION\_WHOLEGRID'  
RESULTS SPEC LAYERNUMB 0  
RESULTS SPEC PORTYPE 1  
RESULTS SPEC EQUALSI 0 1  
RESULTS SPEC SPECKEEMOD 'YES'  
RESULTS SPEC STOP

RESULTS SPEC 'Permeability J' FRACTURE  
RESULTS SPEC SPECNOTCALCVAL -99999  
RESULTS SPEC REGION 'All Layers (Whole Grid)'  
RESULTS SPEC REGIONTYPE 'REGION\_WHOLEGRID'  
RESULTS SPEC LAYERNUMB 0  
RESULTS SPEC PORTYPE 2  
RESULTS SPEC EQUALSI 0 1  
RESULTS SPEC SPECKEEMOD 'YES'  
RESULTS SPEC STOP

RESULTS SPEC 'Permeability I' MATRIX  
RESULTS SPEC SPECNOTCALCVAL -99999  
RESULTS SPEC REGION 'Layer 1 - Whole layer'  
RESULTS SPEC REGIONTYPE 'REGION\_LAYER'  
RESULTS SPEC LAYERNUMB 1  
RESULTS SPEC PORTYPE 1  
RESULTS SPEC CON 30  
RESULTS SPEC REGION 'Layer 2 - Whole layer'  
RESULTS SPEC REGIONTYPE 'REGION\_LAYER'  
RESULTS SPEC LAYERNUMB 2  
RESULTS SPEC PORTYPE 1  
RESULTS SPEC CON 31  
RESULTS SPEC REGION 'Layer 3 - Whole layer'  
RESULTS SPEC REGIONTYPE 'REGION\_LAYER'  
RESULTS SPEC LAYERNUMB 3  
RESULTS SPEC PORTYPE 1  
RESULTS SPEC CON 31  
RESULTS SPEC REGION 'Layer 4 - Whole layer'  
RESULTS SPEC REGIONTYPE 'REGION\_LAYER'

RESULTS SPEC LAYERNUMB 4  
RESULTS SPEC PORTYPE 1  
RESULTS SPEC CON 33  
RESULTS SPEC REGION 'Layer 5 - Whole layer'  
RESULTS SPEC REGIONTYPE 'REGION\_LAYER'  
RESULTS SPEC LAYERNUMB 5  
RESULTS SPEC PORTYPE 1  
RESULTS SPEC CON 29  
RESULTS SPEC REGION 'Layer 6 - Whole layer'  
RESULTS SPEC REGIONTYPE 'REGION\_LAYER'  
RESULTS SPEC LAYERNUMB 6  
RESULTS SPEC PORTYPE 1  
RESULTS SPEC CON 30  
RESULTS SPEC REGION 'Layer 7 - Whole layer'  
RESULTS SPEC REGIONTYPE 'REGION\_LAYER'  
RESULTS SPEC LAYERNUMB 7  
RESULTS SPEC PORTYPE 1  
RESULTS SPEC CON 33  
RESULTS SPEC REGION 'Layer 8 - Whole layer'  
RESULTS SPEC REGIONTYPE 'REGION\_LAYER'  
RESULTS SPEC LAYERNUMB 8  
RESULTS SPEC PORTYPE 1  
RESULTS SPEC CON 35  
RESULTS SPEC REGION 'Layer 9 - Whole layer'  
RESULTS SPEC REGIONTYPE 'REGION\_LAYER'  
RESULTS SPEC LAYERNUMB 9  
RESULTS SPEC PORTYPE 1  
RESULTS SPEC CON 32  
RESULTS SPEC REGION 'Layer 10 - Whole layer'  
RESULTS SPEC REGIONTYPE 'REGION\_LAYER'  
RESULTS SPEC LAYERNUMB 10  
RESULTS SPEC PORTYPE 1  
RESULTS SPEC CON 30  
RESULTS SPEC SPECKEEMOD 'YES'  
RESULTS SPEC STOP

RESULTS SPEC 'Porosity' FRACTURE  
RESULTS SPEC SPECNOTCALCVAL -99999  
RESULTS SPEC REGION 'Layer 1 - Whole layer'  
RESULTS SPEC REGIONTYPE 'REGION\_LAYER'  
RESULTS SPEC LAYERNUMB 1  
RESULTS SPEC PORTYPE 2  
RESULTS SPEC CON 0.004

RESULTS SPEC REGION 'Layer 2 - Whole layer'  
RESULTS SPEC REGIONTYPE 'REGION\_LAYER'  
RESULTS SPEC LAYERNUMB 2  
RESULTS SPEC PORTYPE 2  
RESULTS SPEC CON 0.0042  
RESULTS SPEC REGION 'Layer 3 - Whole layer'  
RESULTS SPEC REGIONTYPE 'REGION\_LAYER'  
RESULTS SPEC LAYERNUMB 3  
RESULTS SPEC PORTYPE 2  
RESULTS SPEC CON 0.0045  
RESULTS SPEC REGION 'Layer 4 - Whole layer'  
RESULTS SPEC REGIONTYPE 'REGION\_LAYER'  
RESULTS SPEC LAYERNUMB 4  
RESULTS SPEC PORTYPE 2  
RESULTS SPEC CON 0.0028  
RESULTS SPEC REGION 'Layer 5 - Whole layer'  
RESULTS SPEC REGIONTYPE 'REGION\_LAYER'  
RESULTS SPEC LAYERNUMB 5  
RESULTS SPEC PORTYPE 2  
RESULTS SPEC CON 0.0035  
RESULTS SPEC REGION 'Layer 6 - Whole layer'  
RESULTS SPEC REGIONTYPE 'REGION\_LAYER'  
RESULTS SPEC LAYERNUMB 6  
RESULTS SPEC PORTYPE 2  
RESULTS SPEC CON 0.0048  
RESULTS SPEC REGION 'Layer 7 - Whole layer'  
RESULTS SPEC REGIONTYPE 'REGION\_LAYER'  
RESULTS SPEC LAYERNUMB 7  
RESULTS SPEC PORTYPE 2  
RESULTS SPEC CON 0.0027  
RESULTS SPEC REGION 'Layer 8 - Whole layer'  
RESULTS SPEC REGIONTYPE 'REGION\_LAYER'  
RESULTS SPEC LAYERNUMB 8  
RESULTS SPEC PORTYPE 2  
RESULTS SPEC CON 0.0032  
RESULTS SPEC REGION 'Layer 9 - Whole layer'  
RESULTS SPEC REGIONTYPE 'REGION\_LAYER'  
RESULTS SPEC LAYERNUMB 9  
RESULTS SPEC PORTYPE 2  
RESULTS SPEC CON 0.003  
RESULTS SPEC REGION 'Layer 10 - Whole layer'  
RESULTS SPEC REGIONTYPE 'REGION\_LAYER'  
RESULTS SPEC LAYERNUMB 10  
RESULTS SPEC PORTYPE 2

RESULTS SPEC CON 0.0031  
RESULTS SPEC SPECKEEMOD 'YES'  
RESULTS SPEC STOP

RESULTS SPEC 'Permeability I' FRACTURE  
RESULTS SPEC SPECNOTCALCVL -99999  
RESULTS SPEC REGION 'Layer 1 - Whole layer'  
RESULTS SPEC REGIONTYPE 'REGION\_LAYER'  
RESULTS SPEC LAYERNUMB 1  
RESULTS SPEC PORTYPE 2  
RESULTS SPEC CON 1830  
RESULTS SPEC REGION 'Layer 2 - Whole layer'  
RESULTS SPEC REGIONTYPE 'REGION\_LAYER'  
RESULTS SPEC LAYERNUMB 2  
RESULTS SPEC PORTYPE 2  
RESULTS SPEC CON 1750  
RESULTS SPEC REGION 'Layer 3 - Whole layer'  
RESULTS SPEC REGIONTYPE 'REGION\_LAYER'  
RESULTS SPEC LAYERNUMB 3  
RESULTS SPEC PORTYPE 2  
RESULTS SPEC CON 1850  
RESULTS SPEC REGION 'Layer 4 - Whole layer'  
RESULTS SPEC REGIONTYPE 'REGION\_LAYER'  
RESULTS SPEC LAYERNUMB 4  
RESULTS SPEC PORTYPE 2  
RESULTS SPEC CON 1645  
RESULTS SPEC REGION 'Layer 5 - Whole layer'  
RESULTS SPEC REGIONTYPE 'REGION\_LAYER'  
RESULTS SPEC LAYERNUMB 5  
RESULTS SPEC PORTYPE 2  
RESULTS SPEC CON 1570  
RESULTS SPEC REGION 'Layer 6 - Whole layer'  
RESULTS SPEC REGIONTYPE 'REGION\_LAYER'  
RESULTS SPEC LAYERNUMB 6  
RESULTS SPEC PORTYPE 2  
RESULTS SPEC CON 2100  
RESULTS SPEC REGION 'Layer 7 - Whole layer'  
RESULTS SPEC REGIONTYPE 'REGION\_LAYER'  
RESULTS SPEC LAYERNUMB 7  
RESULTS SPEC PORTYPE 2  
RESULTS SPEC CON 1950  
RESULTS SPEC REGION 'Layer 8 - Whole layer'  
RESULTS SPEC REGIONTYPE 'REGION\_LAYER'

RESULTS SPEC LAYERNUMB 8  
RESULTS SPEC PORTYPE 2  
RESULTS SPEC CON 1320  
RESULTS SPEC REGION 'Layer 9 - Whole layer'  
RESULTS SPEC REGIONTYPE 'REGION\_LAYER'  
RESULTS SPEC LAYERNUMB 9  
RESULTS SPEC PORTYPE 2  
RESULTS SPEC CON 1290  
RESULTS SPEC REGION 'Layer 10 - Whole layer'  
RESULTS SPEC REGIONTYPE 'REGION\_LAYER'  
RESULTS SPEC LAYERNUMB 10  
RESULTS SPEC PORTYPE 2  
RESULTS SPEC CON 1120  
RESULTS SPEC SPECKEEMOD 'YES'  
RESULTS SPEC STOP

RESULTS SPEC 'Permeability K' FRACTURE  
RESULTS SPEC SPECNOTCALCVAL -99999  
RESULTS SPEC REGION 'All Layers (Whole Grid)'  
RESULTS SPEC REGIONTYPE 'REGION\_WHOLEGRID'  
RESULTS SPEC LAYERNUMB 0  
RESULTS SPEC PORTYPE 2  
RESULTS SPEC CON 150  
RESULTS SPEC SPECKEEMOD 'YES'  
RESULTS SPEC STOP

RESULTS SPEC 'Permeability J' MATRIX  
RESULTS SPEC SPECNOTCALCVAL -99999  
RESULTS SPEC REGION 'All Layers (Whole Grid)'  
RESULTS SPEC REGIONTYPE 'REGION\_WHOLEGRID'  
RESULTS SPEC LAYERNUMB 0  
RESULTS SPEC PORTYPE 1  
RESULTS SPEC EQUALSI 0 1  
RESULTS SPEC SPECKEEMOD 'YES'  
RESULTS SPEC STOP

RESULTS SPEC 'Permeability K' MATRIX  
RESULTS SPEC SPECNOTCALCVAL -99999  
RESULTS SPEC REGION 'Layer 1 - Whole layer'  
RESULTS SPEC REGIONTYPE 'REGION\_LAYER'  
RESULTS SPEC LAYERNUMB 1

RESULTS SPEC PORTYPE 1  
RESULTS SPEC CON 0.3  
RESULTS SPEC REGION 'Layer 2 - Whole layer'  
RESULTS SPEC REGIONTYPE 'REGION\_LAYER'  
RESULTS SPEC LAYERNUMB 2  
RESULTS SPEC PORTYPE 1  
RESULTS SPEC CON 0.31  
RESULTS SPEC REGION 'Layer 3 - Whole layer'  
RESULTS SPEC REGIONTYPE 'REGION\_LAYER'  
RESULTS SPEC LAYERNUMB 3  
RESULTS SPEC PORTYPE 1  
RESULTS SPEC CON 0.31  
RESULTS SPEC REGION 'Layer 4 - Whole layer'  
RESULTS SPEC REGIONTYPE 'REGION\_LAYER'  
RESULTS SPEC LAYERNUMB 4  
RESULTS SPEC PORTYPE 1  
RESULTS SPEC CON 0.33  
RESULTS SPEC REGION 'Layer 5 - Whole layer'  
RESULTS SPEC REGIONTYPE 'REGION\_LAYER'  
RESULTS SPEC LAYERNUMB 5  
RESULTS SPEC PORTYPE 1  
RESULTS SPEC CON 0.29  
RESULTS SPEC REGION 'Layer 6 - Whole layer'  
RESULTS SPEC REGIONTYPE 'REGION\_LAYER'  
RESULTS SPEC LAYERNUMB 6  
RESULTS SPEC PORTYPE 1  
RESULTS SPEC CON 0.3  
RESULTS SPEC REGION 'Layer 7 - Whole layer'  
RESULTS SPEC REGIONTYPE 'REGION\_LAYER'  
RESULTS SPEC LAYERNUMB 7  
RESULTS SPEC PORTYPE 1  
RESULTS SPEC CON 0.33  
RESULTS SPEC REGION 'Layer 8 - Whole layer'  
RESULTS SPEC REGIONTYPE 'REGION\_LAYER'  
RESULTS SPEC LAYERNUMB 8  
RESULTS SPEC PORTYPE 1  
RESULTS SPEC CON 0.35  
RESULTS SPEC REGION 'Layer 9 - Whole layer'  
RESULTS SPEC REGIONTYPE 'REGION\_LAYER'  
RESULTS SPEC LAYERNUMB 9  
RESULTS SPEC PORTYPE 1  
RESULTS SPEC CON 0.32  
RESULTS SPEC REGION 'Layer 10 - Whole layer'  
RESULTS SPEC REGIONTYPE 'REGION\_LAYER'

RESULTS SPEC LAYERNUMB 10  
RESULTS SPEC PORTYPE 1  
RESULTS SPEC CON 0.3  
RESULTS SPEC SPECKEEMOD 'YES'  
RESULTS SPEC STOP

RESULTS SPEC 'Porosity' MATRIX  
RESULTS SPEC SPECNOTCALCVAL -99999  
RESULTS SPEC REGION 'Layer 1 - Whole layer'  
RESULTS SPEC REGIONTYPE 'REGION\_LAYER'  
RESULTS SPEC LAYERNUMB 1  
RESULTS SPEC PORTYPE 1  
RESULTS SPEC CON 0.12  
RESULTS SPEC REGION 'Layer 2 - Whole layer'  
RESULTS SPEC REGIONTYPE 'REGION\_LAYER'  
RESULTS SPEC LAYERNUMB 2  
RESULTS SPEC PORTYPE 1  
RESULTS SPEC CON 0.125  
RESULTS SPEC REGION 'Layer 3 - Whole layer'  
RESULTS SPEC REGIONTYPE 'REGION\_LAYER'  
RESULTS SPEC LAYERNUMB 3  
RESULTS SPEC PORTYPE 1  
RESULTS SPEC CON 0.13  
RESULTS SPEC REGION 'Layer 4 - Whole layer'  
RESULTS SPEC REGIONTYPE 'REGION\_LAYER'  
RESULTS SPEC LAYERNUMB 4  
RESULTS SPEC PORTYPE 1  
RESULTS SPEC CON 0.14  
RESULTS SPEC REGION 'Layer 5 - Whole layer'  
RESULTS SPEC REGIONTYPE 'REGION\_LAYER'  
RESULTS SPEC LAYERNUMB 5  
RESULTS SPEC PORTYPE 1  
RESULTS SPEC CON 0.135  
RESULTS SPEC REGION 'Layer 6 - Whole layer'  
RESULTS SPEC REGIONTYPE 'REGION\_LAYER'  
RESULTS SPEC LAYERNUMB 6  
RESULTS SPEC PORTYPE 1  
RESULTS SPEC CON 0.138  
RESULTS SPEC REGION 'Layer 7 - Whole layer'  
RESULTS SPEC REGIONTYPE 'REGION\_LAYER'  
RESULTS SPEC LAYERNUMB 7  
RESULTS SPEC PORTYPE 1  
RESULTS SPEC CON 0.128

RESULTS SPEC REGION 'Layer 8 - Whole layer'  
RESULTS SPEC REGIONTYPE 'REGION\_LAYER'  
RESULTS SPEC LAYERNUMB 8  
RESULTS SPEC PORTYPE 1  
RESULTS SPEC CON 0.126  
RESULTS SPEC REGION 'Layer 9 - Whole layer'  
RESULTS SPEC REGIONTYPE 'REGION\_LAYER'  
RESULTS SPEC LAYERNUMB 9  
RESULTS SPEC PORTYPE 1  
RESULTS SPEC CON 0.14  
RESULTS SPEC REGION 'Layer 10 - Whole layer'  
RESULTS SPEC REGIONTYPE 'REGION\_LAYER'  
RESULTS SPEC LAYERNUMB 10  
RESULTS SPEC PORTYPE 1  
RESULTS SPEC CON 0.123  
RESULTS SPEC SPECKEEMOD 'YES'  
RESULTS SPEC STOP

RESULTS SPEC 'Temperature' MATRIX  
RESULTS SPEC SPECNOTCALCVAL -99999  
RESULTS SPEC REGION 'All Layers (Whole Grid)'  
RESULTS SPEC REGIONTYPE 'REGION\_WHOLEGRID'  
RESULTS SPEC LAYERNUMB 0  
RESULTS SPEC PORTYPE 1  
RESULTS SPEC CON 139  
RESULTS SPEC SPECKEEMOD 'YES'  
RESULTS SPEC STOP

RESULTS SPEC 'Oil Saturation' MATRIX  
RESULTS SPEC SPECNOTCALCVAL -99999  
RESULTS SPEC REGION 'All Layers (Whole Grid)'  
RESULTS SPEC REGIONTYPE 'REGION\_WHOLEGRID'  
RESULTS SPEC LAYERNUMB 0  
RESULTS SPEC PORTYPE 1  
RESULTS SPEC CON 0.8  
RESULTS SPEC SPECKEEMOD 'YES'  
RESULTS SPEC STOP

RESULTS SPEC 'Water Saturation' MATRIX  
RESULTS SPEC SPECNOTCALCVAL -99999  
RESULTS SPEC REGION 'All Layers (Whole Grid)'

RESULTS SPEC REGIONTYPE 'REGION\_WHOLEGRID'  
RESULTS SPEC LAYERNUMB 0  
RESULTS SPEC PORTYPE 1  
RESULTS SPEC CON 0.2  
RESULTS SPEC SPECKEEMOD 'YES'  
RESULTS SPEC STOP

RESULTS SPEC 'Grid Top'  
RESULTS SPEC SPECNOTCALCVAL -99999  
RESULTS SPEC REGION 'Layer 1 - Whole layer'  
RESULTS SPEC REGIONTYPE 'REGION\_LAYER'  
RESULTS SPEC LAYERNUMB 1  
RESULTS SPEC PORTYPE 1  
RESULTS SPEC CON 4500  
RESULTS SPEC SPECKEEMOD 'YES'  
RESULTS SPEC STOP

RESULTS SPEC 'Grid Thickness'  
RESULTS SPEC SPECNOTCALCVAL -99999  
RESULTS SPEC REGION 'All Layers (Whole Grid)'  
RESULTS SPEC REGIONTYPE 'REGION\_WHOLEGRID'  
RESULTS SPEC LAYERNUMB 0  
RESULTS SPEC PORTYPE 1  
RESULTS SPEC CON 10  
RESULTS SPEC SPECKEEMOD 'YES'  
RESULTS SPEC STOP

## Appendix 2

### Similarity Report

Cavit Atalar | User Info | Messages | Instructor ▼ | English ▼ | Community | ? Help | Logout



Assignments | Students | Grade Book | Libraries | Calendar | Discussion | Preferences

NOW VIEWING: HOME > MASTER > MUSTAFA

About this page  
This is your assignment inbox. To view a paper, select the paper's title. To view a Similarity Report, select the paper's Similarity Report icon in the similarity column. A ghosted icon indicates that the Similarity Report has not yet been generated.

### MUSTAFA

INBOX | NOW VIEWING: NEW PAPERS ▼

Submit File Online Grading Report | Edit assignment settings | Email non-submitters

<input type="checkbox"/>	AUTHOR	TITLE	SIMILARITY	GRADE	RESPONSE	FILE	PAPER ID	DATE
<input type="checkbox"/>	Mustafa Hamad	ABSTRACT	0% 	--	--		1630313490	11-Aug-2021
<input type="checkbox"/>	Mustafa Hamad	CONCLUSION	0% 	--	--		1630313501	11-Aug-2021
<input type="checkbox"/>	Mustafa Hamad	CHAPTER 1	1% 	--	--		1630314110	11-Aug-2021
<input type="checkbox"/>	Mustafa Hamad	CHAPTER 4	1% 	--	--		1630314428	11-Aug-2021
<input type="checkbox"/>	Mustafa Hamad	CHAPTER 3	2% 	--	--		1630314343	11-Aug-2021
<input type="checkbox"/>	Mustafa Hamad	THESIS	5% 	--	--		1631973930	16-Aug-2021
<input type="checkbox"/>	Mustafa Hamad	CHAPTER 2	9% 	--	--		1631973864	16-Aug-2021



Prof. Dr. Salih SANER  
Thesis Supervisor

**Appendix 3**  
**Ethical Approval Letter**



**YAKIN DOĞU ÜNİVERSİTESİ**  
**ETHICAL APPROVAL DOCUMENT**

Date: 28/06/2021

To the **Institute of Graduate Studies**

The research project titled “**IMPLEMENTING THE HOT WATER-WAG FOR ENHANCING HEAVY OIL RECOVERY IN A FRACTURED CARBONATE RESERVOIR**” has been evaluated. Since the researcher will not collect primary data from humans, animals, plants or earth, this project does not need through the ethics committee.

Title: **Prof. Dr.**

Name Surname: **Salih SANER**

Signature:

Role in the Research Project: **Supervisor**